AEDC-TN-59-84

WIND TUNNEL TESTS ON AN AERIAL TARGET MODEL AT TRANSONIC AND SUPERSONIC SPEEDS

By

W. L. Chew and W. E. Carleton
PWT, ARO, Inc.

July 1959

ARNOLD ENGINEERING
DEVELOPMENT CENTER
AIR RESEARCH AND DEVELOPMENT COMMAND
U S A F

WIND TUNNEL TESTS ON AN AERIAL TARGET MODEL AT TRANSONIC AND SUPERSONIC SPEEDS

By

W. L. Chew and W. E. Carleton

PWT, ARO, Inc.

July 1959

ARO Project No. 231869

Contract No. AF 40(600)-800

AF - AEDC
Tullahoma, Tennessee

CONTENTS

ILLUSTRATIONS

ABSTRACT

Static stability characteristics of the Aerophysics Development Corporation 0.22-scale aerial target model with attached launching lugs were investigated in the 1-Foot Transonic and Supersonic Tunnels of the AEDC Propulsion Wind Tunnel Facility. Test data were obtained at Mach numbers of 0.8, 1.0, 1.2, 1.4 and 1.5 through an angle-of-attack range from -3 to +12 deg in the transonic tunnel and Mach numbers of 1.5 and 2.0 through an angle-of-attack range from -3 to +8 deg in the supersonic tunnel. Reynolds numbers, based on maximum body diameter, were in the range from 0.52 to 0.68 million. Data showing the aerodynamic characteristics of the basic model and with launching lugs attached are presented as well as a comparison of the transonic and supersonic tunnel data at Mach number 1.5.

The data show that the static stability characteristics of the aerial target model were only slightly affected by the attachment of launching lugs. Forebody axial force coefficients of the body-wing-tail configuration were increased by 38 to 48 percent with the launching lugs attached. Slight changes in normal force-curve slope and model stability were indicated as the model was rolled from 0 to ±45 deg. Changes in the roll-control effectiveness as affected by rolling the model from 0 to ±45 deg were indicated.

NOMENCLATURE

General

A	Reference area, maximum cross-sectional area, $\frac{\pi d^2}{4}$, sq ft
d	Maximum body diameter, ft
M_∞	Free-stream Mach number
p_∞	Free-stream static pressure, psf
q_∞	Free-stream dynamic pressure, $0.7\, p_\infty M_\infty{}^2$, psf
R	Reynolds number based on maximum body diameter, $V_\infty d/\nu$
T_t	Stilling chamber total temperature, °F
V_∞	Free-stream velocity, ft/sec
X_{cp}	Center of pressure location in reference body diameters measured from the model c.g. location, C_m/C_N. Positive when forward of model c.g. location

α	Angle of attack, deg
ϕ	Roll angle, positive in the clockwise direction looking upstream, deg. ϕ = 0 deg position when the plane of the wing is normal to the pitch plane at i_W and α = 0 deg
ψ	Yaw angle, positive in the right hand direction, looking forward, deg
C_{N_α}	Rate of change of normal force coefficient with angle of attack, 1/deg
C_N	Normal force coefficient, normal force/q_∞ A
C_m	Pitching moment coefficient, pitching moment/q_∞ Ad, positive in a nose up direction, all moments referenced to model c.g. location (see Fig. 1)
$C_{A,F}$	Forebody axial force coefficient, forebody axial force/q_∞ A
C_ℓ	Rolling moment coefficient, rolling moment/q_∞ Ad
C_Y	Side force coefficient, side force/q_∞ A
C_n	Yawing moment coefficient, yawing moment/q_∞ Ad, positive in a nose right direction when looking forward, all moments referenced to model c.g. location
ν	Kinematic viscosity, ft^2/sec
i_W	Incidence of both wing panels, deg. A positive direction of i_W corresponds to raising each wing panel leading edge at ϕ = 0 deg.
a_W	Wing panel differential setting, deg. The settings constitute a differential deflection from a given value of i_W of equal magnitude in each wing panel and of such direction as to result in a more positive contribution to the rolling moment by each wing panel for a positive setting.
i_t	Incidence of both horizontal tail fins for configuration T, ϕ = 0 deg. A positive direction of i_t corresponds to raising each tail fin leading edge at ϕ = 0.
a_t	Setting of both tail fin roll-control surfaces, deg. The setting of each control surface equal in magnitude and of such direction as to result in a positive contribution to the rolling moment by each tail fin for a positive setting.

Model Identification

BWT	Body plus wing plus tail (see Fig. 1)

BWT(L_1 -45)	Body plus wing plus tail plus three configuration no. 1 launch lugs orientated at 45 deg counterclockwise from the top of the model looking upstream (see Figs. 2. and 3a)
BWT(L_2 -45)	Body plus wing plus tail plus three configuration no. 2 launch lugs orientated at 45 deg counterclockwise from the top of the model looking upstream (see Figs. 2 and 3b)
BWT(L_4 -45)	Body plus wing plus tail plus three configuration no. 4 launch lugs orientated 45 deg counterclockwise from the top of the model looking upstream (see Figs. 2 and 3c)
BWT(L_4 -122)	Body plus wing plus tail plus three configuration no. 4 launch lugs orientated at 122 deg counterclockwise from the top of the model looking upstream

INTRODUCTION

At the request of the Air Proving Ground Center, Eglin Air Force Base, additional tests of an aerial target model were conducted in the 1-Foot Transonic and Supersonic Tunnels, Propulsion Wind Tunnel Facility, Arnold Engineering Development Center (PWT-AEDC), for the Aerophysics Development Corporation. The respective test dates were July 28 through July 31 and August 22 through September 4, 1958. Additional runs were made on January 19 and 20, March 17 and 26, 1959.

The 0.22-scale model used in these tests was the same basic model previously tested and reported in Ref. 1 with the addition of attached launching lugs. The purpose of this investigation was to determine an optimum launch lug configuration consistent with existing launchers and to determine static stability characteristics at various launch attitudes for finalizing the design of the aerial target. The Mach number range for these tests was extended to Mach number 2.0 to provide for launching from aircraft (F-104) flying at higher speeds than were covered by the previous tests reported in Ref. 1. Axial force and lateral stability data which were not obtained in the previous test because of balance malfunctions were obtained during these tests.

Parameters investigated included launch lug configurations, incidence of the wing, roll attitudes, and differential deflections of the tail roll-control surfaces.

The configurations were investigated at Mach numbers of 0.8, 1.0, 1.2, 1.4 and 1.5 in the Transonic Tunnel and Mach numbers 1.5 and 2.0 in the Supersonic Tunnel.

The angle-of-attack range for these tests extended from -3 to +12 deg and -3 to +8 deg in the Transonic and Supersonic Tunnels, respectively. The test Reynolds numbers, based on maximum body diameter, were in the range from 0.52 to 0.68 million.

APPARATUS

TEST ARTICLE

The 0.22-scale, sting-supported aerial target model consisted of a body of revolution with a cruciform tail assembly, movable wing, and launch rail attachment lugs. The model was supplied by the Aerophysics Development Corporation. The model assembly with

---

Manuscript released by authors June 1959.

overall dimensions is shown in Fig. 1. Detailed description of the wing, tail fins, and model construction is contained in Ref. 1.

Detailed dimensions of the three lug configurations tested are shown in Fig. 2. The maximum cross section of each lug is the same. Three lugs for each configuration L_1, L_2 and L_4 were attached to the model as indicated in Fig. 3a, 3b and 3c. The lugs were normally attached to the model along a longitudinal ray oriented at 45 deg counterclockwise from the top of the model looking forward. Provisions also were made in the model for attaching the lugs along a second longitudinal ray 122 deg counterclockwise from the top of the model.

TUNNEL DESCRIPTION

1-Foot Transonic. The 1-Foot Transonic Tunnel is a continuous-flow, non-return wind tunnel equipped with a plenum evacuation system (see Ref. 2). The tunnel is equipped with a two-dimensional flexible nozzle capable of establishing air speeds in the test section up to Mach number 1.50.

The test section consists of four parallel perforated walls forming a test section 12 by 12 inches in cross-section and 37.5 inches in length. The walls used for the investigation were 1/8-in. thick with 1/8-in. diam holes inclined 60 deg into the airstream as indicated in Fig. 4a. Relative location of the model, sting, and model support in the test section are also shown in Fig. 4a.

1-Foot Supersonic. The 1-Foot Supersonic Tunnel is a continuous-flow, non-return wind tunnel equipped with a plenum evacuation system. The tunnel is located in the Engine Test Facility (ETF) and utilizes the compressor and exhauster capabilities of that facility. The tunnel is equipped with a two-dimensional flexible nozzle capable of establishing air speeds in the test section from Mach number 1.5 to 5.0. A more complete description of the test facility and operating characteristics are presented in Ref. 2.

The test section for this test consisted of four perforated walls forming a test section 12 by 12 inches in cross-section and 30 inches in length. The walls used for the investigation were 1/8-in. thick with 1/8-in. diam holes inclined 60 deg into the airstream as indicated in Fig. 4b. For these tests the top and bottom perforated walls were diverged 15.9 minutes each for Mach numbers of 1.5 and 2.0. Figure 4b also shows the relative location of the model, sting, and model support in the test section. The model support system in the 1-Foot Supersonic Tunnel is installed so that the model pitch plane is horizontal.

Figures 5a and b show the model installed in the transonic tunnel test section in a normal flight attitude and in the supersonic tunnel test section with the plane of the wing normal to the pitch plane.

INSTRUMENTATION

A six component, internal strain gage balance (AEDC-PWT 6-.75-.1-.52M) was used in the 1-Foot Transonic Tunnel and a similar balance (AEDC-PWT 6-.75-.2-.52M) was used in the 1-Foot Supersonic Tunnel to measure model forces and moments. The readout was in the form of counts on an analog-to-digital converter. Base pressure was measured utilizing a pressure transducer and a servo amplifier for readout. The data were manually punched on tape and entered into a digital computer for calculations of final reduced aerodynamic coefficients.

PROCEDURE

TUNNEL OPERATION

1-Foot Transonic. Condensation in the test section at transonic speeds was prevented by raising the stagnation temperature. The stagnation temperature range was from 160 to 219° F. Local ambient weather conditions during the initial test period restricted the maximum Mach number to 1.4. During a later period when the ambient weather conditions were favorable, data were obtained at Mach number 1.5. The average stagnation pressure was approximately 2850 psfa. Mach numbers of 0.8 and 1.0 were established in the test section with the sonic nozzle contour in conjunction with the proper combination of tunnel pressure ratio and plenum evacuation rate. Supersonic speeds were obtained with the flexible nozzle and with plenum suction used to stablize the flow in the test section.

The model was pitched through the angle-of-attack range (-3 to 12 deg) while a constant Mach number was maintained for each model configuration. Throughout the investigation the tail assembly was maintained with the tail fins at zero incidence and the tail fin roll-control surfaces deflected -6 deg. The initial test runs were made to determine the optimum lug configuration based on minimum drag. These runs included lug configurations L_1, L_2 and L_4. The optimum lug configuration (L_4) was then tested with various wing deflections (0, 2, 4, and 6 deg) and model roll positions (-45, 0, 45, and 90 deg) at Mach numbers 0.8, 1.0, 1.2, 1.4 and 1.5. For the various roll positions the balance was maintained in a fixed position and the model rolled with respect to the balance.

1-Foot Supersonic. The stagnation pressure and temperature in the 1-Foot Supersonic Tunnel were maintained at approximately 2850 psfa and 120°F. Supersonic speeds were obtained with the flexible nozzle and plenum evacuation.

The model was pitched through the angle-of-attack range (-3 to 8 deg) while a constant Mach number was maintained for each model configuration. The angle-of-attack range of the model pitch mechanism was limited to ±8 deg. The model with the optimum lug configuration (L_4) was tested with various wing deflection angles (0, 2, 4, and 6 deg) and model roll positions (-45, 0, 45, and 90 deg) at Mach numbers 1.5 and 2.0.

CORRECTIONS

The model angle of attack was corrected for deflections caused by aerodynamic loads and for tunnel flow inclination. The correction for load deflection was approximately 1.37 deg at maximum load. Corrections applied as a result of tunnel flow inclination were as follows:

Mach Number	$\Delta\alpha$, deg
0.8	.02
1.0	.03
1.2	.14
1.4	.09
1.5	-.15
2.0	-.17

PRECISION

The estimated precision of measurements is given in the following table:

	Mach Number					
	0.8	1.0	1.2	1.4	1.5	2.0
C_N	±0.034	±0.029	±0.038	±0.025	±0.041	±0.045
C_m	±0.041	±0.028	±0.045	±0.029	±0.049	±0.051
C_ℓ	±0.008	±0.007	±0.009	±0.006	±0.012	±0.014
$C_{A,F}$	±0.016	±0.013	±0.012	±0.011	±0.021	±0.015
C_Y	±0.026	±0.024	±0.026	±0.019	±0.039	±0.044
C_n	±0.036	±0.040	±0.048	±0.029	±0.052	±0.053
α	±0.10 deg	±0.10 deg	±0.10 deg	±0.10 deg	±0.10 deg	±0.10 deg
ψ	±0.10 deg	±0.10 deg	±0.10 deg	±0.10 deg	±0.10 deg	±0.10 deg
M	±0.003	±0.003	±0.005	±0.007	±0.005	±0.005

The uncertainty quoted above for Mach number is based on the variation of Mach number in the region of the test article as determined from the tunnel empty calibration. The precision in setting Mach number is ±.003 for M = 0.8 through 1.4 and ±.005 for M = 1.5 and 2.0. The statistical method used to determine the errors assumed the applicability of a normal distribution function and probability odds of 20-1 (Ref. 3).

RESULTS AND DISCUSSION

Test results are presented for Mach numbers 0.8, 1.0, 1.2, 1.4, 1.5, and 2.0. The model forces and moments measured during the investigation have been reduced to coefficients by using the balance axis coordinate system without regard to model roll attitude. All coefficients are based on the body maximum cross-sectional area and maximum diameter.

Aerodynamic coefficients for the basic body-wing-tail (BWT) configuration with the wing at zero degrees and the roll-control surfaces on the vertical tail fins deflected -6 deg are presented in Fig. 6. Coefficients for the model when inverted are also included in these figures.

OPTIMUM LUG CONFIGURATION

The variation in forebody axial force coefficients with Mach number at $C_N = 0$ for the body-wing-tail configuration with and without the three launch lug configurations attached are presented in Fig. 7. At Mach numbers of 0.8 and 1.0 the increase in axial force coefficient for the L_1 and L_2 lug configurations ranged from 57 to 92 percent higher than the axial force coefficient obtained on the body-wing-tail configuration without launch lugs. As a result of the excessive axial force obtained with the L_1 and L_2 lug configurations, data were not obtained at Mach numbers above 1.0 on these configurations. The results in Fig. 7 indicate that the axial force coefficients for the L_4 lug configuration was appreciably lower than those obtained with the L_1 and L_2 lug configurations. On this basis the L_4 lug configuration was considered optimum for this investigation.

LAUNCH LUG POSITION

The mission of the aerial target requires that the target have the capability of being launched from aircraft with launch rails mounted on the wing tips or under the wing. To determine the effect of launching the target from the two positions, the L_4 lugs were attached to the model at positions 45 and 122 deg counterclockwise from the vertical looking forward with the model in a normal flight attitude. The effect of lug position on the aerodynamic characteristics are presented in Fig. 8 for Mach numbers of 0.8, 1.0, and 1.2. The aerodynamic characteristics were not sufficiently different for the two positions of lug attachment to justify obtaining additional data at the 122 deg position.

AERODYNAMIC CHARACTERISTICS OF THE BWT (L4 -45) CONFIGURATION

The aerodynamic characteristics of the aerial target model with the launch lugs (L_4 -45) attached for various wing deflection angles (i_W = 0, 2, 4, and 6 deg) and roll angles (ϕ = 0, ±45, and 90 deg) are presented in Figs. 9 through 15. The Mach 1.5 data were those obtained in the 1-Foot Supersonic Tunnel. A comparison of the results at Mach number 1.5 from both the transonic and supersonic tunnels are presented in subsequent figures.

Normal Force and Pitching Moments. The effects of roll angle on the variations in normal force coefficients with angle of attack and pitching moment coefficients are shown in Figs. 9 and 10. The results in Fig. 9 show only slight differences in the variations of normal force coefficient with angle of attack up to 3 deg for each model roll angle. Above 3 deg angle of attack, normal force coefficients increase at a higher rate with increasing angle of attack for the model in a normal

flight attitude than when the model is rolled to either ±45 deg. Rolling the model from 0 to either ±45 deg resulted in an increase in the static longitudinal stability for each wing setting as indicated in Fig. 10.

Side Force and Yawing Moment. Side force coefficients and yawing moment coefficients for various wing angles are presented in Figs. 11 and 12. These results were obtained by rolling the model 90 deg.

Forebody Axial Force. The effect of roll angle (0 and ±45 deg) on the model forebody axial force coefficients for each deflected wing angle is presented in Fig. 13. Only small variations in forebody axial force coefficients with variations in normal force coefficients are indicated as the model was rolled.

Rolling Moments. The effects of the -6 deg deflected roll-control surfaces on the rolling moment characteristics as the roll attitude of the aerial target model was varied are presented in Fig. 14. With the model in a zero roll attitude, for each deflected wing angle setting (i_W = 0, 2, 4, and 6 deg) only minor changes in rolling moment coefficients are indicated with increasing normal force coefficients. With increasing normal force, the rolling moment effectiveness increased when the model was in a 45 deg roll attitude and decreased when the model was in a roll attitude of -45 deg. With the model in a 45 deg roll attitude, the launch lugs were oriented along the model in the plane of pitch, and the roll-control surfaces were in a plane 45 deg with respect to the pitch plane. Thus, the roll-control surfaces were less affected by body and lug interference with increasing normal force coefficients. However, when the model was in the -45 deg roll attitude, the lugs were oriented in the yaw plane. The interference of the body and lugs on the upper roll-control surface increased with increasing normal force coefficients, resulting in a decrease in rolling moment effectiveness.

Center of Pressure Locations. Center of pressure locations, C_m/C_N, in body diameters from the moment reference center are shown in Fig. 15. Included on each Mach number plot at α = 0 are dC_m/dC_N evaluated at C_N = 0. The results indicate a rearward movement of the center of pressure as the model is rolled from 0 to ±45 deg. This trend would be expected since the forward lifting surfaces (wing panels) become less effective at ±45 deg roll.

COMPARISON OF TRANSONIC AND SUPERSONIC TUNNEL DATA AT MACH NUMBER 1.5

Preliminary analysis of the data indicated that the values of C_{N_α} obtained at Mach number 1.5 in the supersonic tunnel were slightly low with respect to the trend of C_{N_α} vs Mach number obtained in the

transonic tunnel. Consequently, additional normal force and pitching moment data were obtained with the model in the transonic tunnel at Mach number 1.5 during a later period (January 1959) when the climatic conditions were favorable with respect to condensation in the test region. A comparison between the transonic and supersonic tunnel data showing the variations in normal force coefficients with angle of attack for each roll angle and wing setting is presented in Fig. 16. For each wing deflection angle and model roll angle, the curves of normal force coefficient versus angle of attack from the transonic tunnel have higher slopes as the angle of attack is increased than those obtained in the supersonic tunnel.

The variations in pitching moment coefficient with normal force coefficient for the same configurations are shown in Fig. 17. These data show better agreement for the model at zero roll attitude than at plus or minus 45 deg roll positions.

The comparison of results between the two tunnels at Mach number 1.5 for the model rolled to 90 deg to obtain side forces and yawing moment coefficients for each wing angle are presented in Figs. 18 and 19. The differences in the variations in side force coefficients with angle of yaw (Fig. 18) between the two tunnels are of the same order of magnitude as that which occurred for the normal force variations. The comparison of the variations in yawing moment coefficients with side force coefficients (Fig. 19) show excellent agreement.

Since the geometry of the test section liners for the two tunnels are different by a factor of approximately two in the wall open area ratios (Fig. 4a and 4b), additional data were obtained in the supersonic tunnel at Mach number 1.5 with test section wall liners geometrically similar to the walls of the transonic tunnel. These data comparisons are presented in Figs. 20 and 21 for model with zero wing angle and roll angles of 0 and 45 deg, respectively, and are in better agreement with the transonic tunnel data.

The discrepancies in the data at Mach number 1.5 are therefore attributed to the difference in the tunnel walls which result in slightly different effective flow angles over the model at a given angle of attack. These effects arise from minor wall disturbances or incomplete cancellation of reflected shocks, and would be most pronounced on configurations such as those of this test which possess fore and aft lifting surfaces. Existence of some discrepancies at $M = 1.5$ is not surprising since the original wall liners for the two tunnels were designed for optimum performance in the intermediate Mach number range of each tunnel (i.e. 1.2 in the transonic tunnel and 2.0 in the supersonic tunnel). Wall development studies are continuing in an effort to resolve this inconsistency.

CONCLUSIONS

Tests of the Aerophysics Development Corporation's 0.22-scale aerial target model with attached launching lugs in the AEDC 1-Foot Transonic and Supersonic Tunnels resulted in the following conclusions:

1. The static longitudinal stability characteristics of the aerial target model were affected only slightly by the attachment of launching lugs.
2. The increase in forebody axial force coefficient for the optimum lug configuration ranged from 38 to 48 percent higher than the forebody axial force coefficient obtained on the body-wing-tail configuration without launch lugs.
3. The aerodynamic characteristics of the aerial target model were affected only slightly by the two positions of launch lug attachment.
4. The slope of the normal force curve was higher for the aerial target model in a normal flight attitude than when rolled to ±45 deg.
5. The static longitudinal stability increased for each wing setting as the model was rolled from 0 to either ±45 deg.
6. Only small variations in forebody axial force coefficients with variations in normal force coefficients were evident as the model was rolled.
7. Only minor changes in rolling moment coefficients were indicated with increasing normal force coefficients for the model in a normal flight attitude. The roll-control effectiveness increased with increasing normal force coefficient when the model was rolled to 45 deg and decreased when rolled to -45 deg.

REFERENCES

1. Chew, William L. and Carleton, W. E. "Wind Tunnel Tests on an Aerial Target Model at Transonic Speeds in the 1-Foot Transonic Tunnel." AEDC-TN-58-41, August 1958.
2. Test Facilities Handbook, (2nd Edition). "Propulsion Wind Tunnel Facility, Vol. 3." Arnold Engineering Development Center, January 1959.
3. "Aerodynamic Measurements." Gas Turbine Laboratory, Massachusetts Institute of Technology, Cambridge, Massachusetts, 1953.

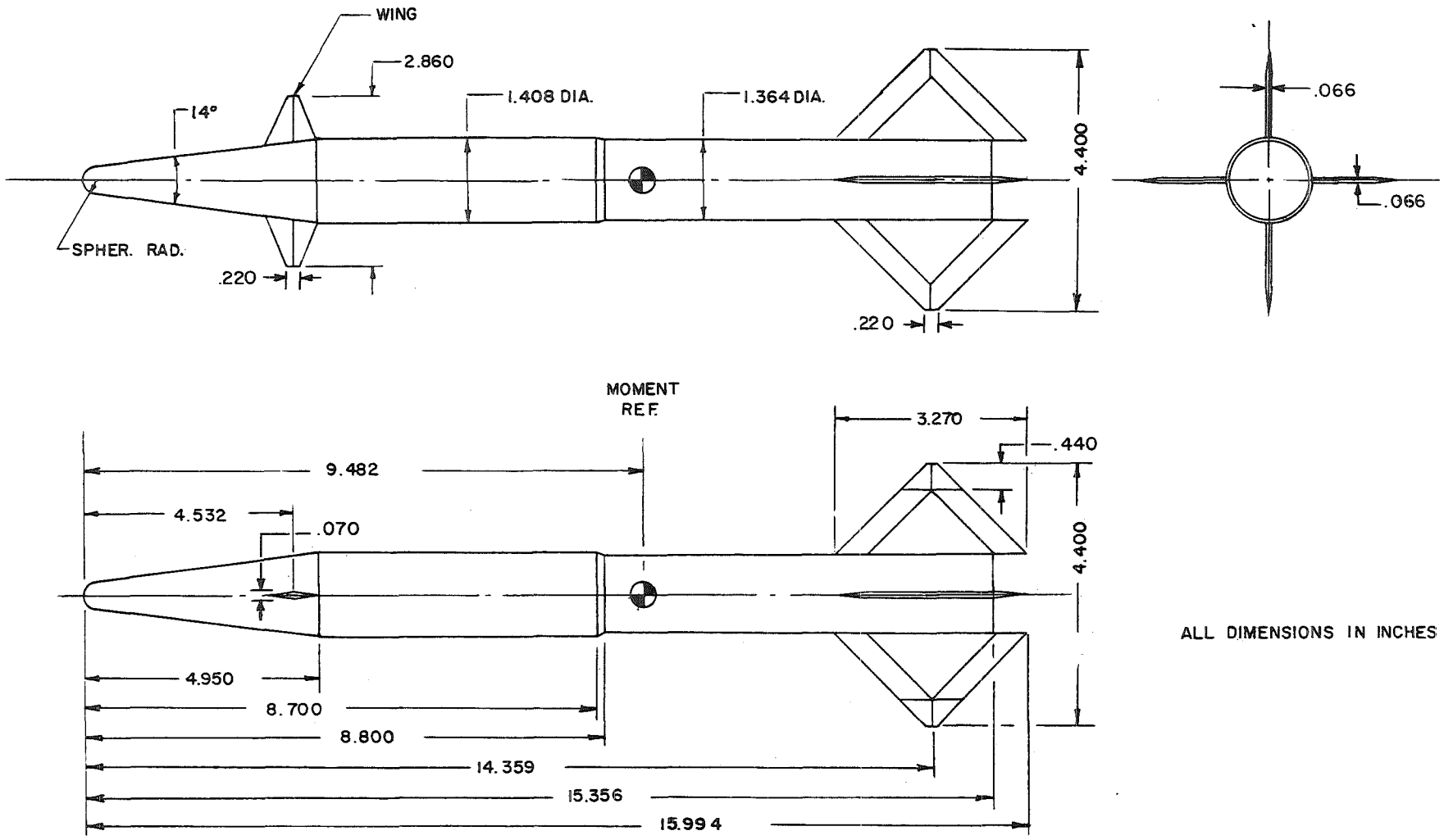

Fig. 1 Aerial Target Model

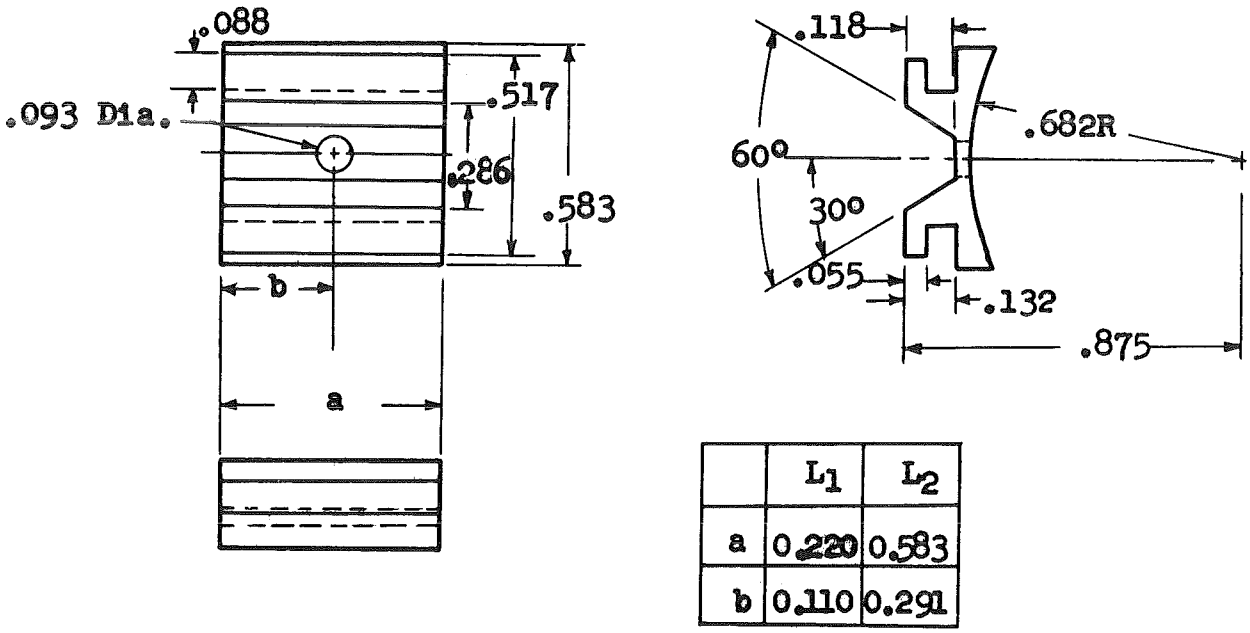

	L_1	L_2
a	0.220	0.583
b	0.110	0.291

a. L_1 and L_2

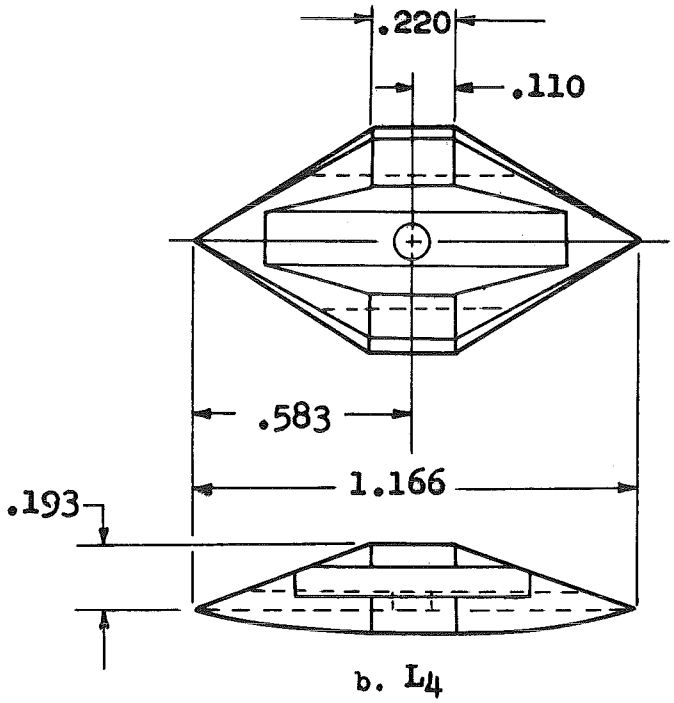

b. L_4

Note: All dimensions in inches.

Fig. 2 Detailed Dimensions of Aerial Target Model Launch Lugs

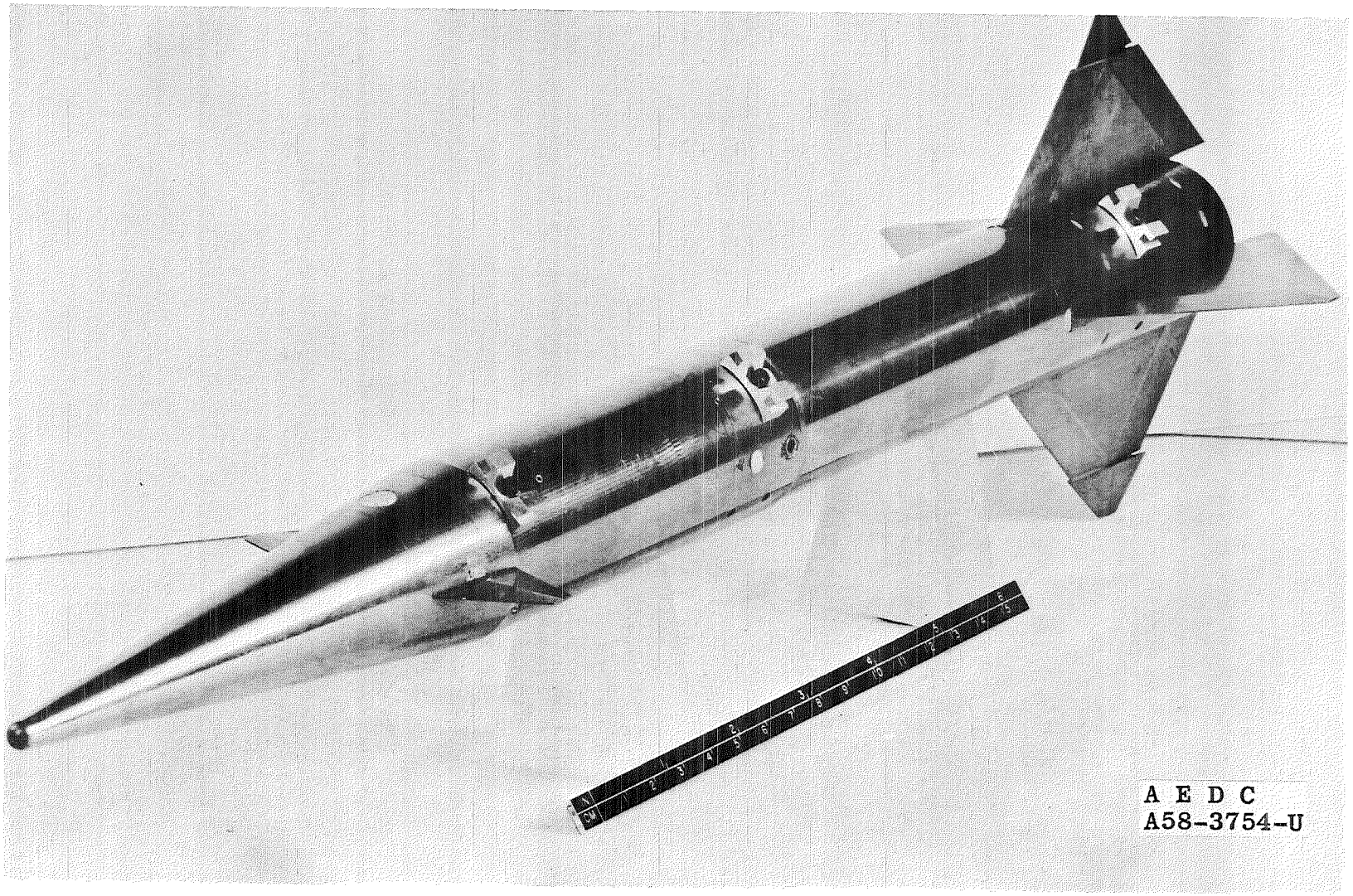

a. Configuration (L_1 – 45) Launch Lugs

Fig. 3 Launch Lug Configurations Attached to the Model

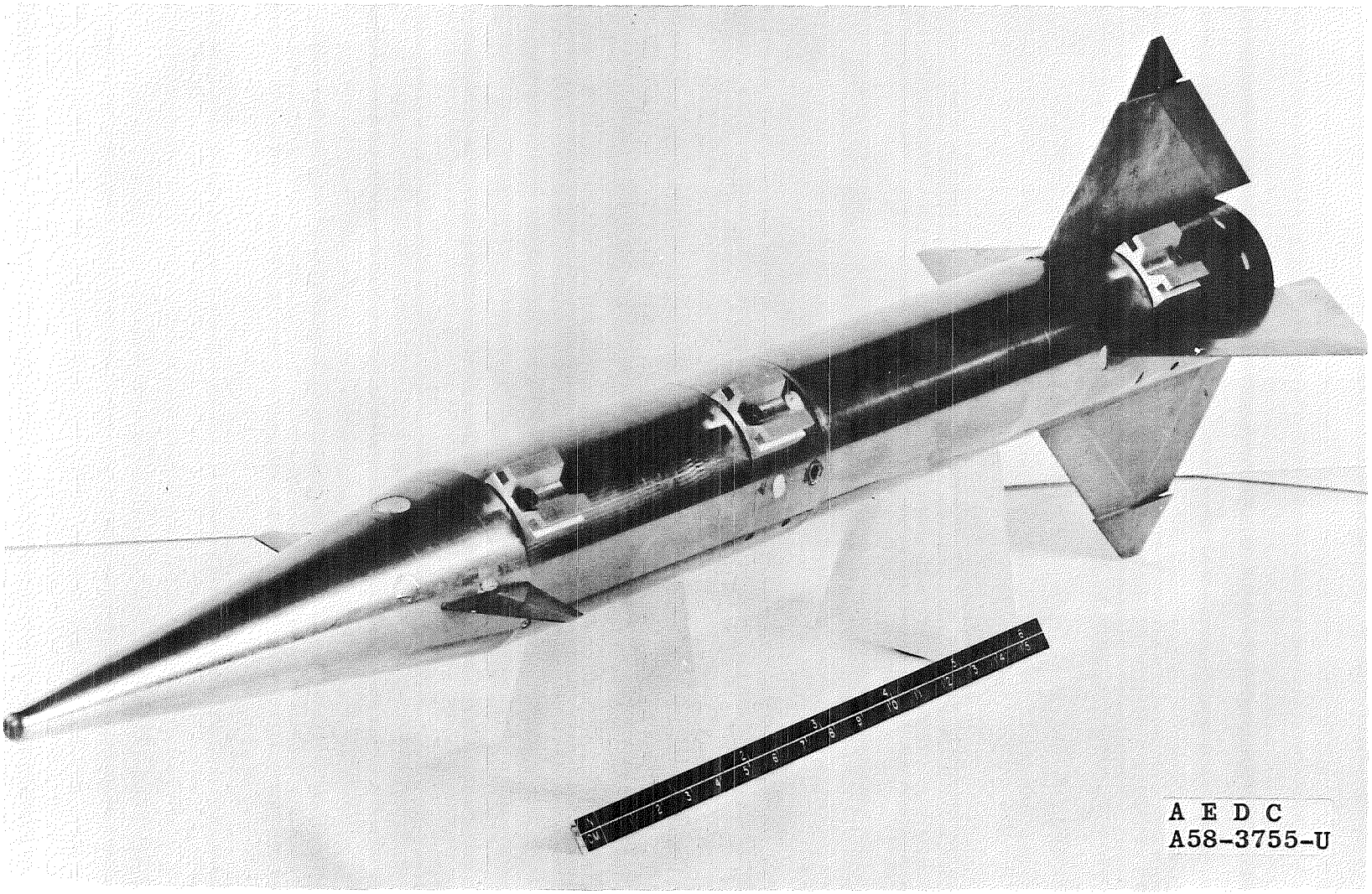

b. Configuration (L_2 −45) Launch Lugs

Fig. 3 Continued

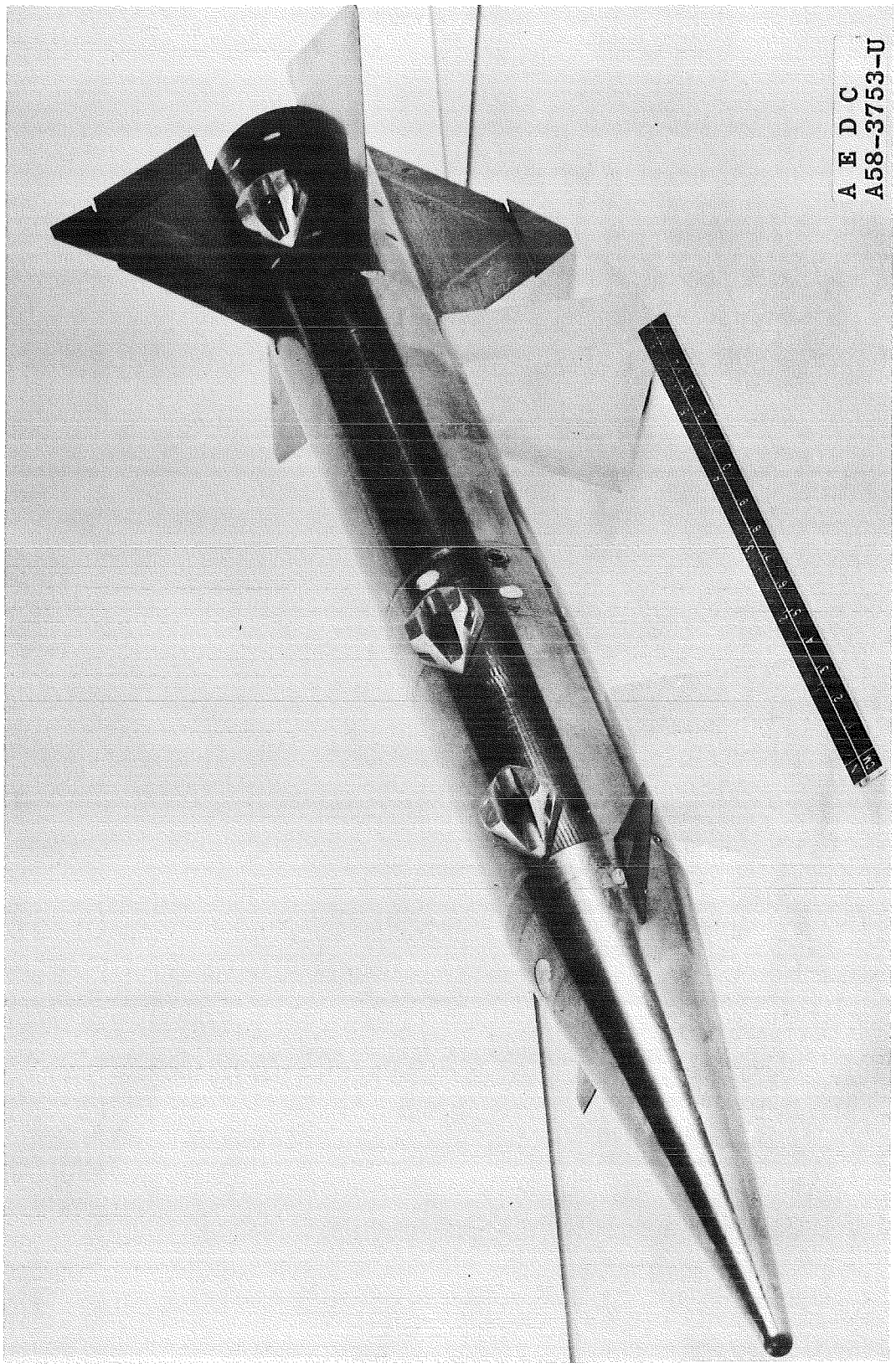

c. Configuration (L_4 –45) Launch Lugs

Fig. 3 Concluded

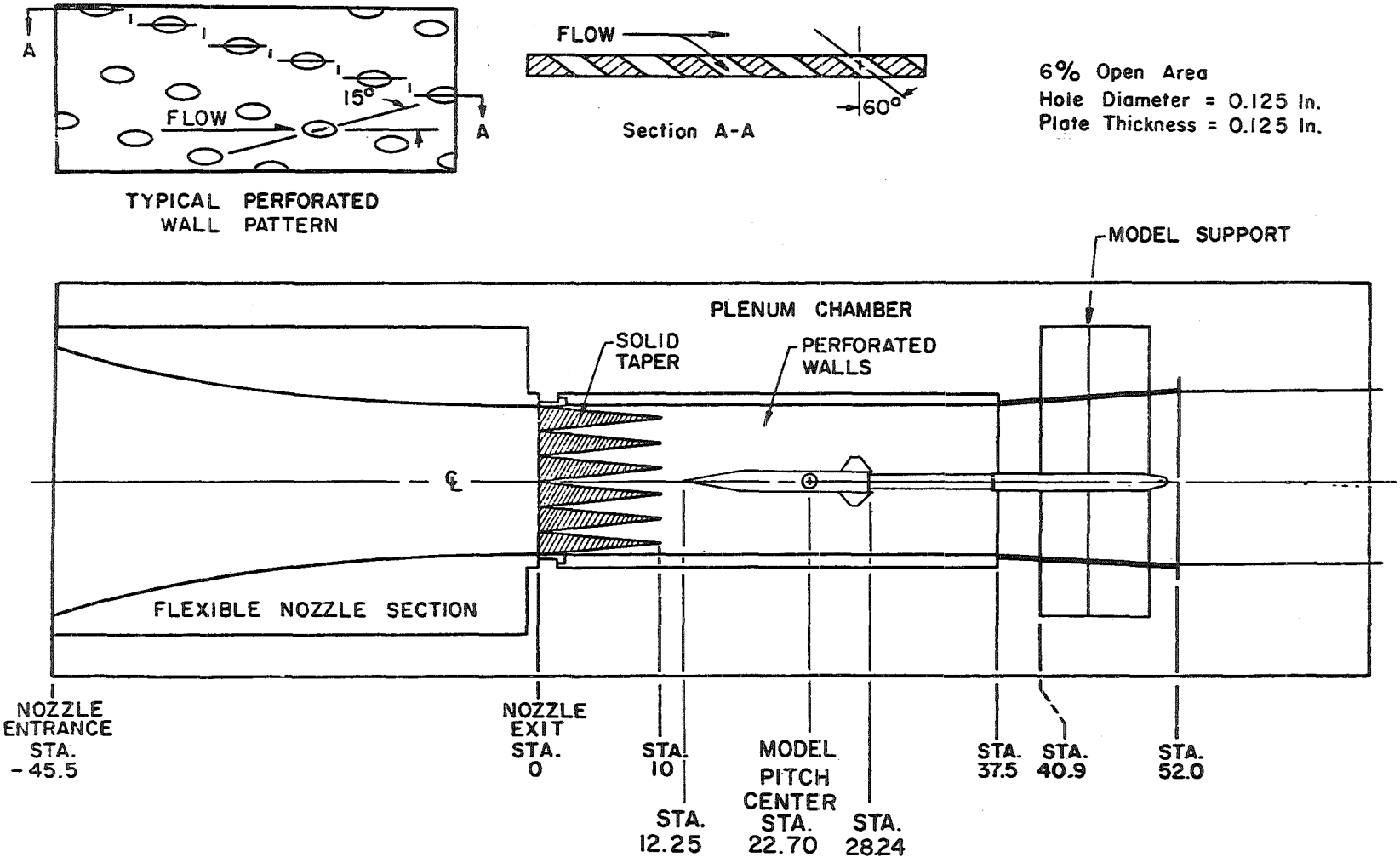

a. 1-Foot Transonic Tunnel

Fig. 4 Schematic of Test Sections Showing Model Position

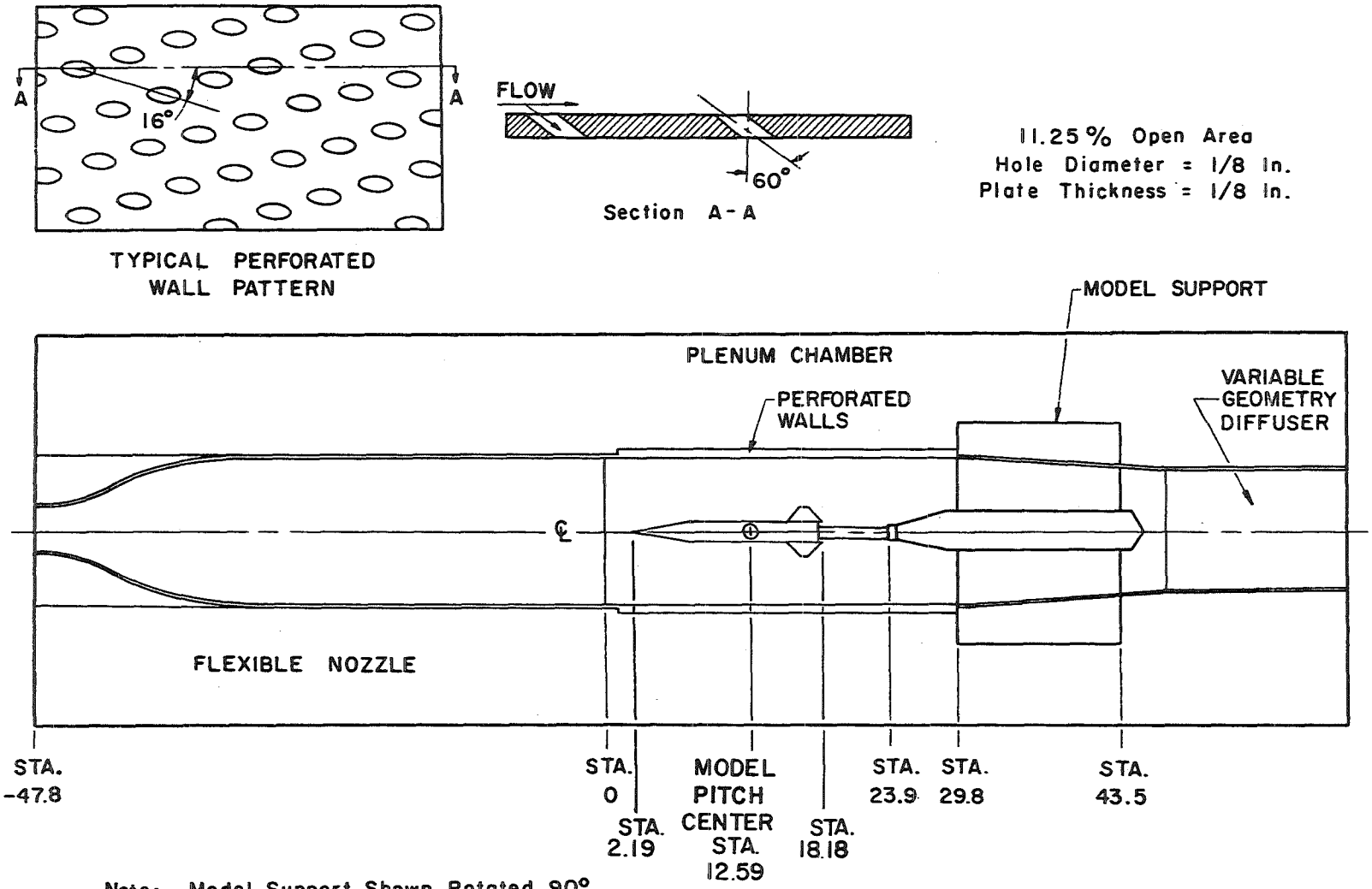

b. 1-Foot Supersonic Tunnel

Fig. 4 Concluded

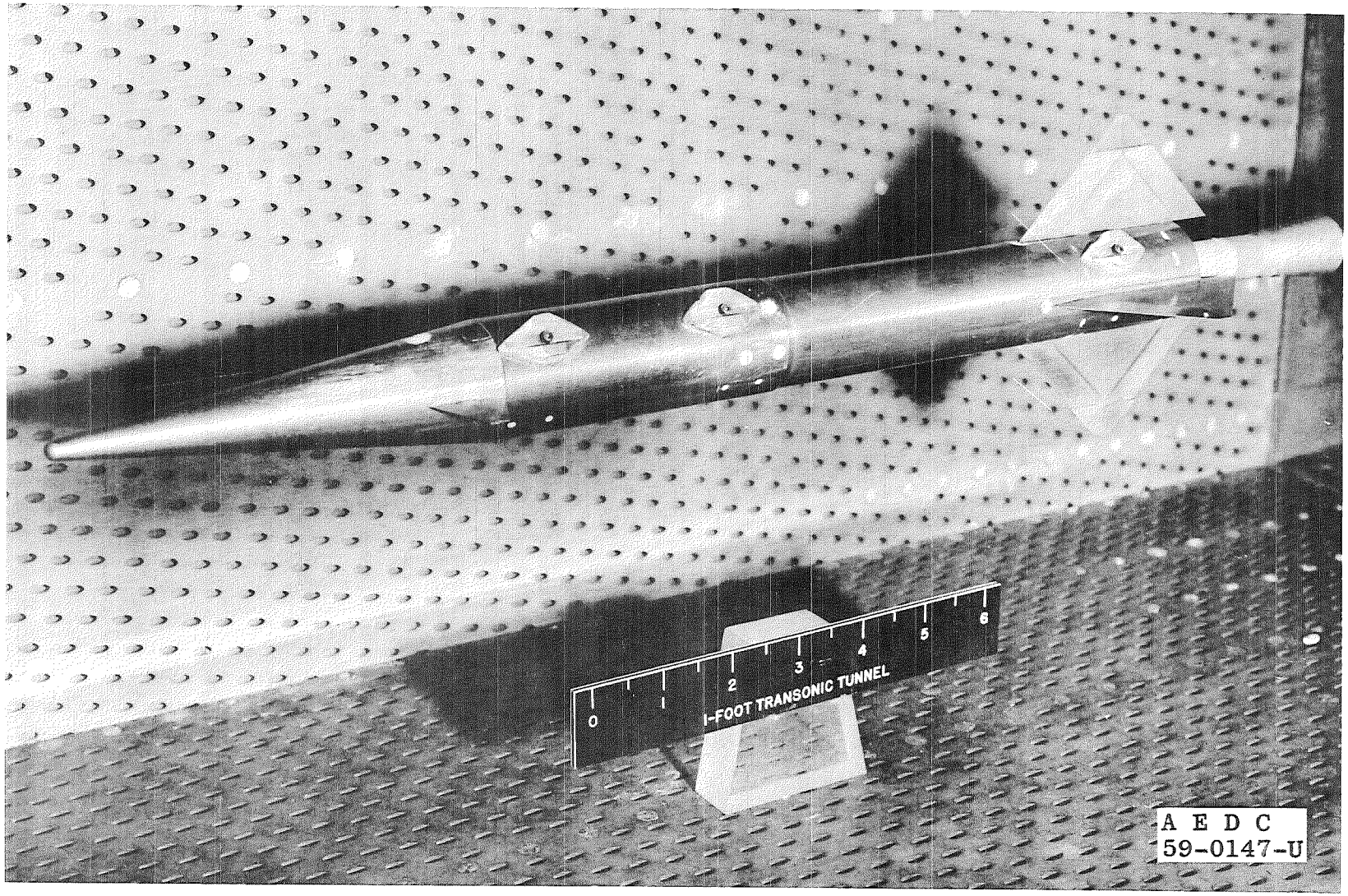

a. 1-Foot Transonic Tunnel

Fig. 5 Configuration BWT (L_4 −45) Installation in the Test Section

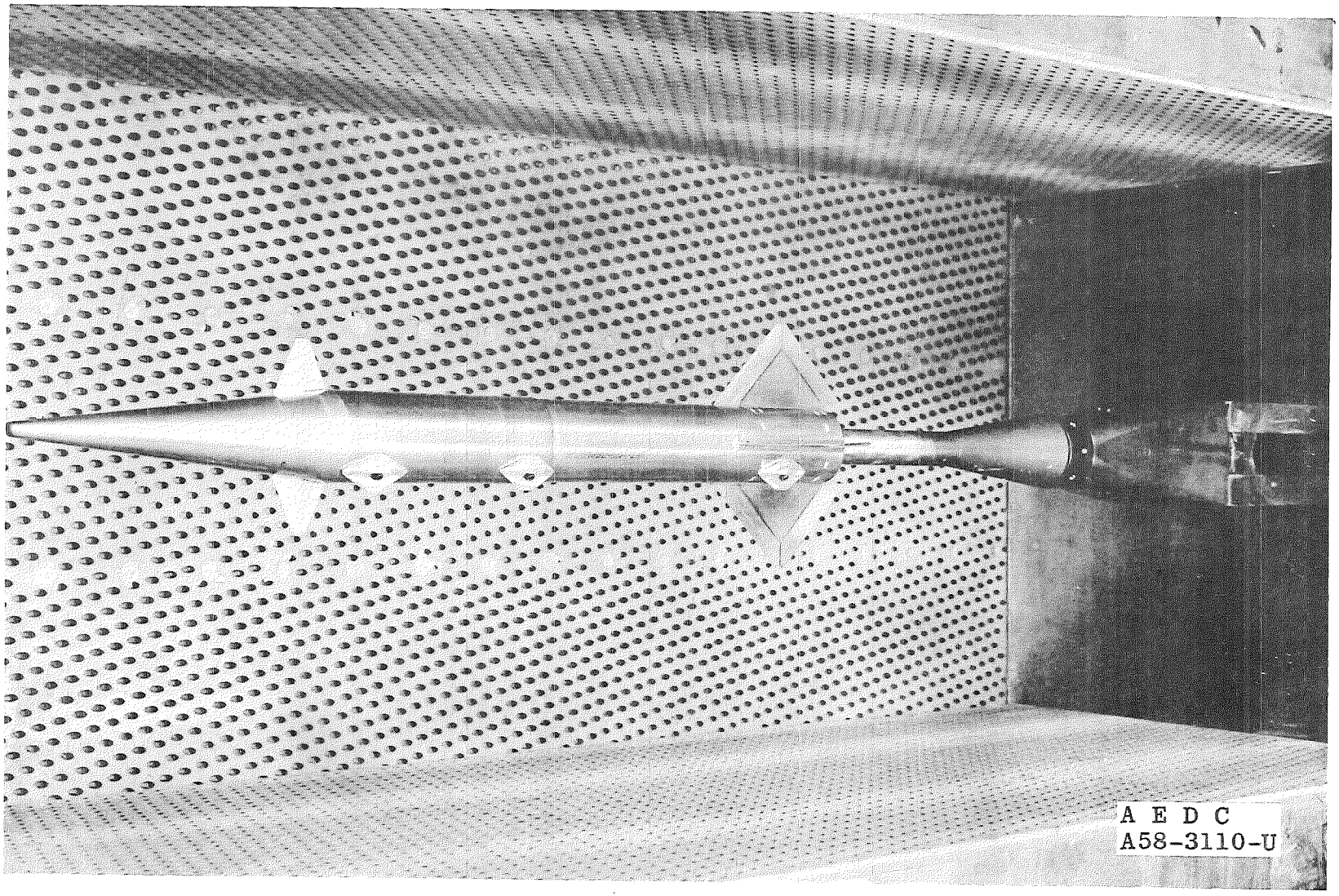

b. 1-Foot Supersonic Tunnel

Fig. 5 Concluded

Real Temperature Data
Shell Temperature Data
Shell Temperature Data
Real Temperature Data

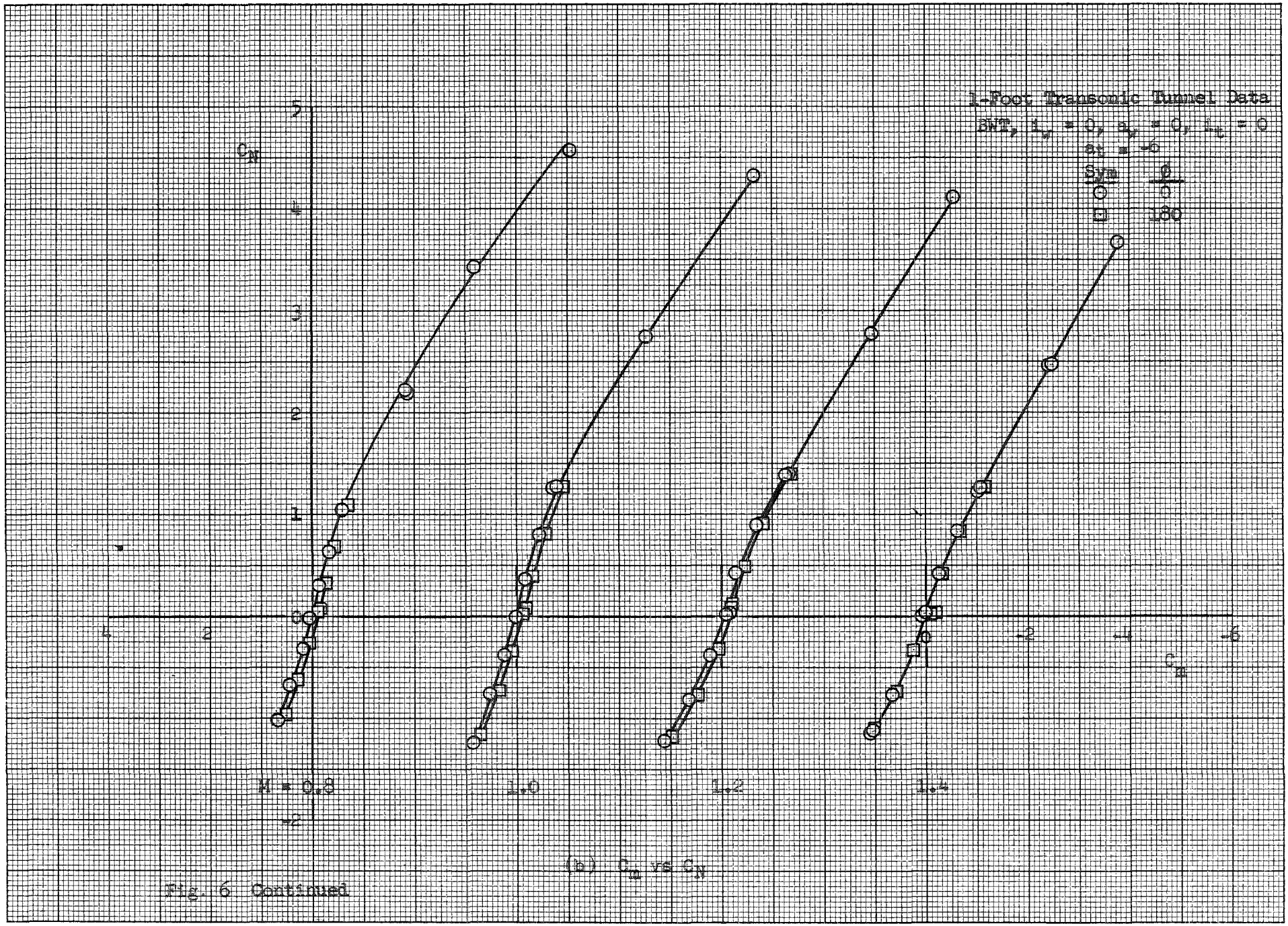

(b) C_m vs C_N

Fig. 6 Continued

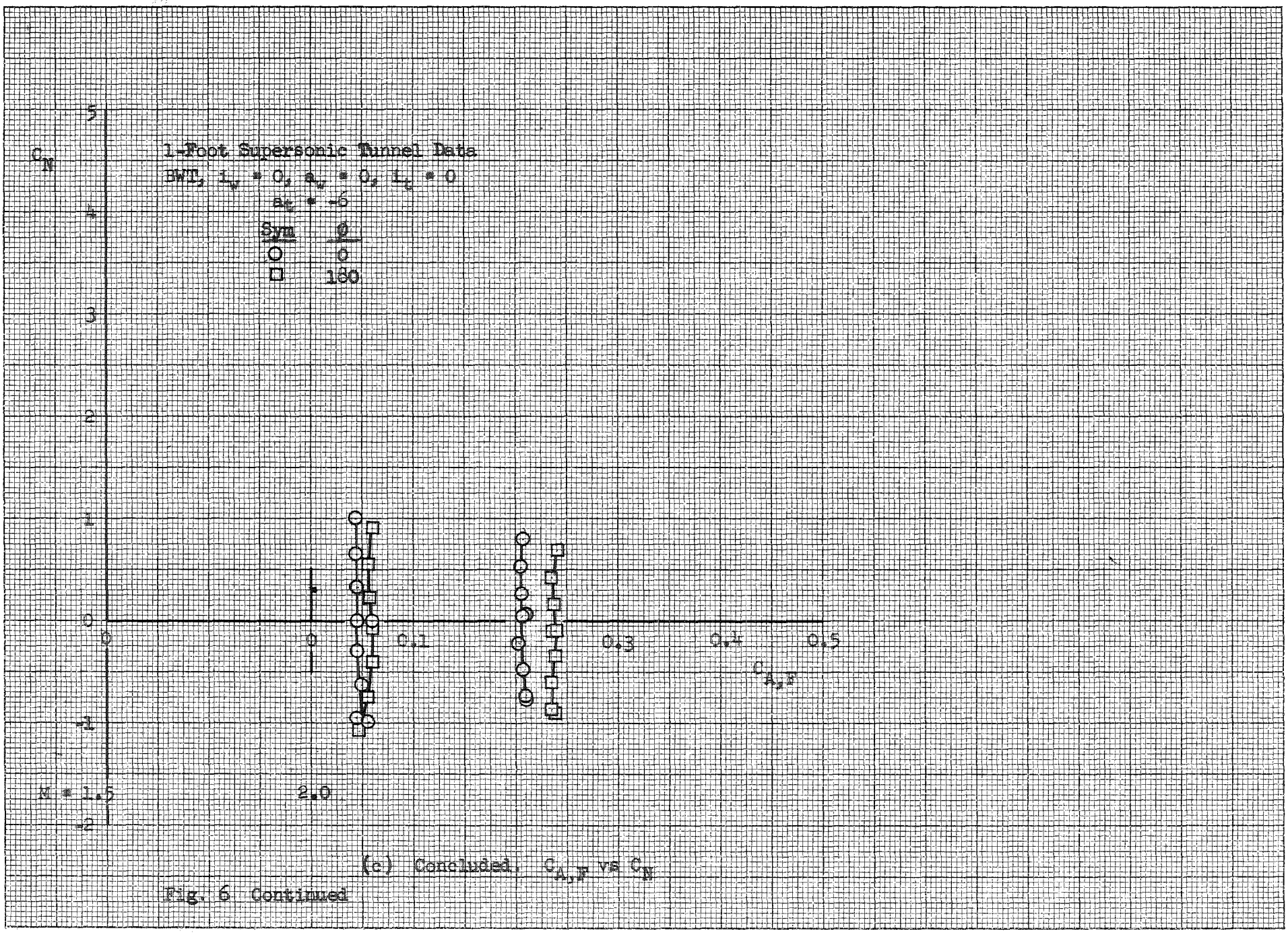

(e) Concluded, $C_{A,F}$ vs C_N

Fig. 6 Continued

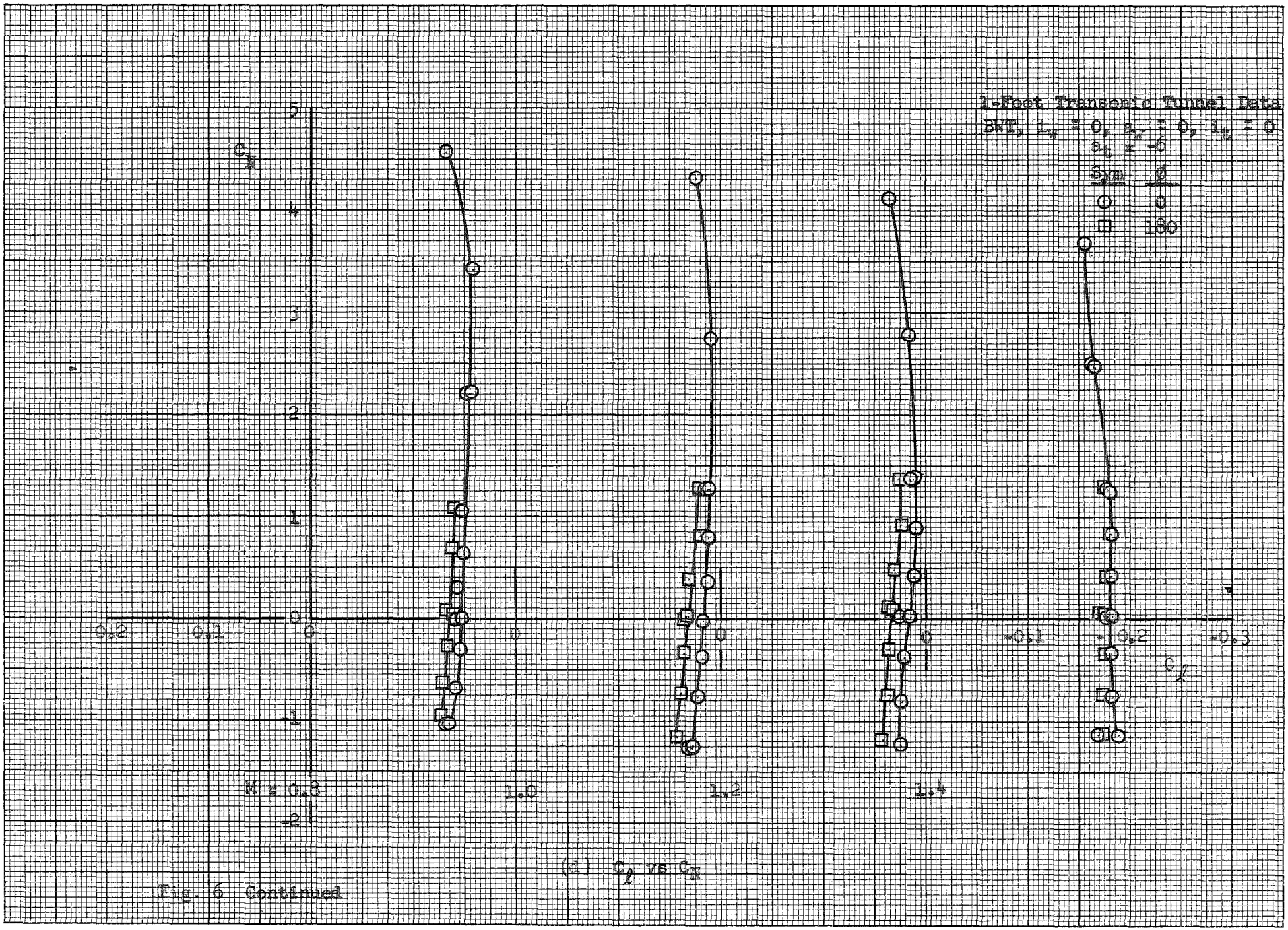

Fig. 6 Continued

Fig. 5 Continued
Conductivity, S/cm
Temperature, °C
Sr
Ca
Ba
Mg
Be
Ra

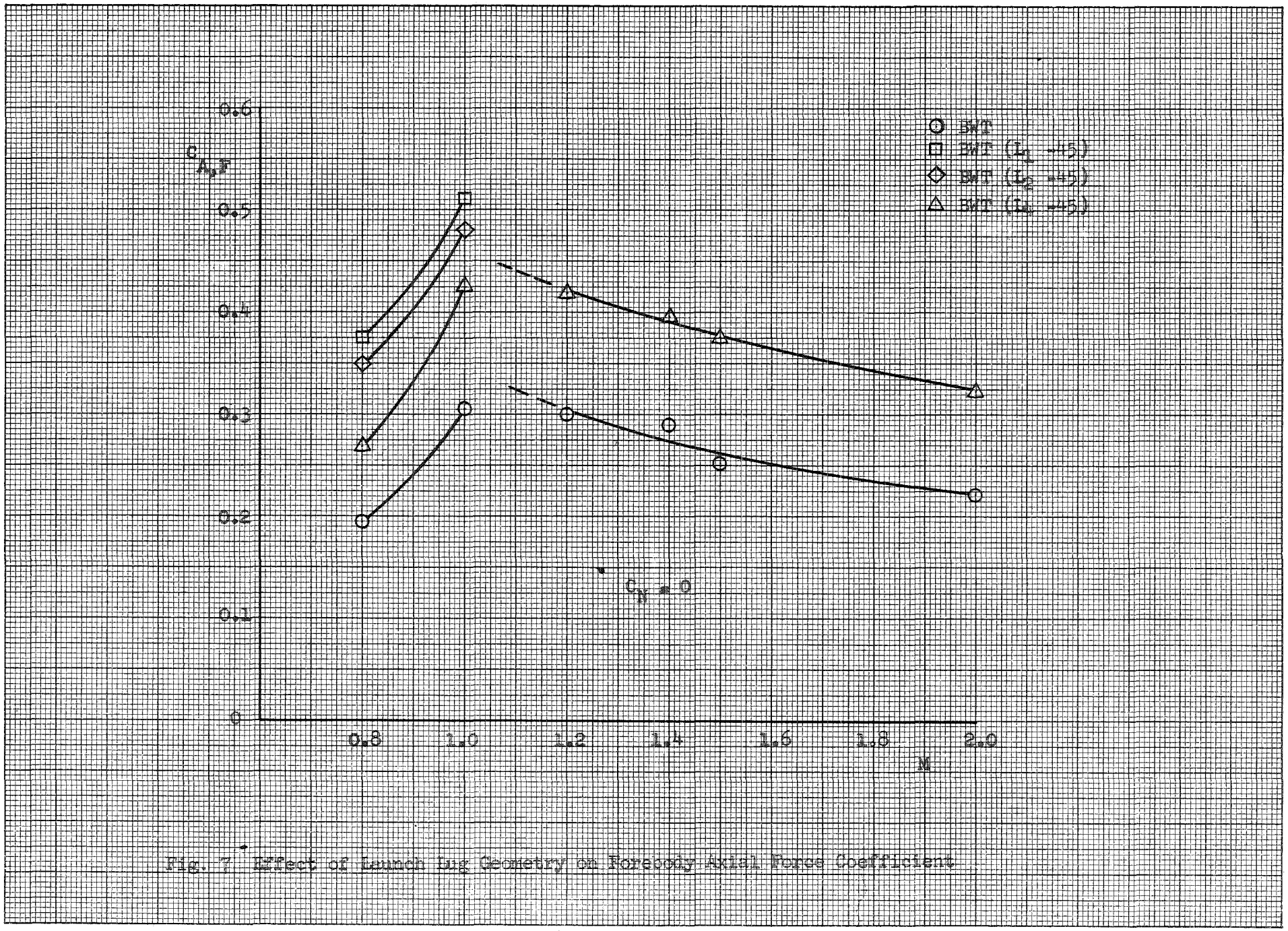

Fig. 7 Effect of Launch Lug Geometry on Forebody Axial Force Coefficient

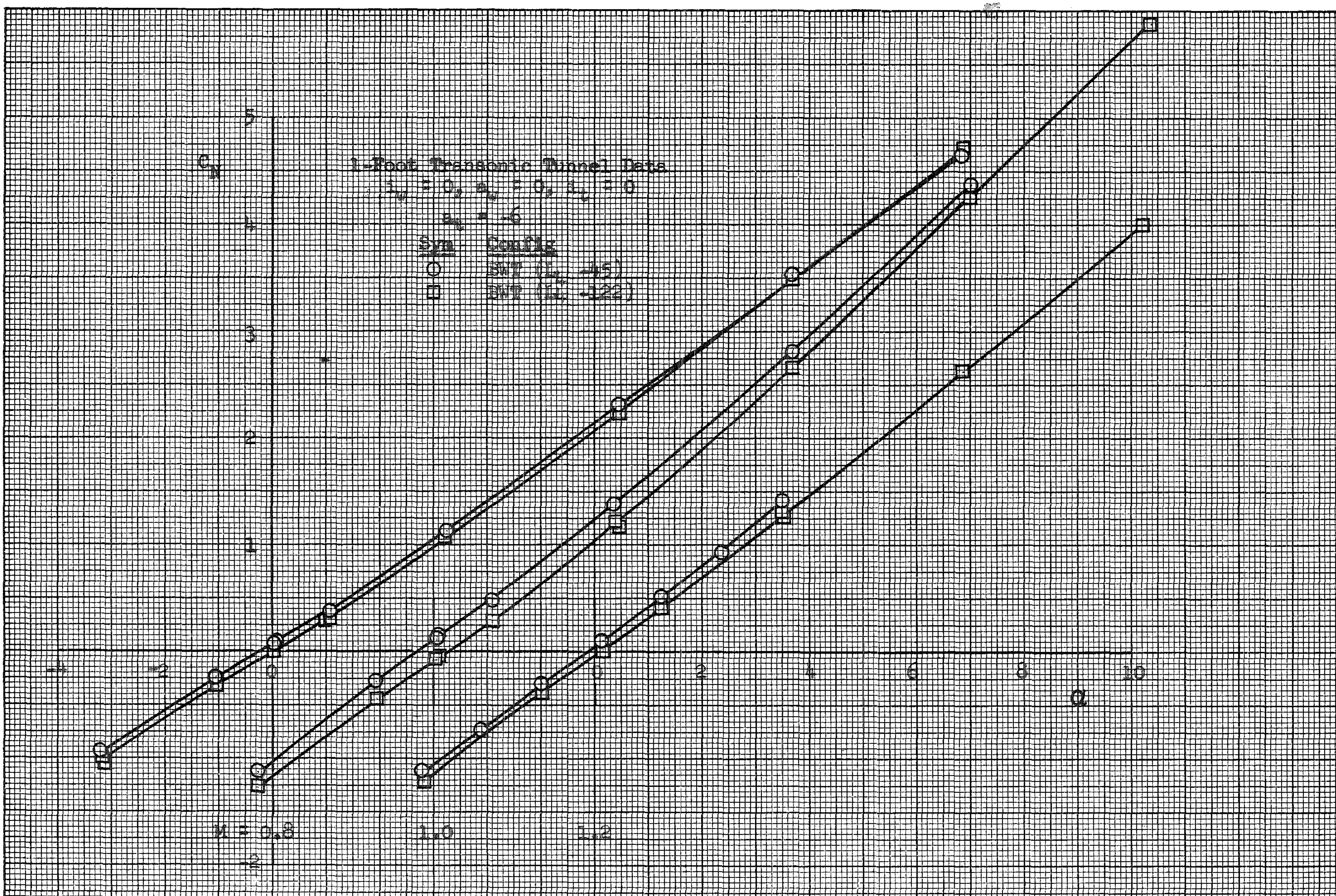

(a) C_N vs α

Fig. 8 Effect of Launch Lug Position on the Aerodynamic Characteristic of Configuration BWT

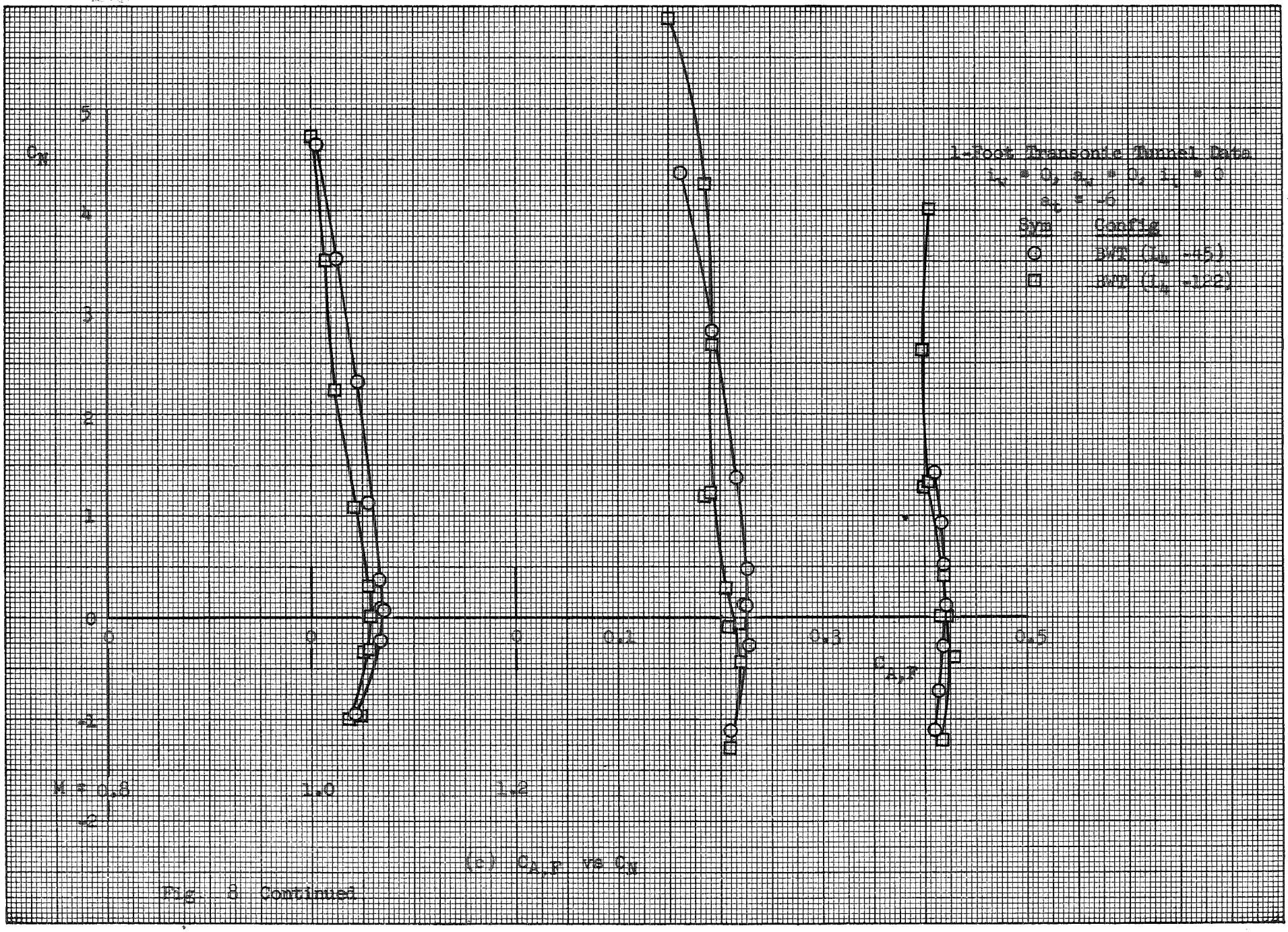

(c) $C_{A,F}$ vs C_W

Fig. 8 Continued.

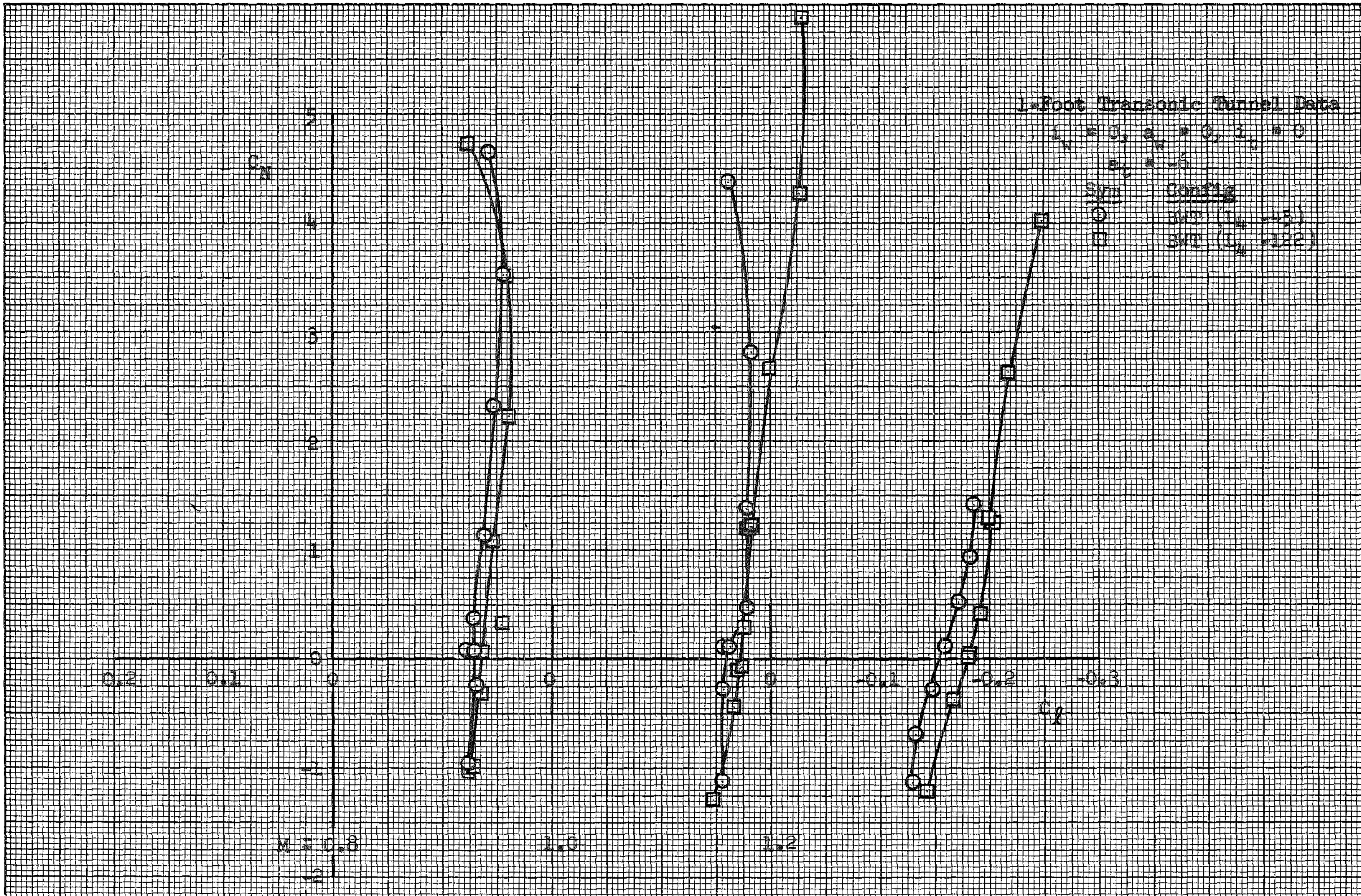

(h) C_l vs C_N

Fig. 8 Continued

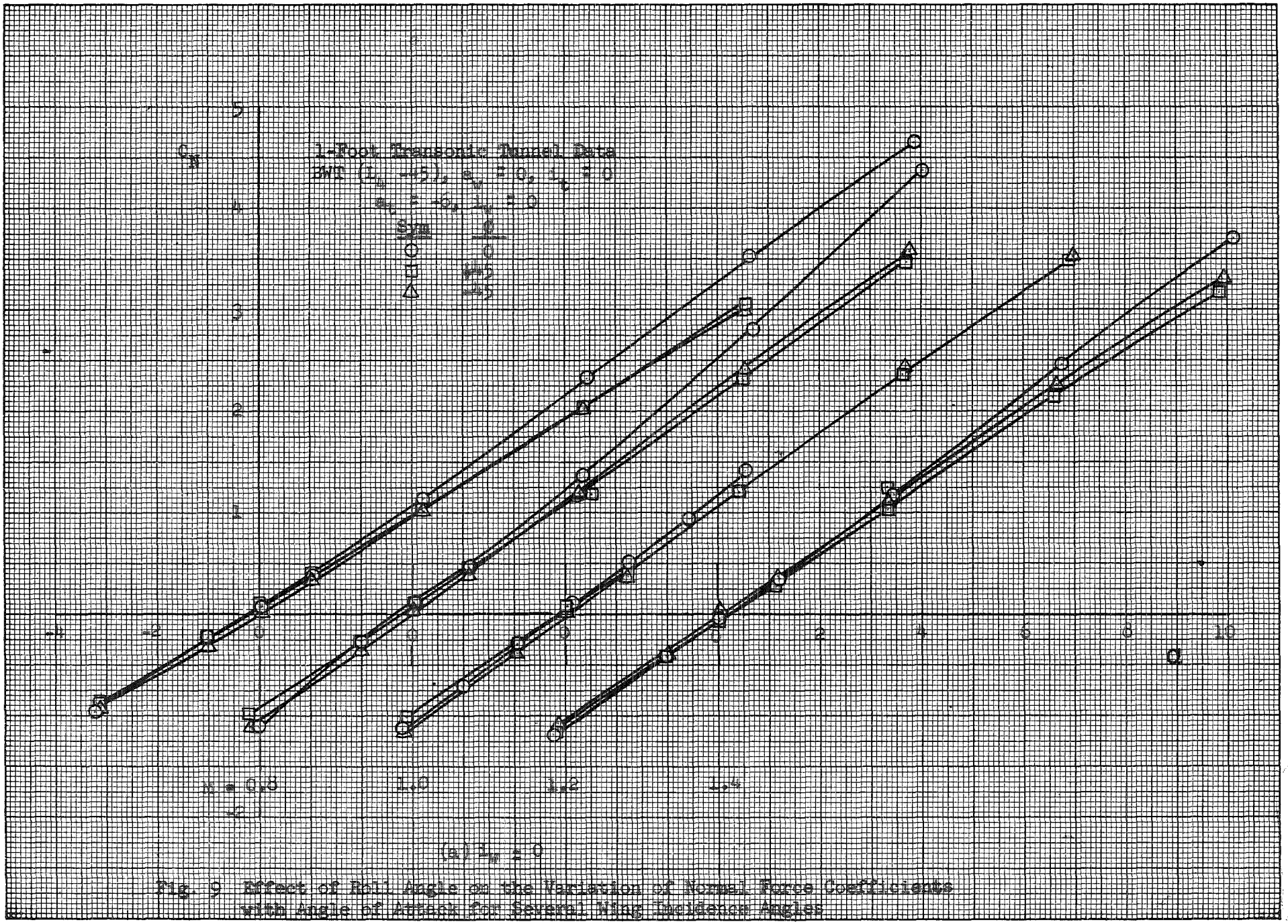

Fig. 9 Effect of Roll Angle on the Variation of Normal Force Coefficients with Angle of Attack for Several Wing Incidence Angles

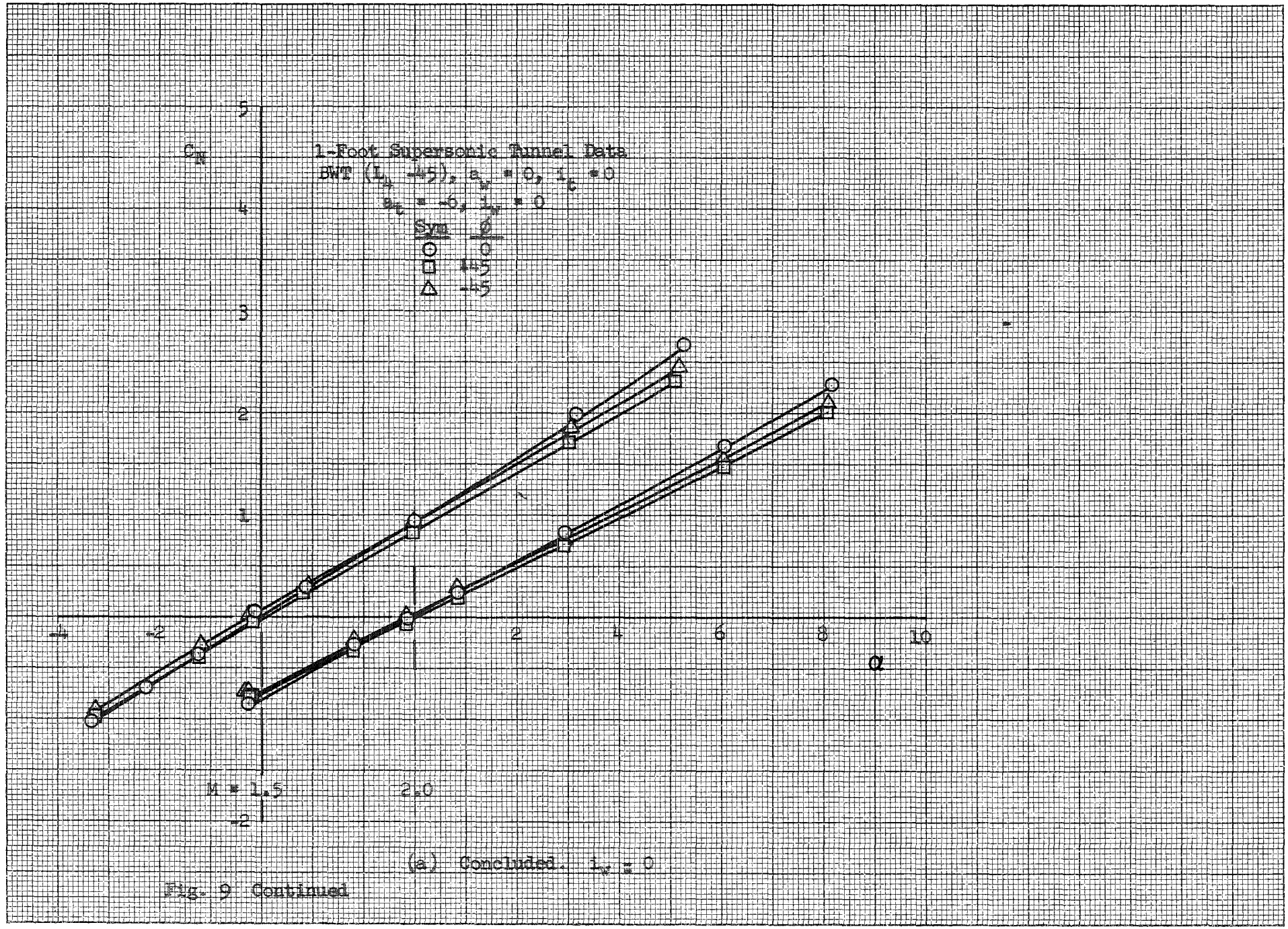

(a) Concluded. i_w = 0

Fig. 9 Continued

Fig. 6 continued
Post-Triassic fluvial facts
Triassic fluvial facts
Post-Triassic marine facts
Triassic marine facts
Pre-Triassic facts
Pre-Triassic fluvial facts
Pre-Triassic marine facts
Post-Triassic fluvial facts
Post-Triassic marine facts
Triassic fluvial facts
Triassic marine facts
Pre-Triassic facts
Pre-Triassic fluvial facts
Pre-Triassic marine facts
KEUFFEL & ESSER CO.
MADE IN U.S.A.

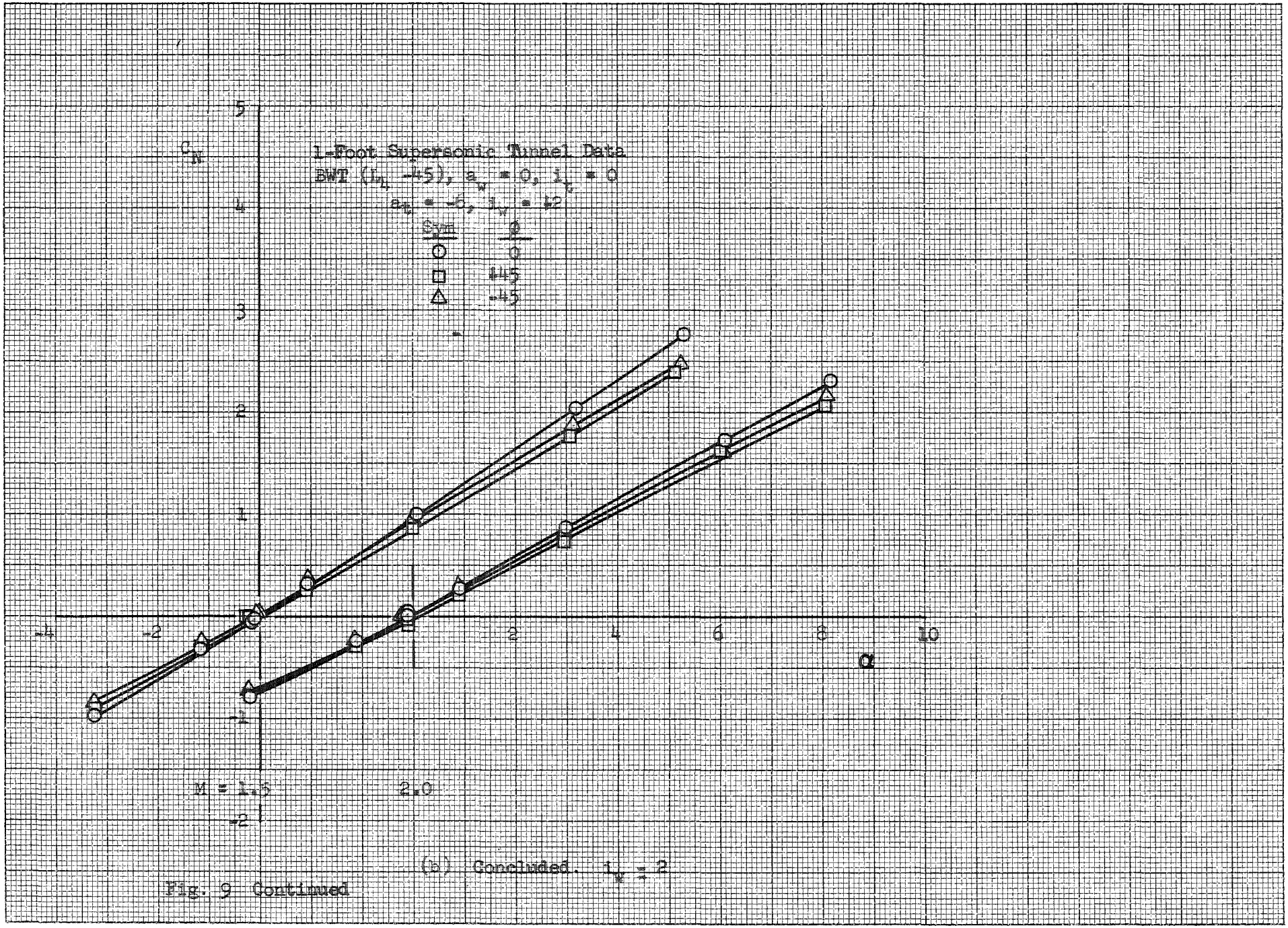

(b) Concluded. i_w = 2

Fig. 9 Continued

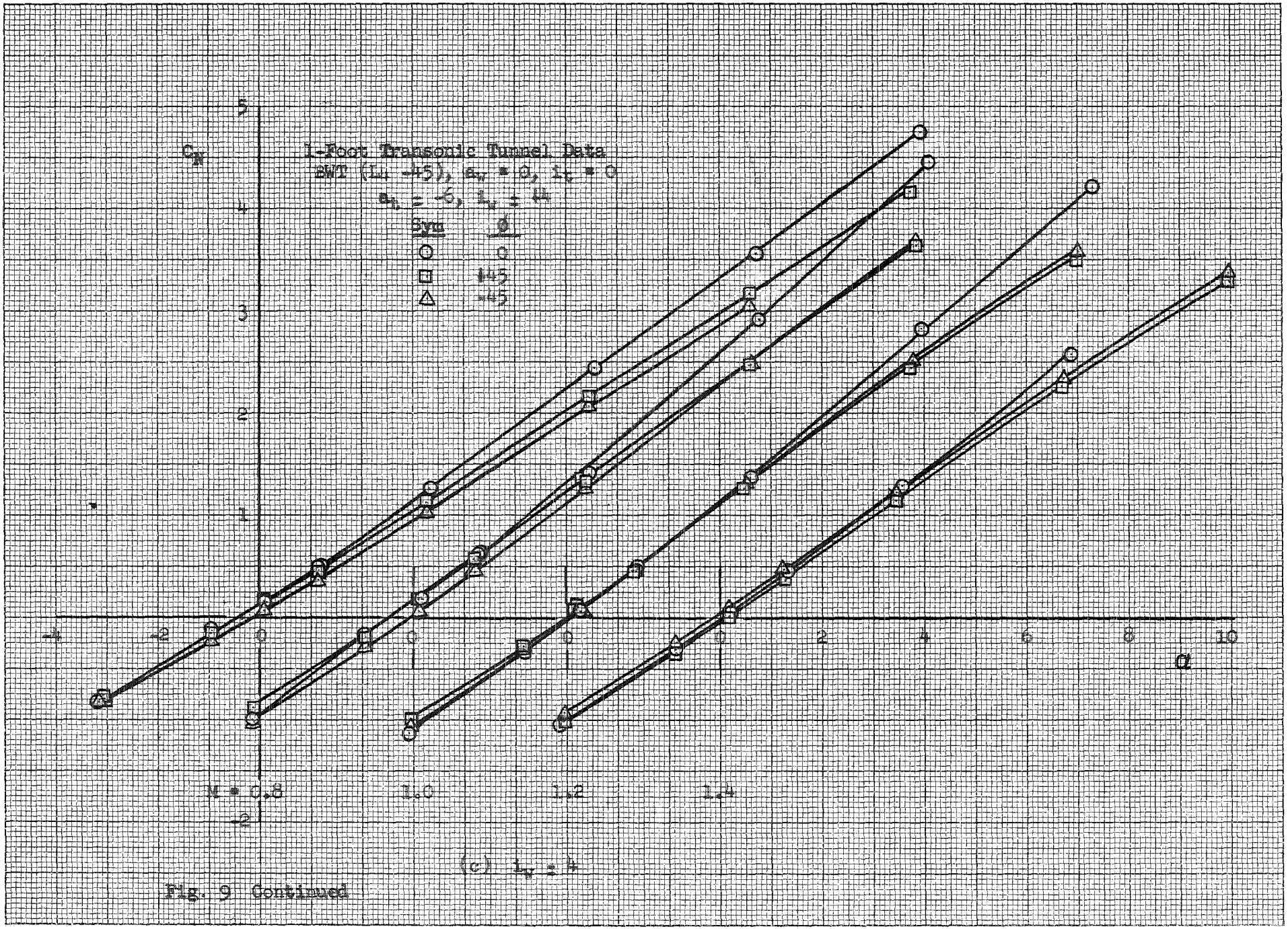

Fig. 9 Continued

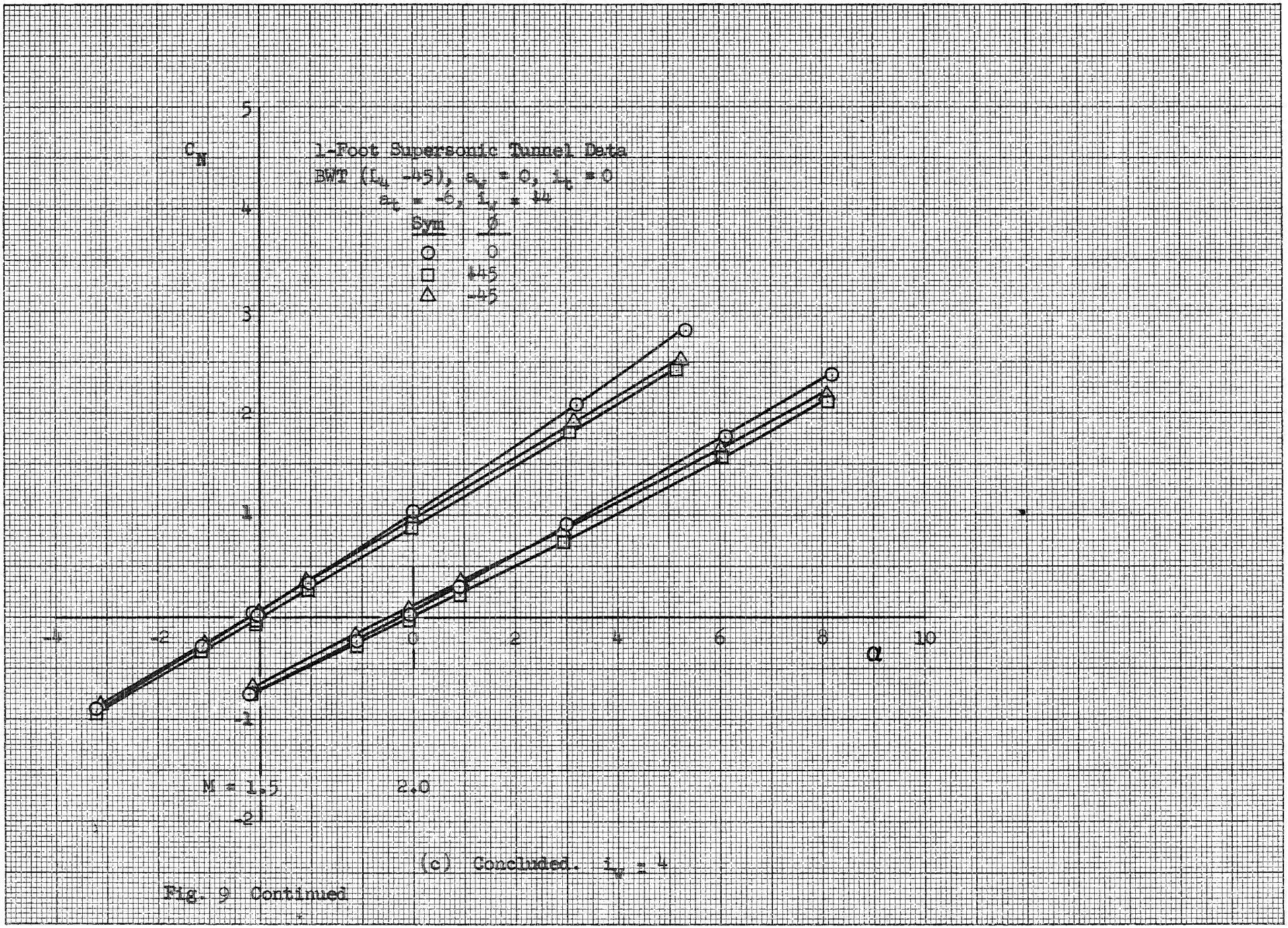

(c) Concluded. i_w = 4

Fig. 9 Continued

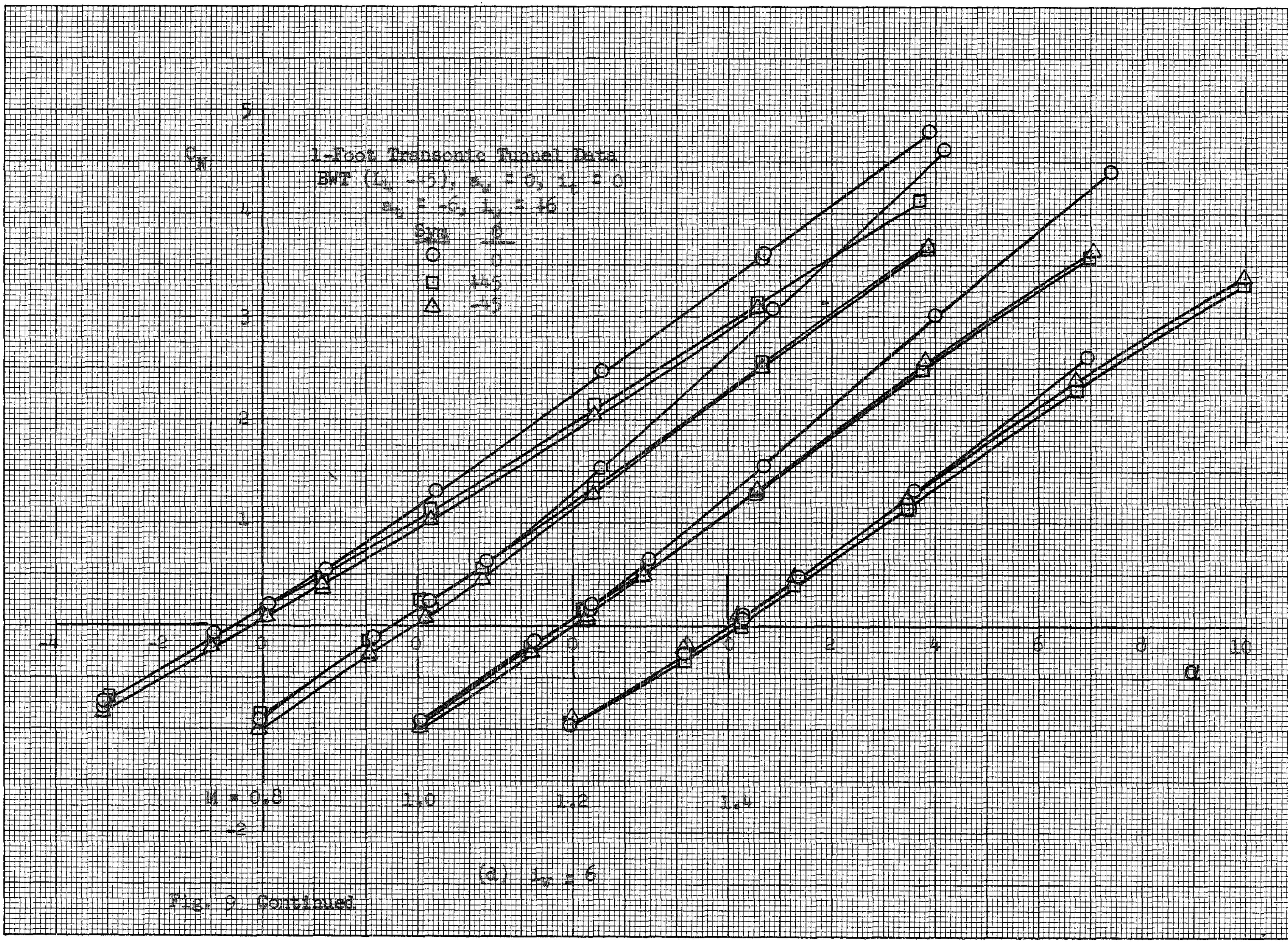

(d) i_v = 6

Fig. 9 Continued

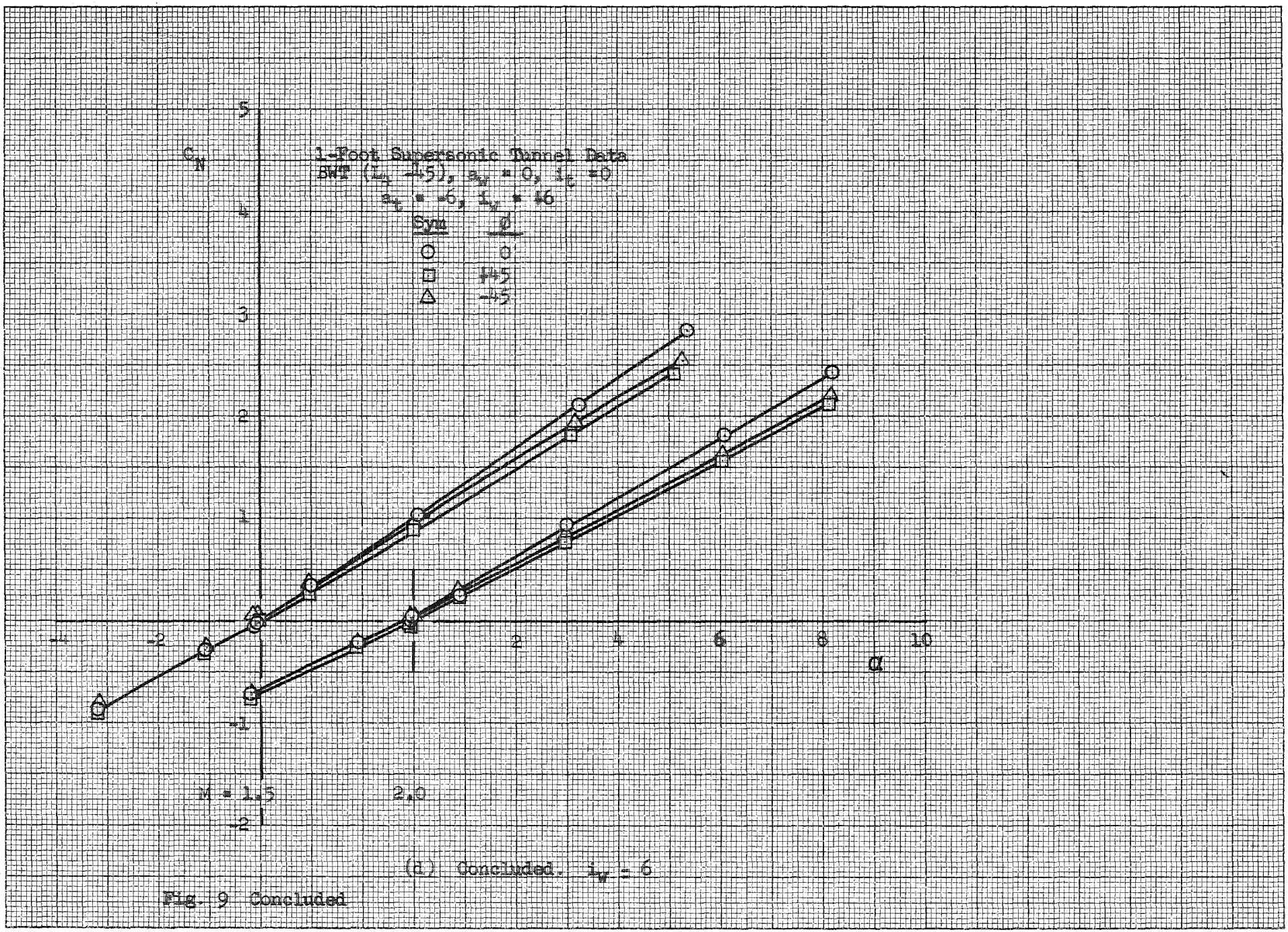

(d) Concluded. i_w = 6

Fig. 9 Concluded

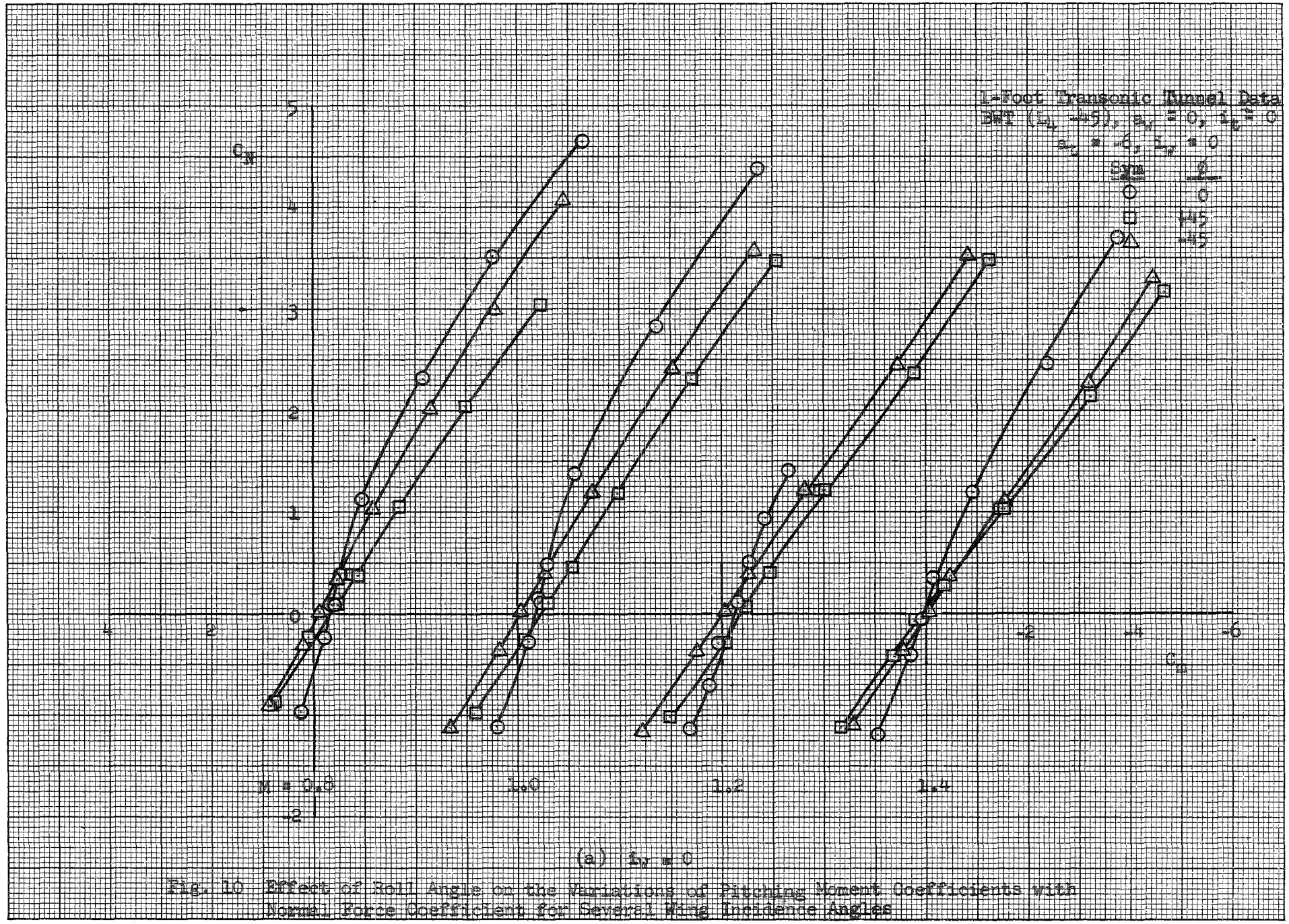

Fig. 10 Effect of Roll Angle on the Variations of Pitching Moment Coefficients with Normal Force Coefficient for Several Wing Incidence Angles

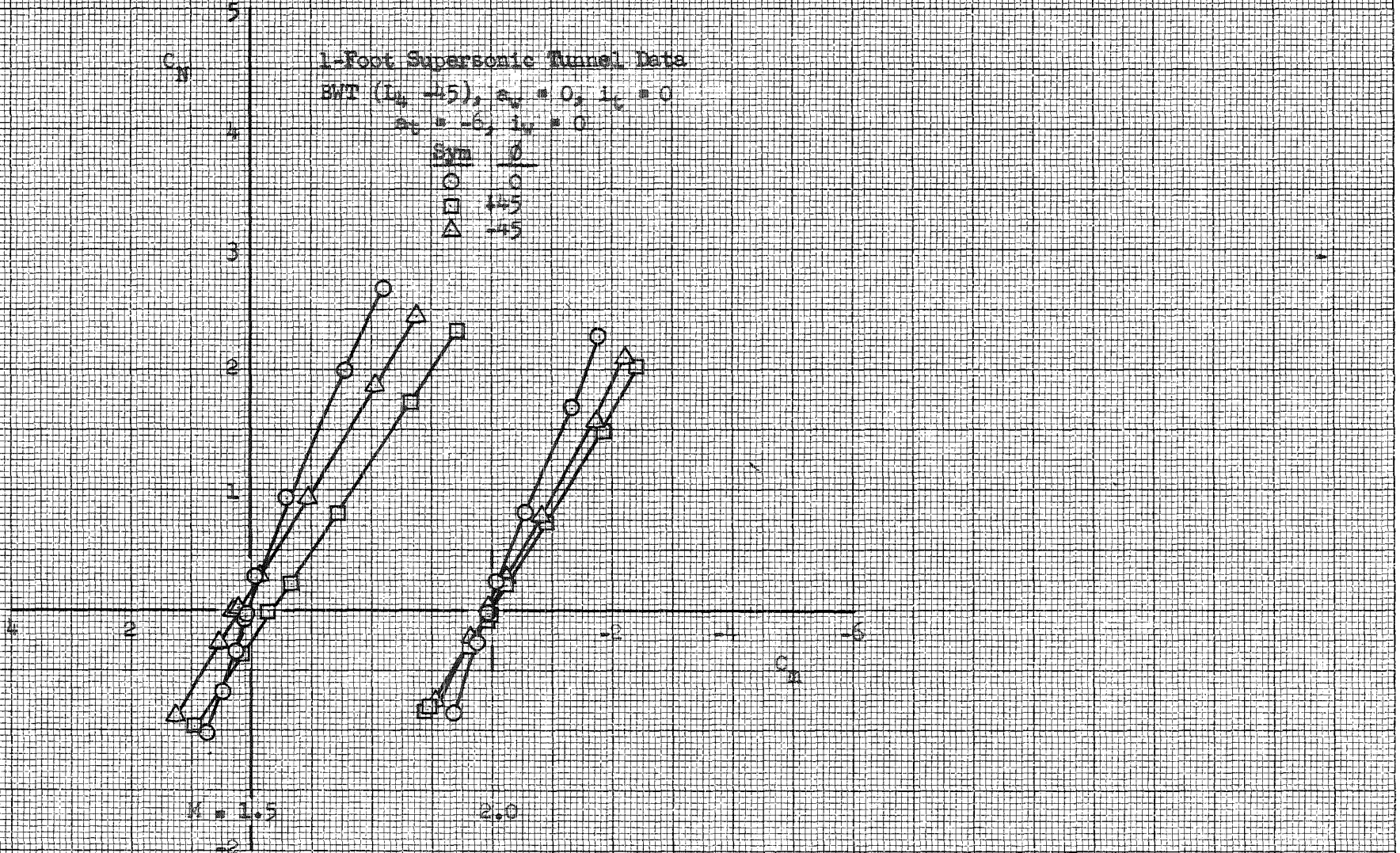

(a) Concluded. i_w = 0

Fig. 10 Continued.

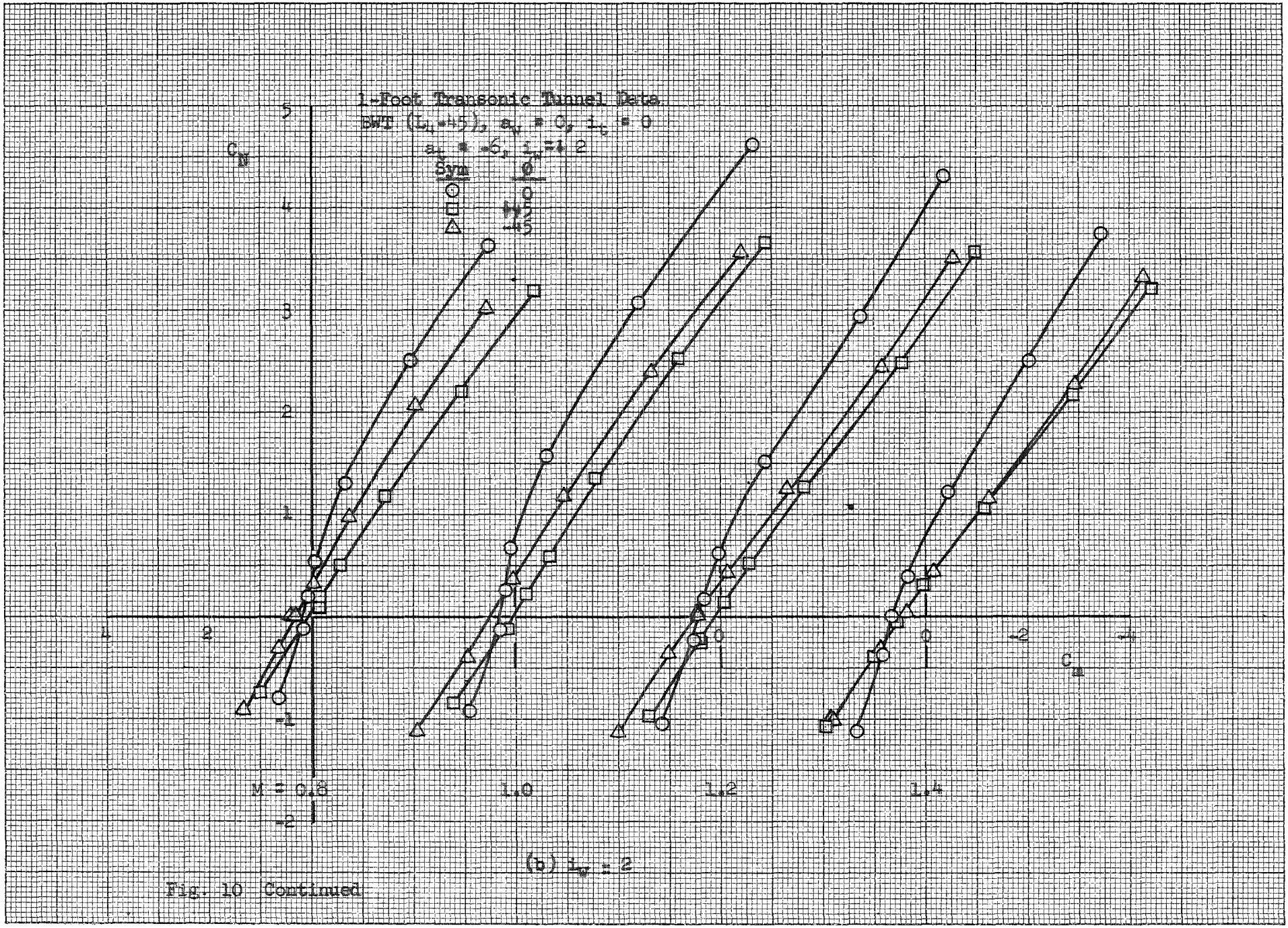

(b) i_w = 2

Fig. 10 Continued

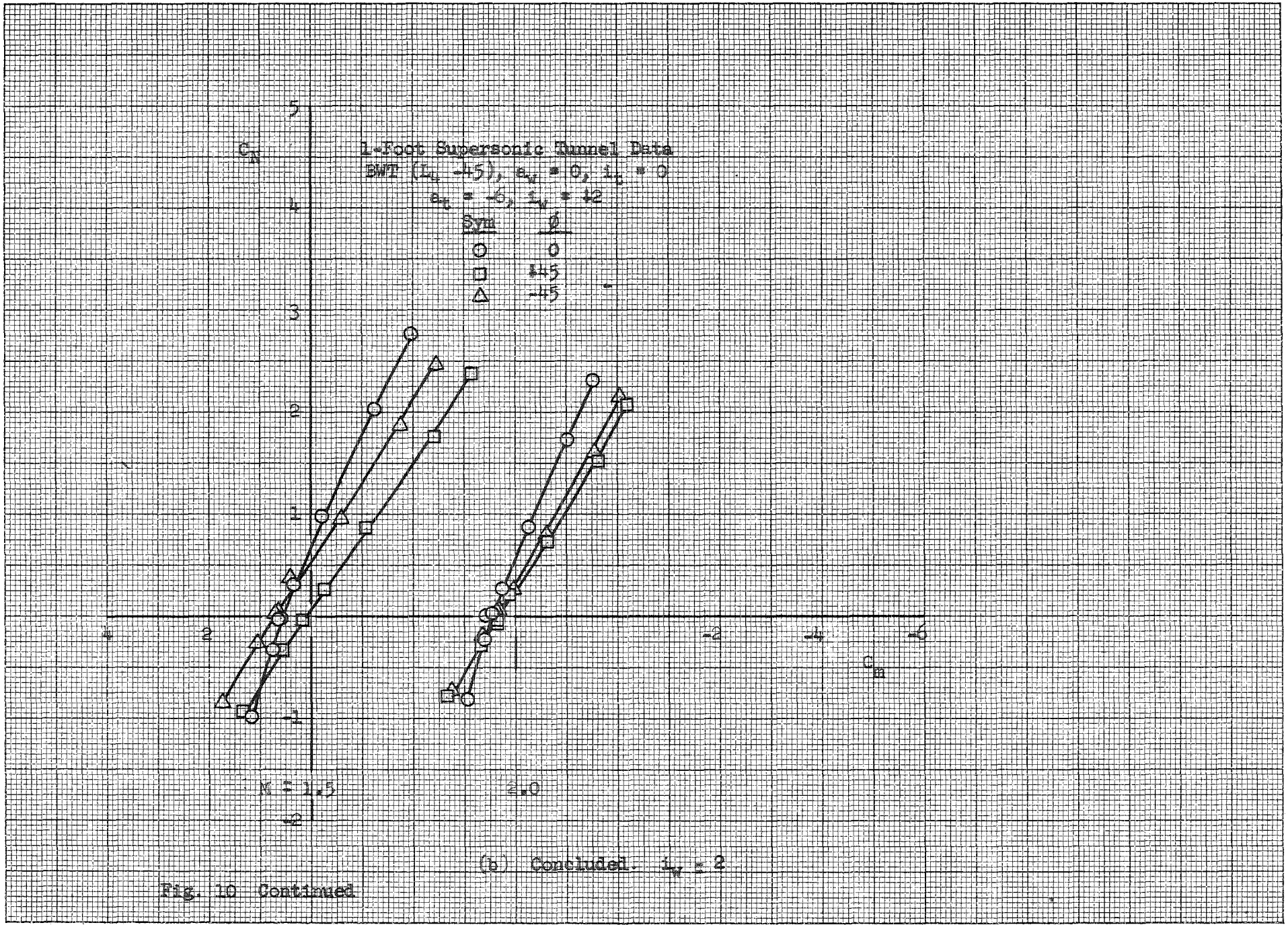

(b) Concluded. i_w = 2

Fig. 10 Continued

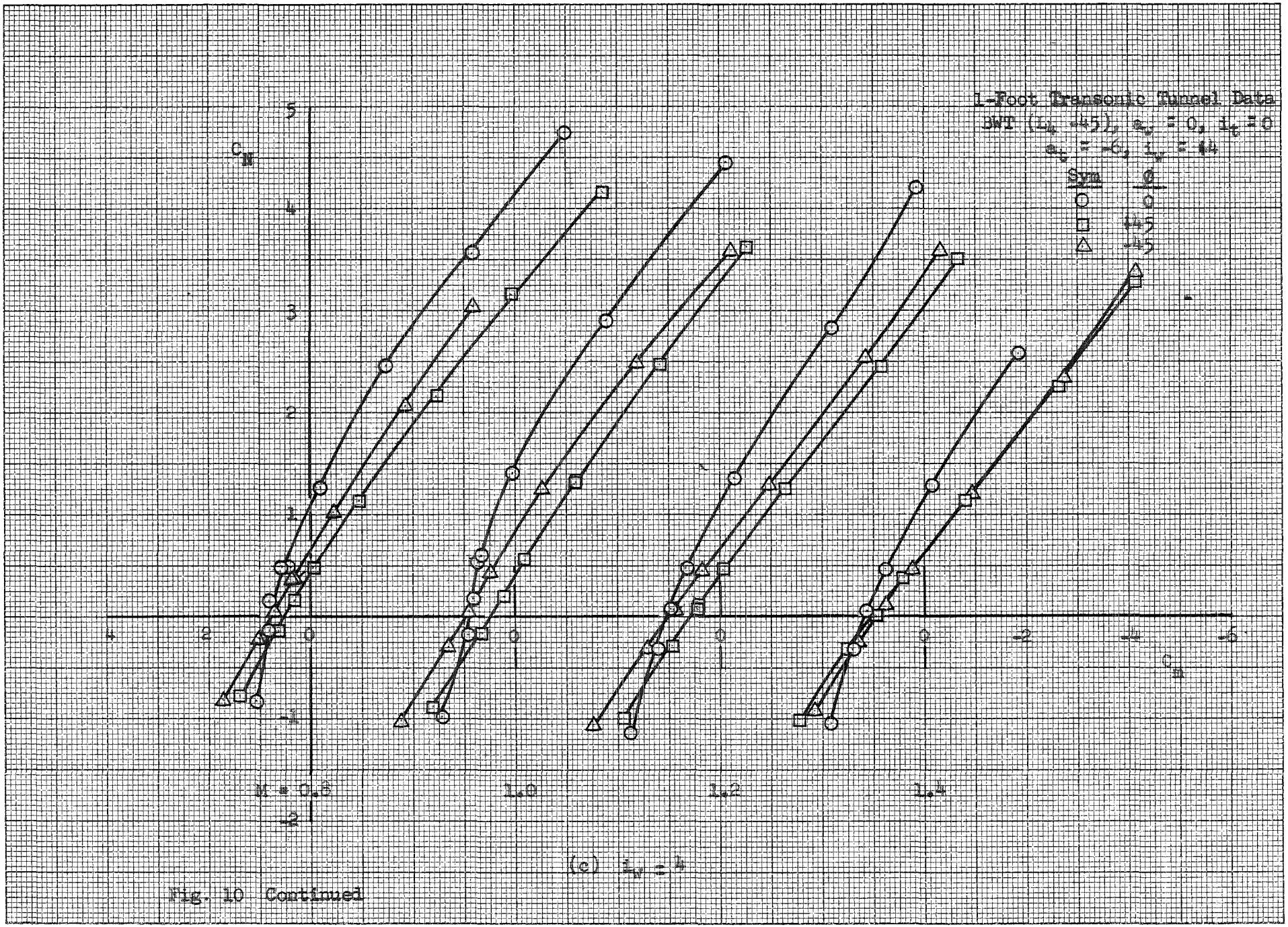

(c) i_w = 4

Fig. 10 Continued

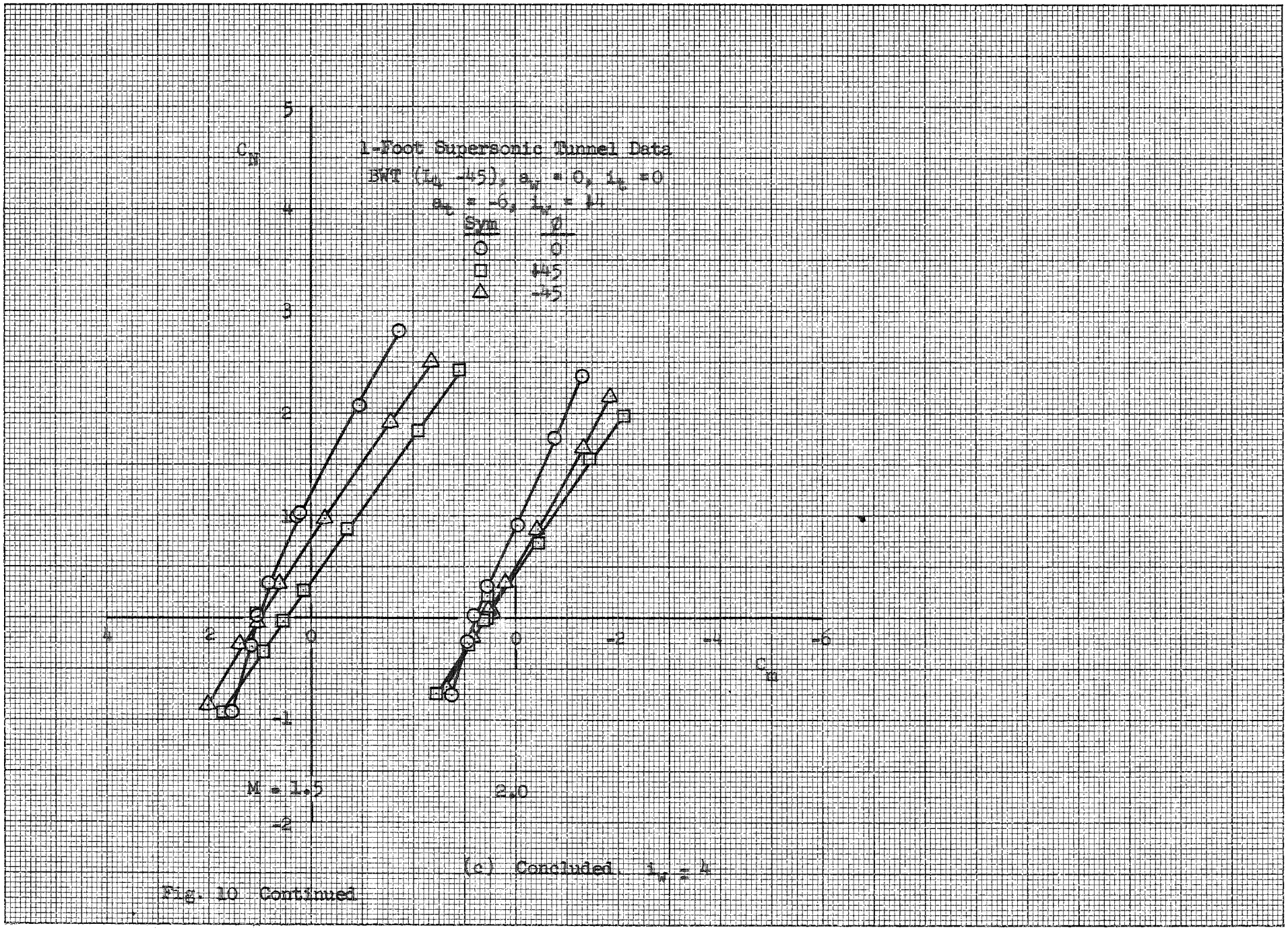

(c) Concluded i_w = 4

Fig. 10 Continued

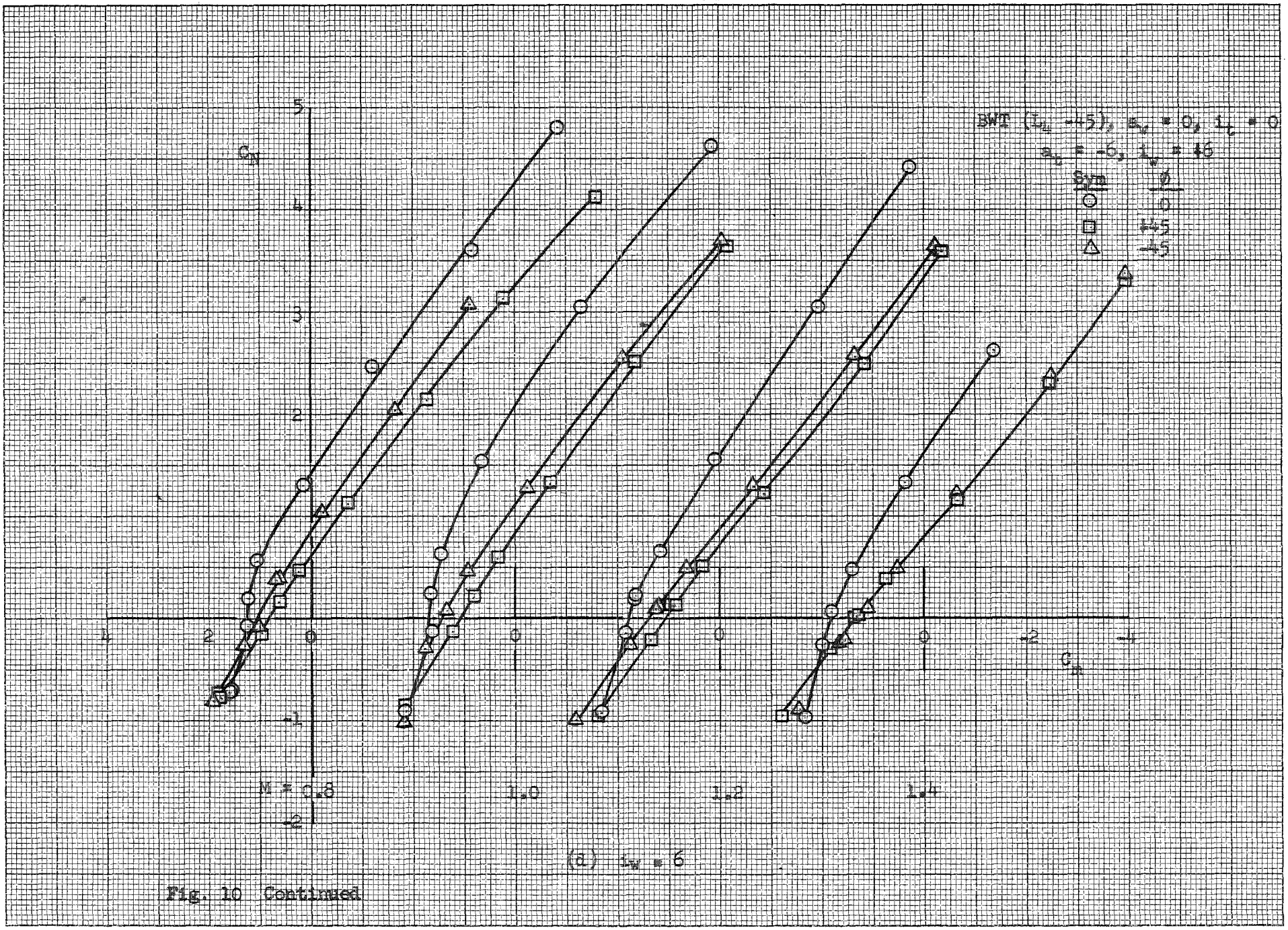

Fig. 10 Continued

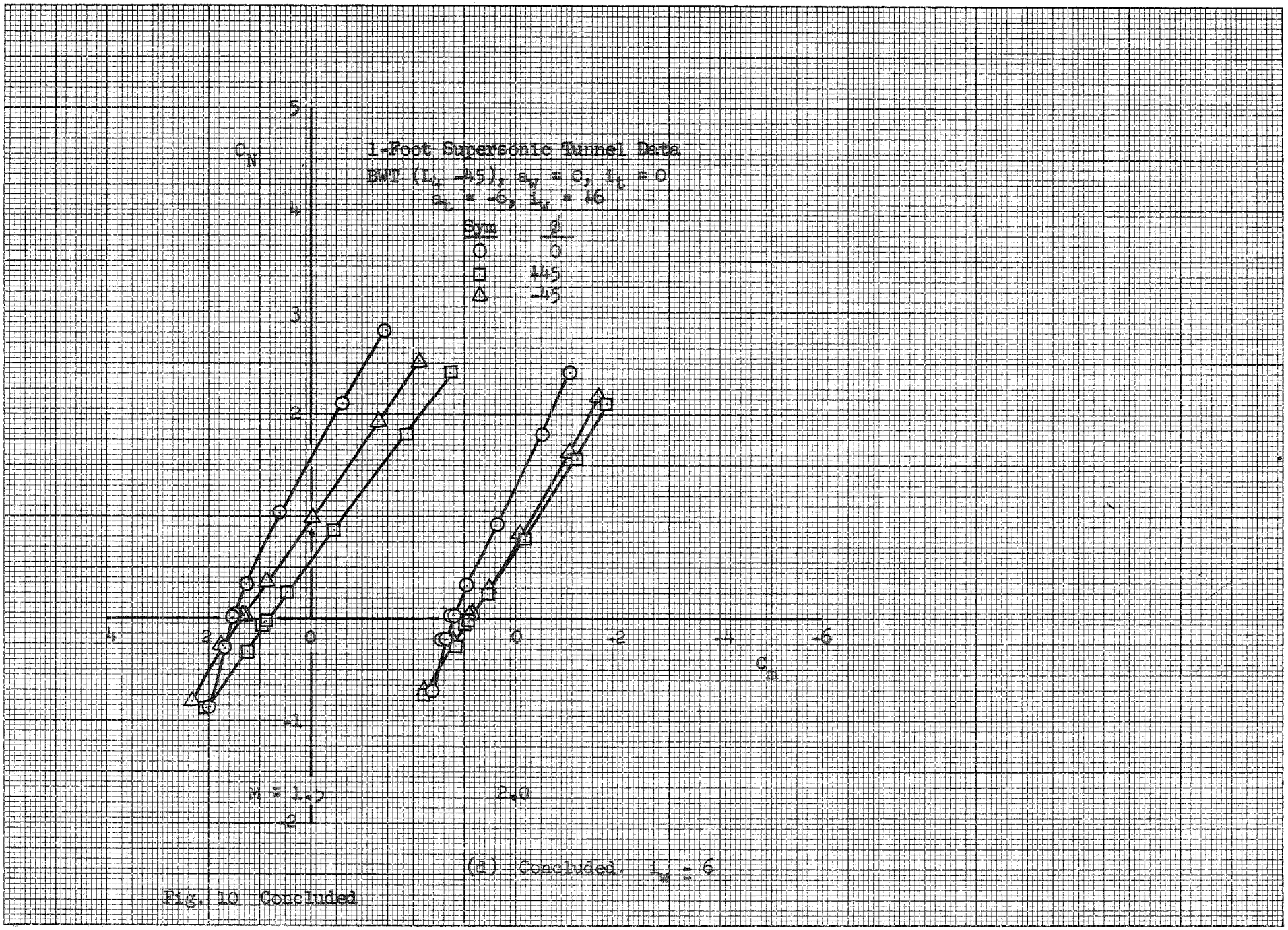

(d) Concluded. i_t = -6

Fig. 10 Concluded

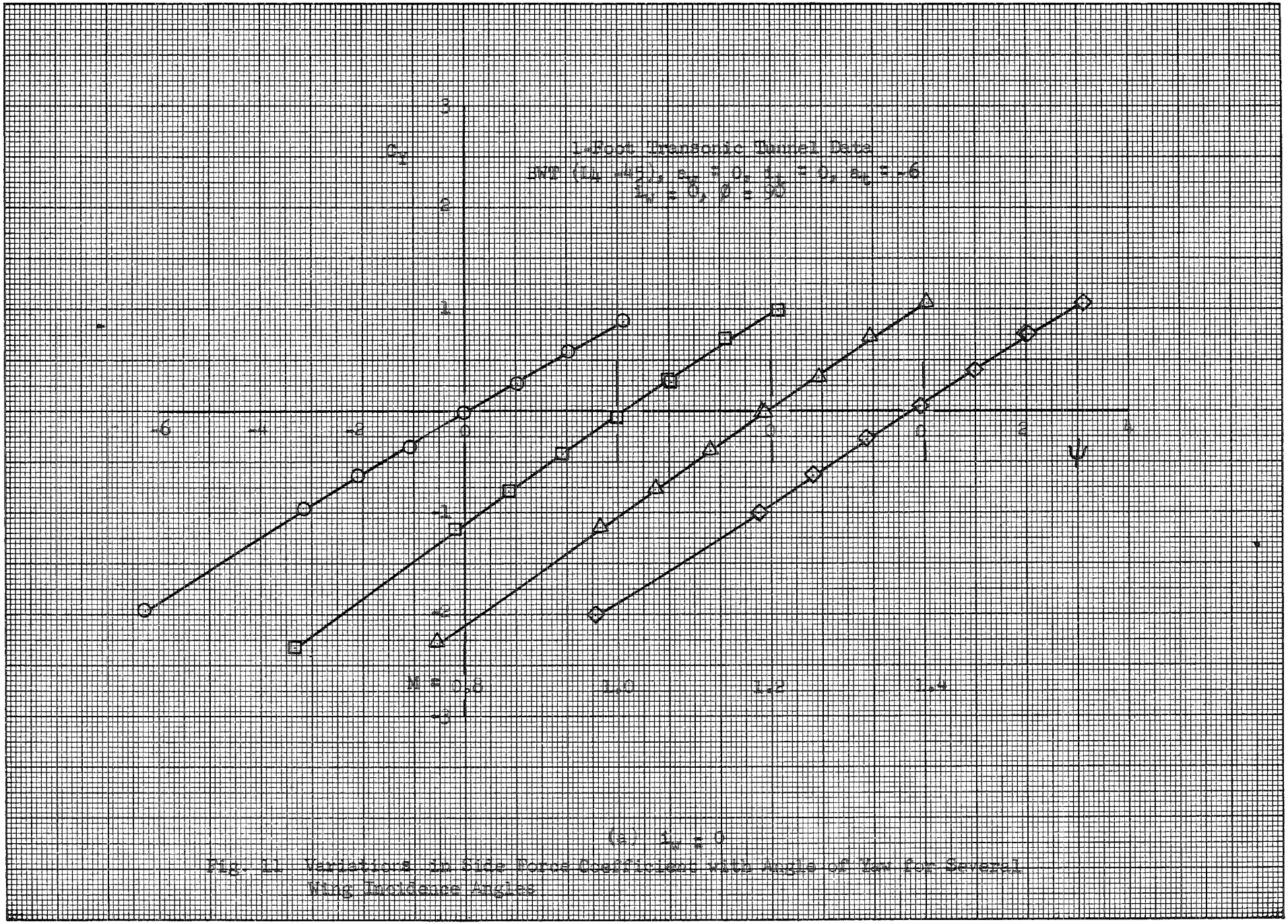

Fig. 11 Variations in Side Force Coefficient with Angle of Yaw for Several Wing Incidence Angles

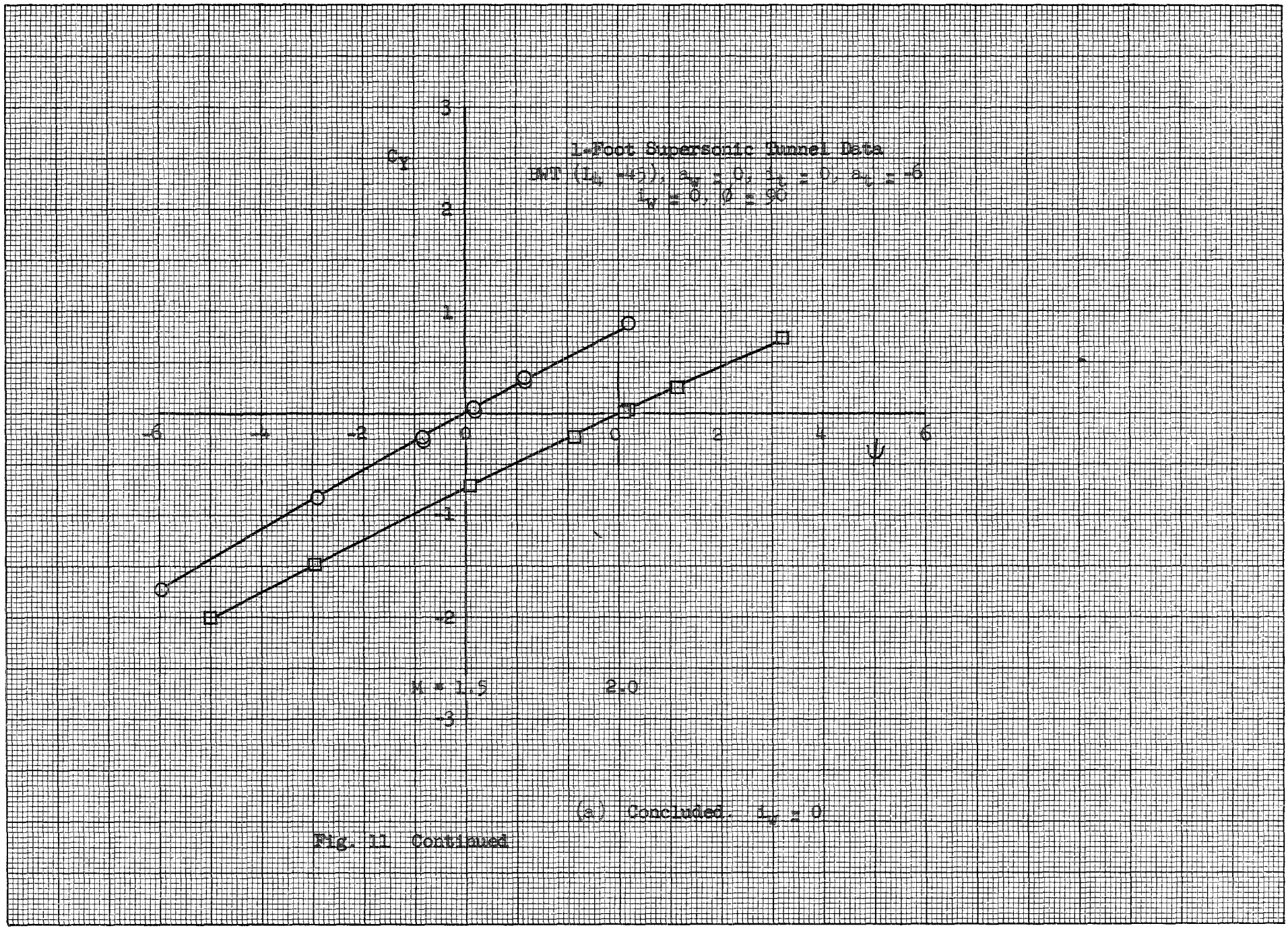

(a) Concluded. $i_w = 0$

Fig. 11 Continued

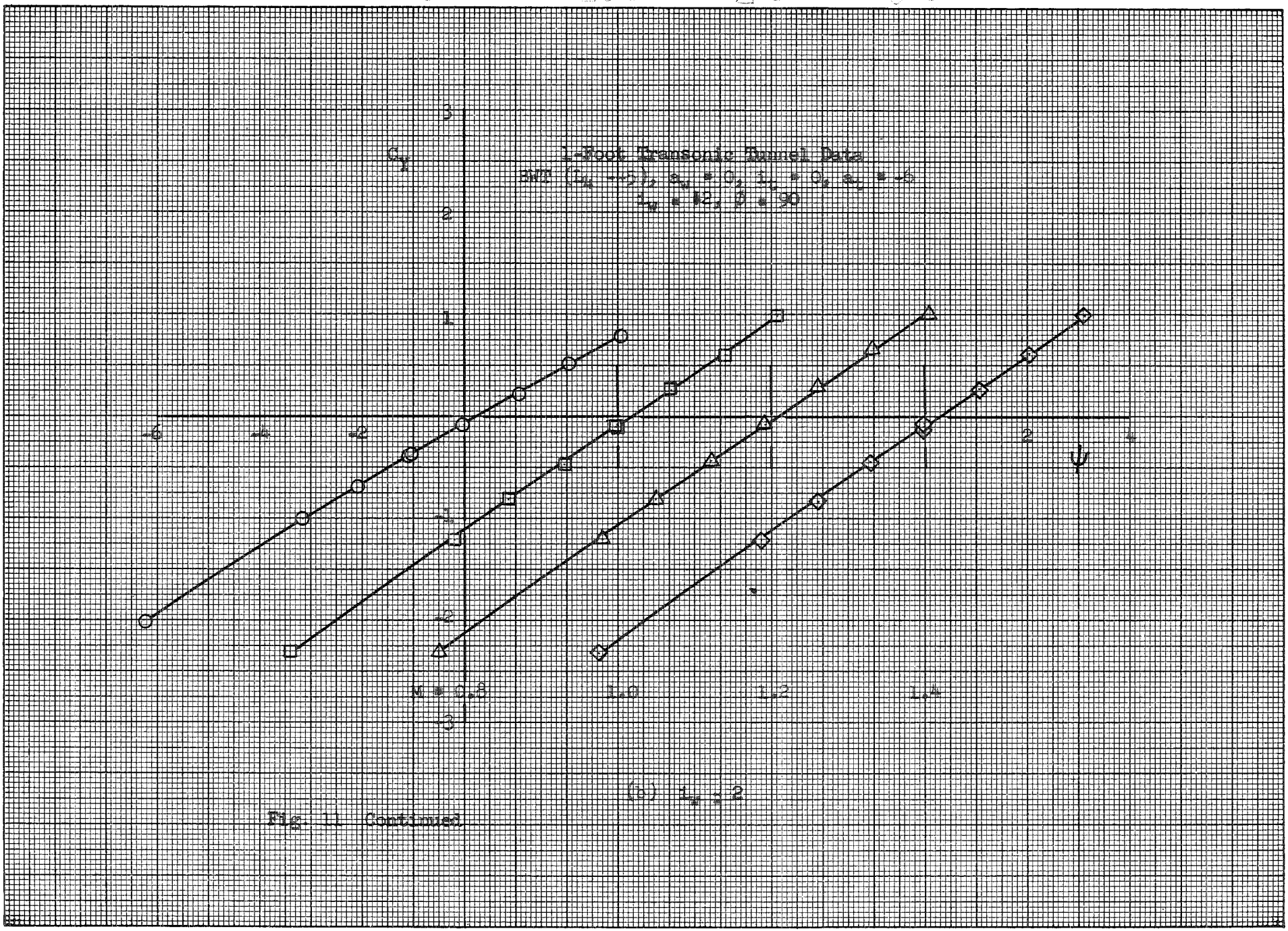

(b) $i_w = 2$

Fig. 11 Continued.

C.33 □/0

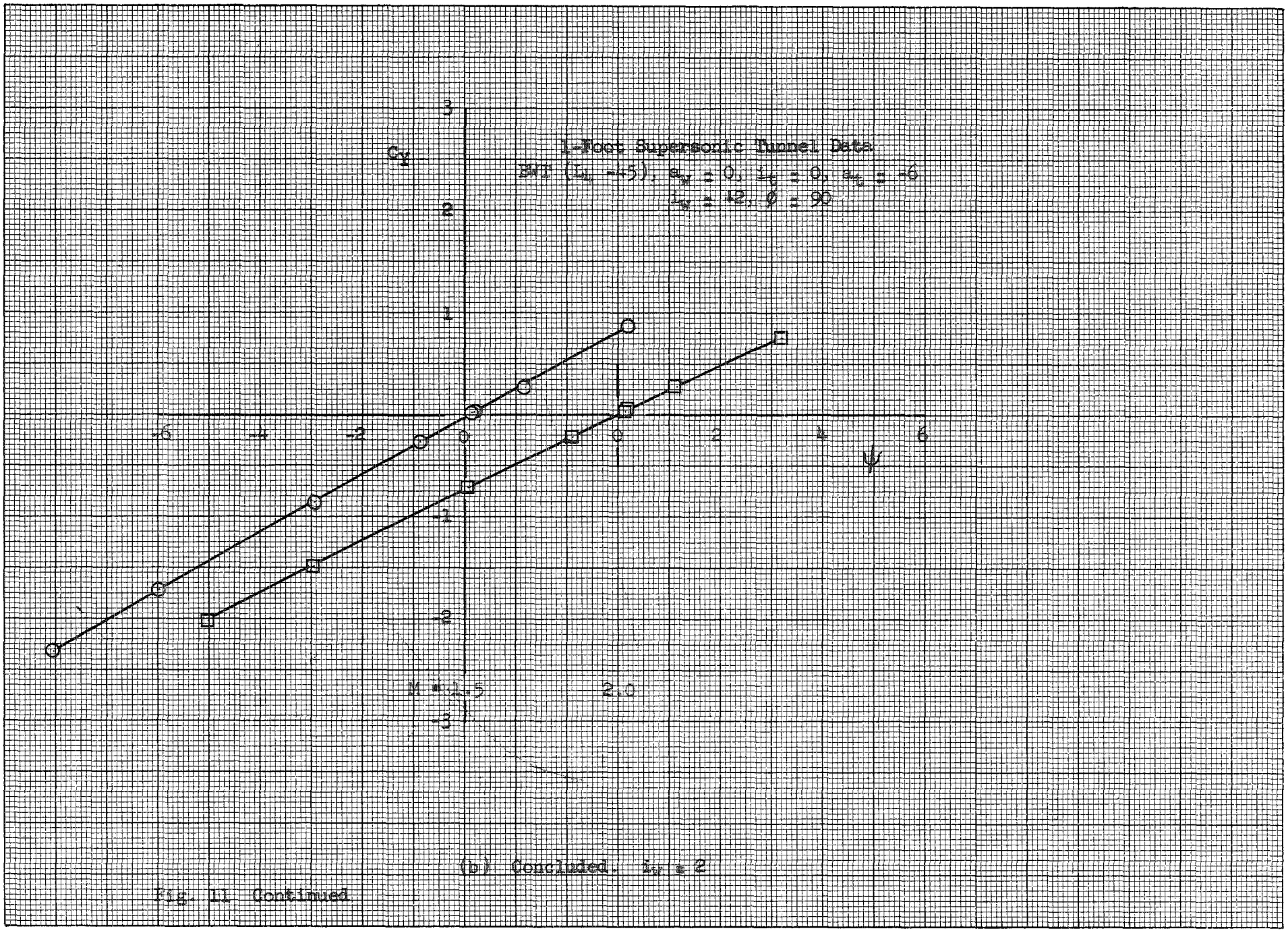

(b) Concluded. i_t = 2

Fig. 11 Continued.

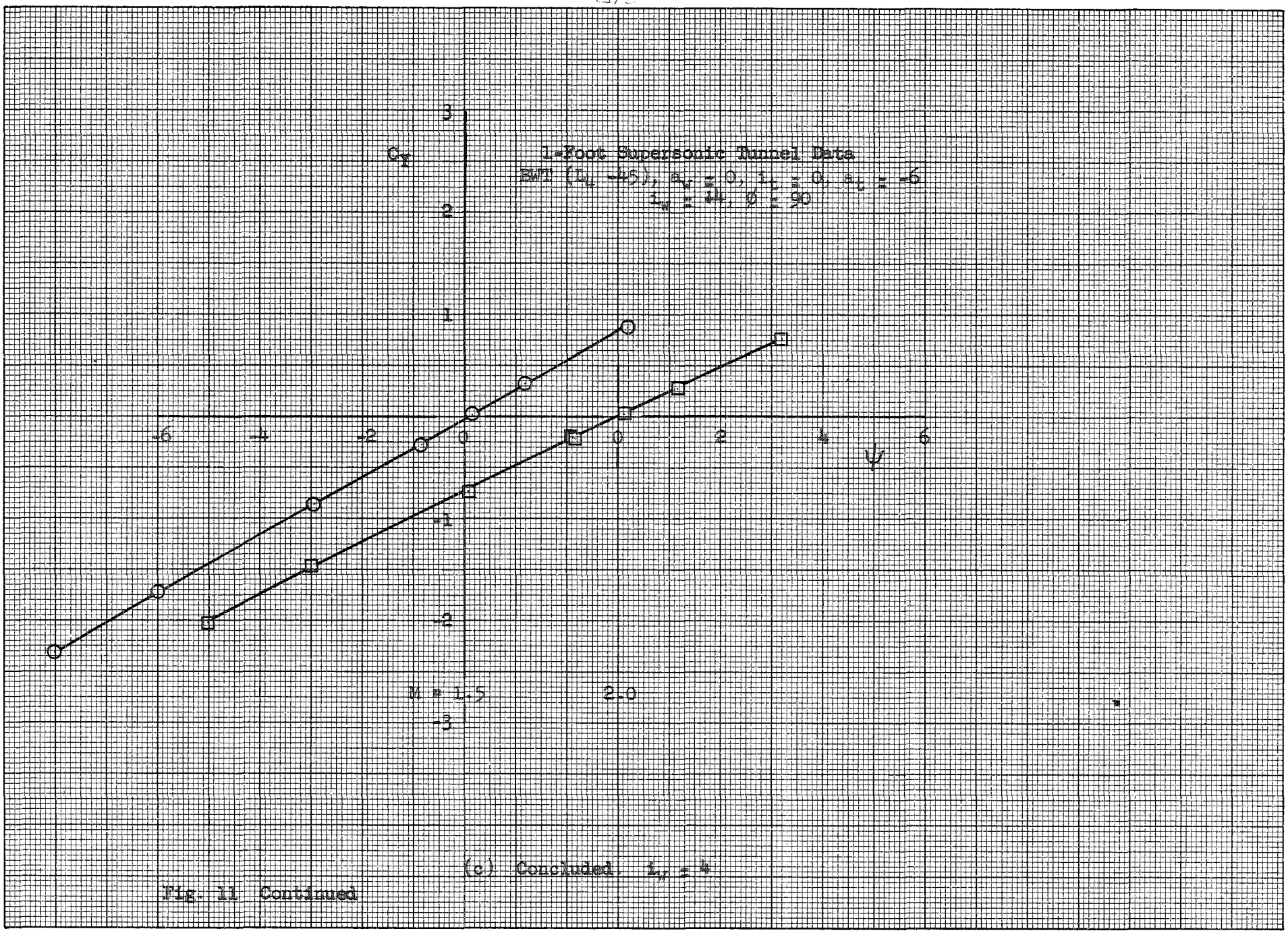

(c) Concluded. $i_w = 4$

Fig. 11 Continued

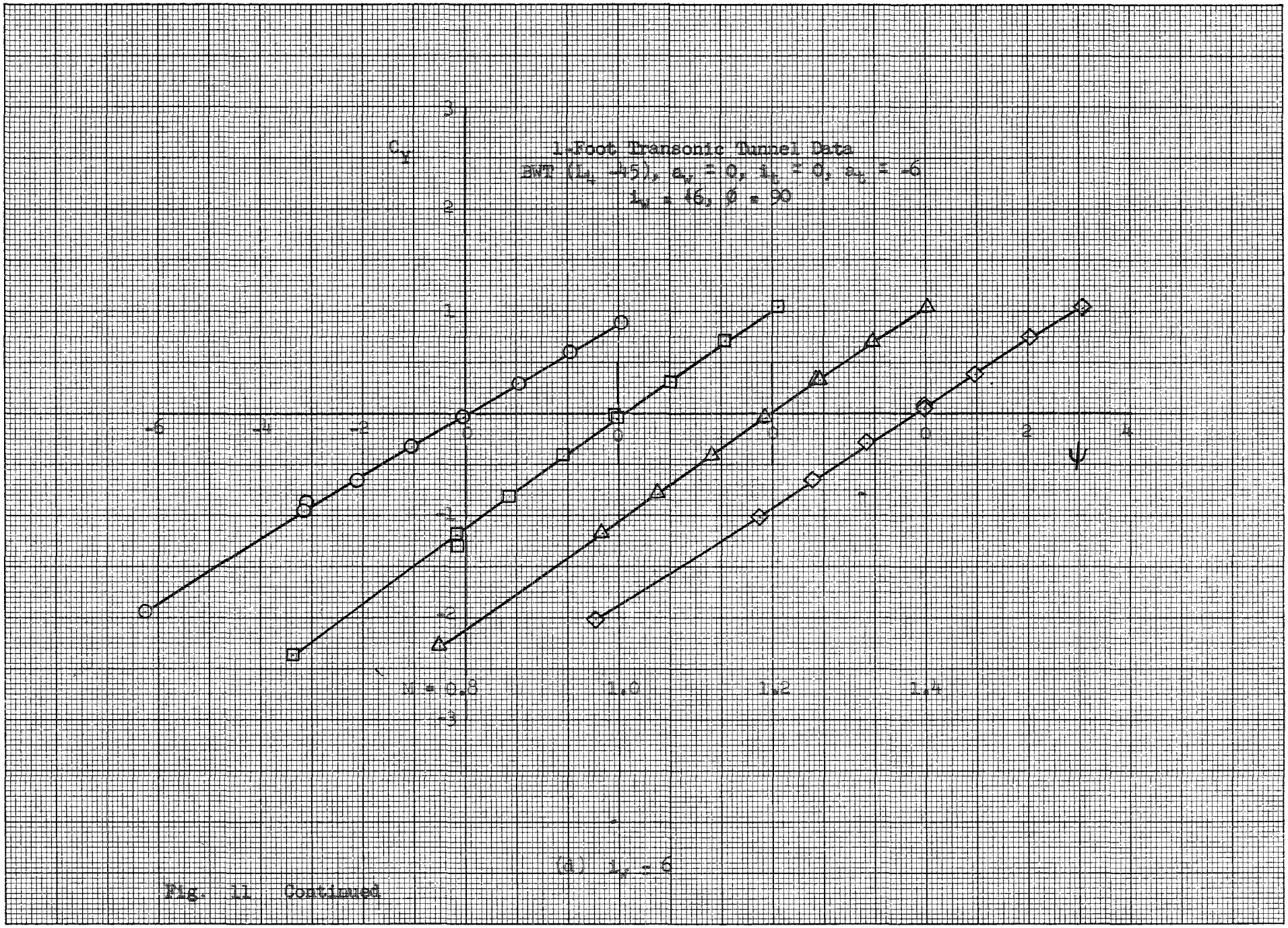

Fig. 11 Continued.

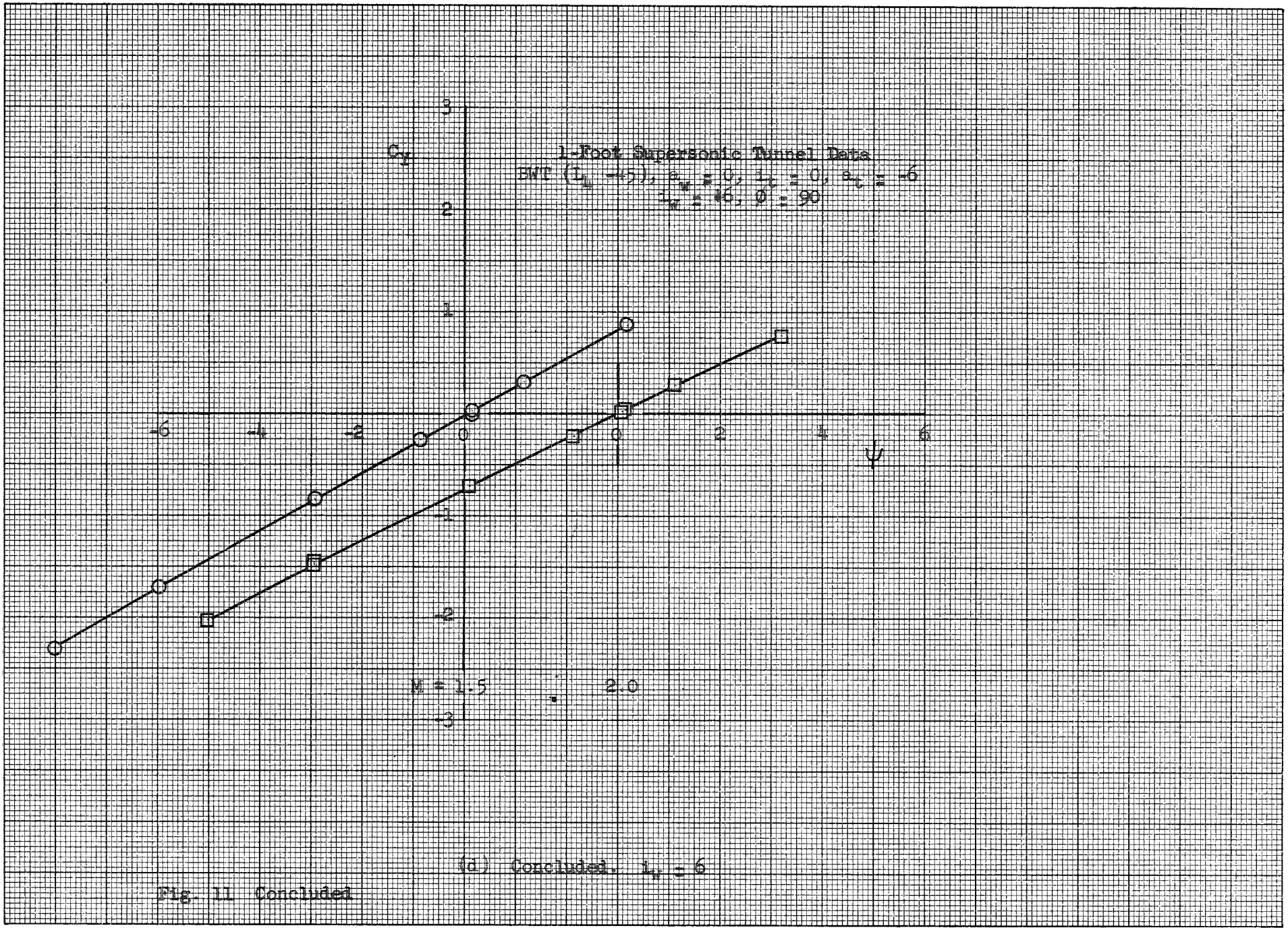

(d) Concluded. L_w = 6

Fig. 11 Concluded

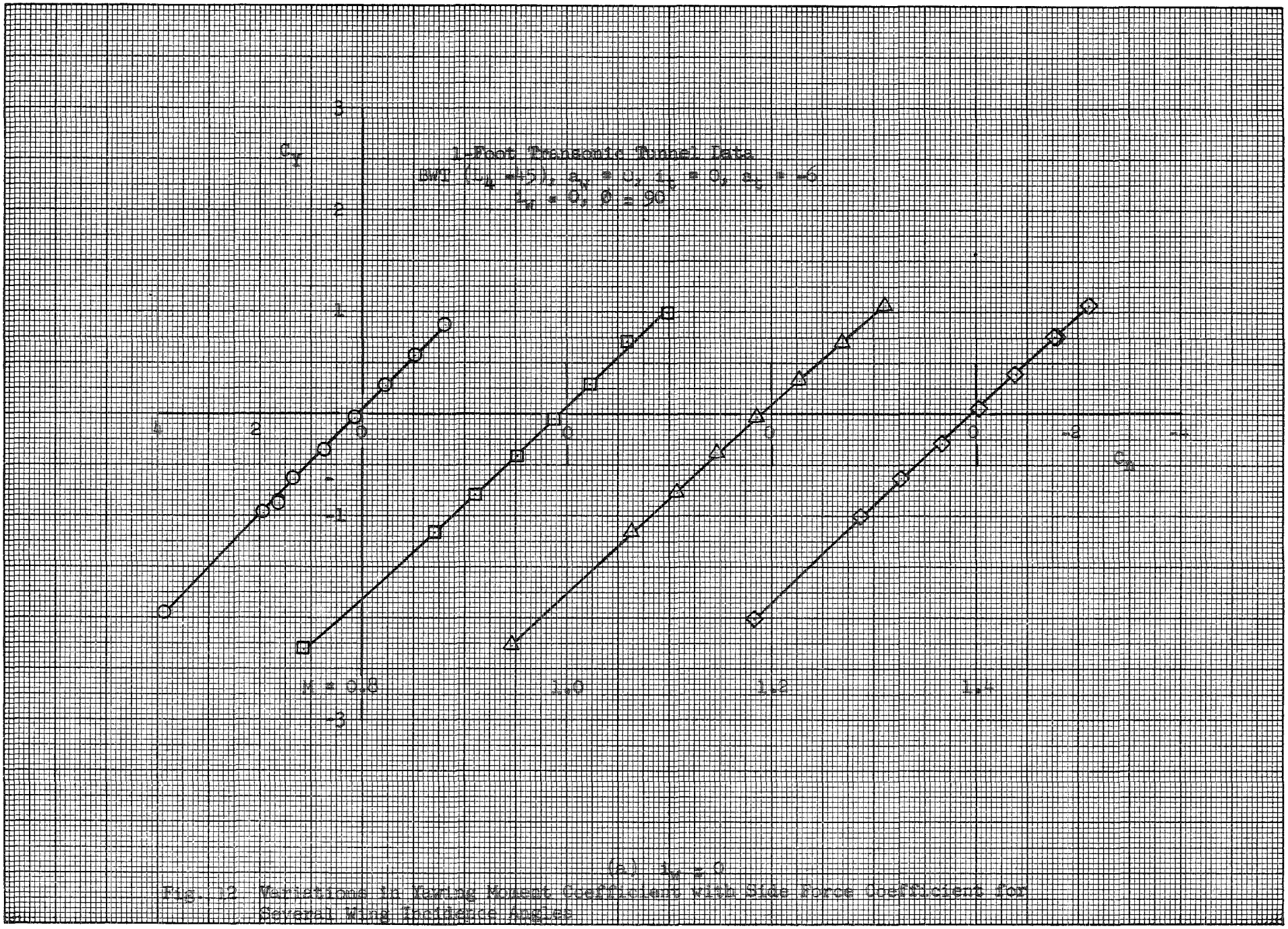

Fig. 12 Variations in Yawing Moment Coefficients with Side Force Coefficient for Several Wing Incidence Angles

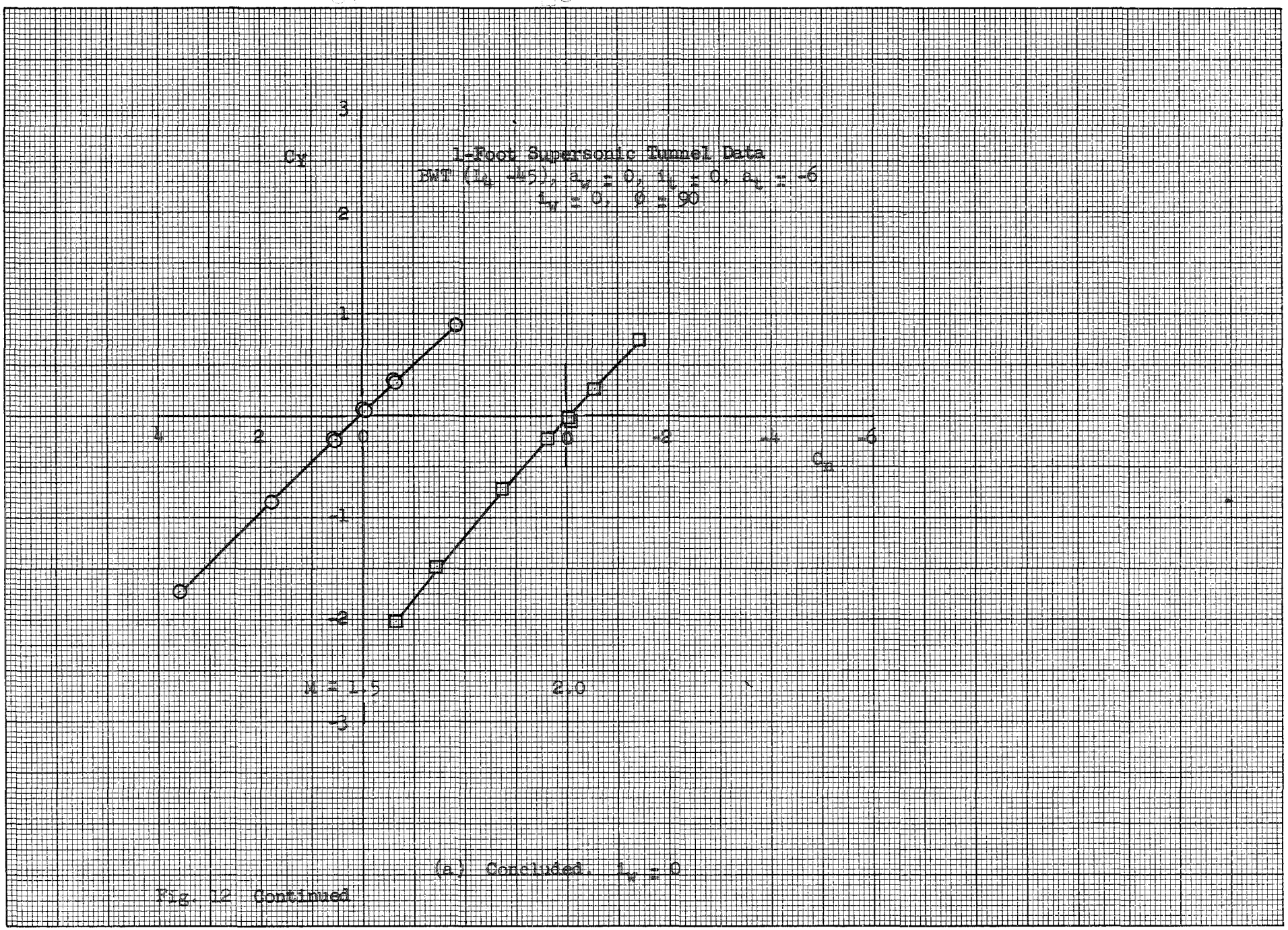

(a) Concluded. i_w = 0

Fig. 12 Continued

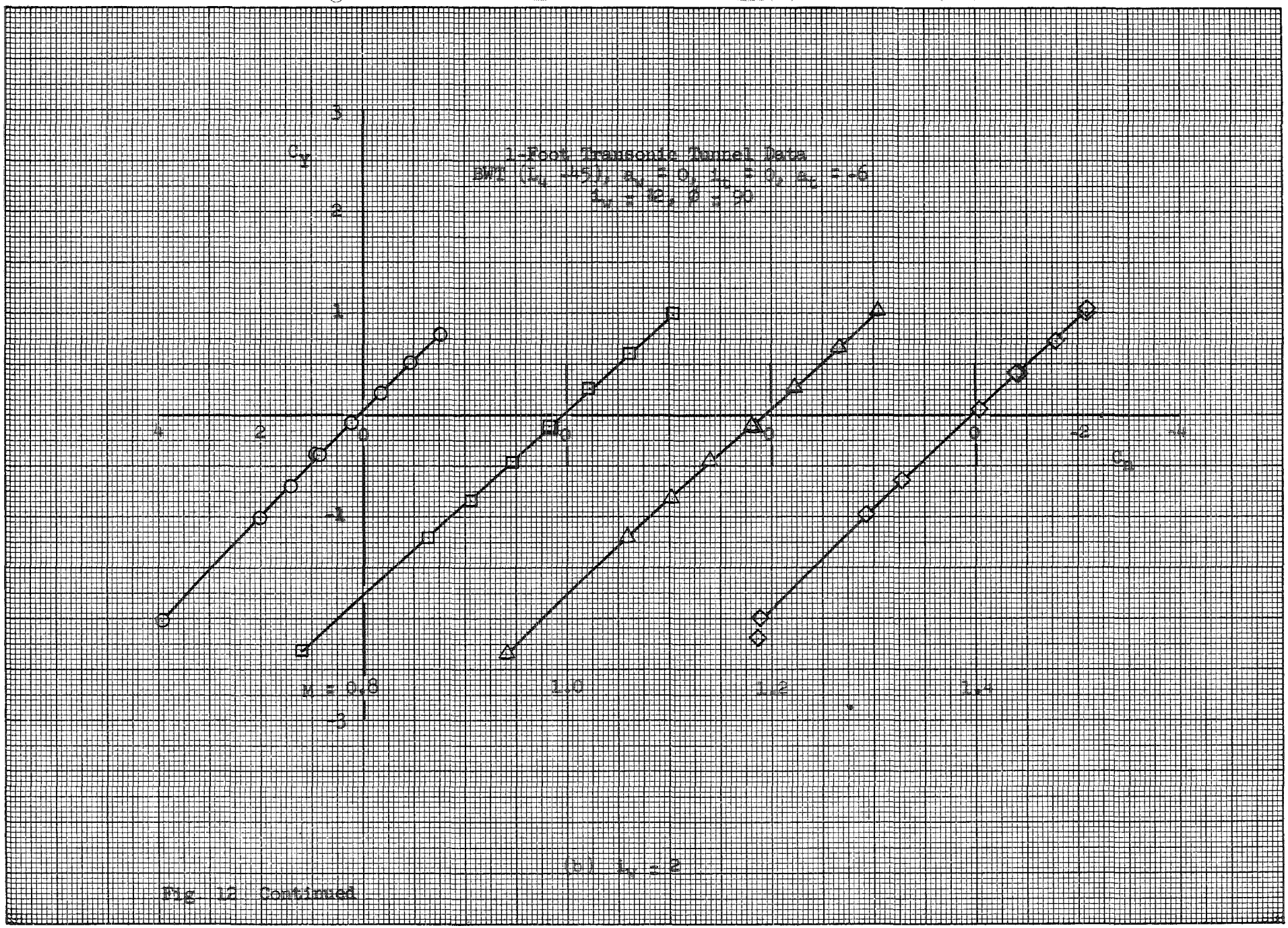

Fig. 12 Continued

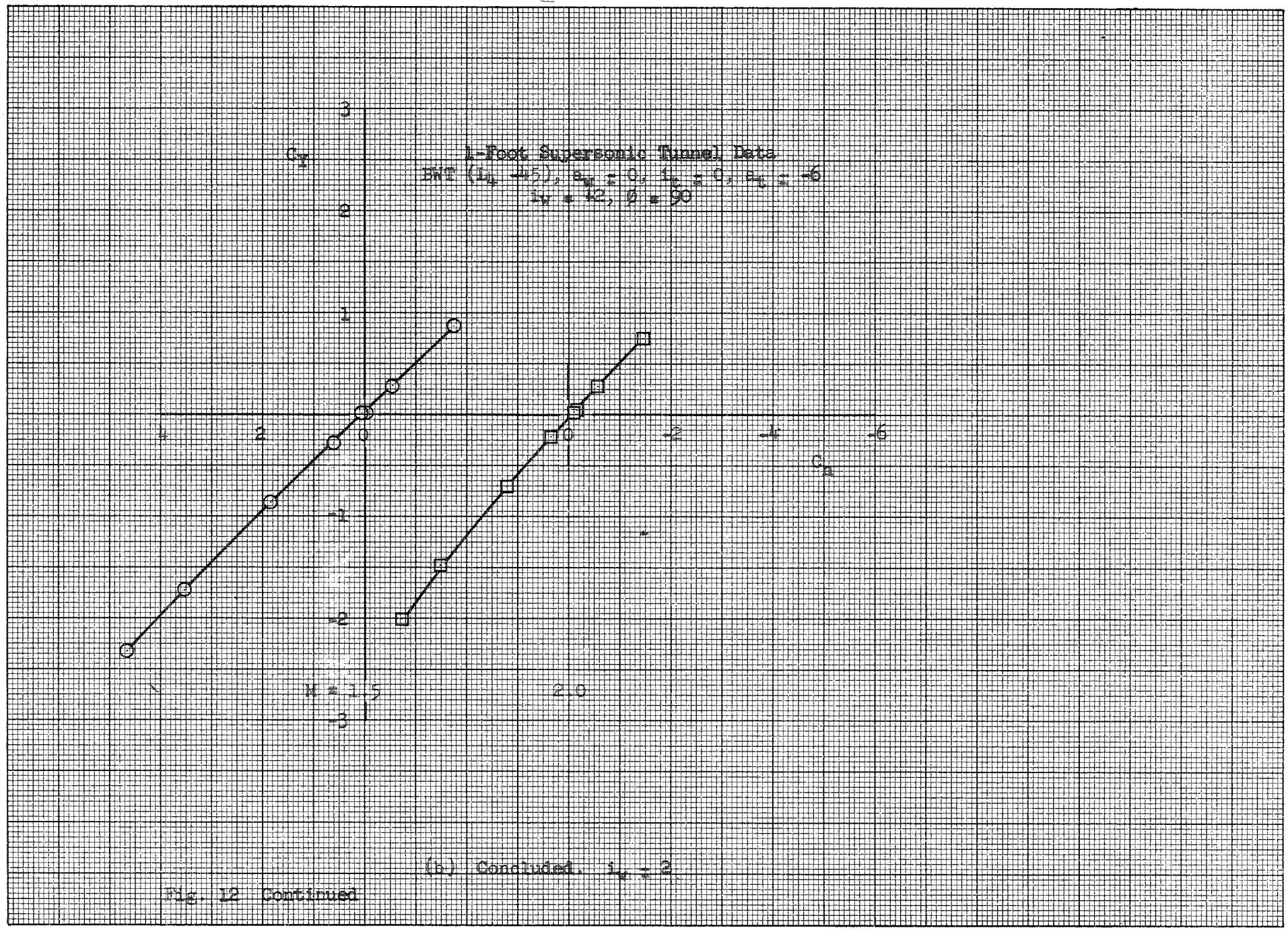

(b) Concluded. i_v = 2

Fig. 12 Continued

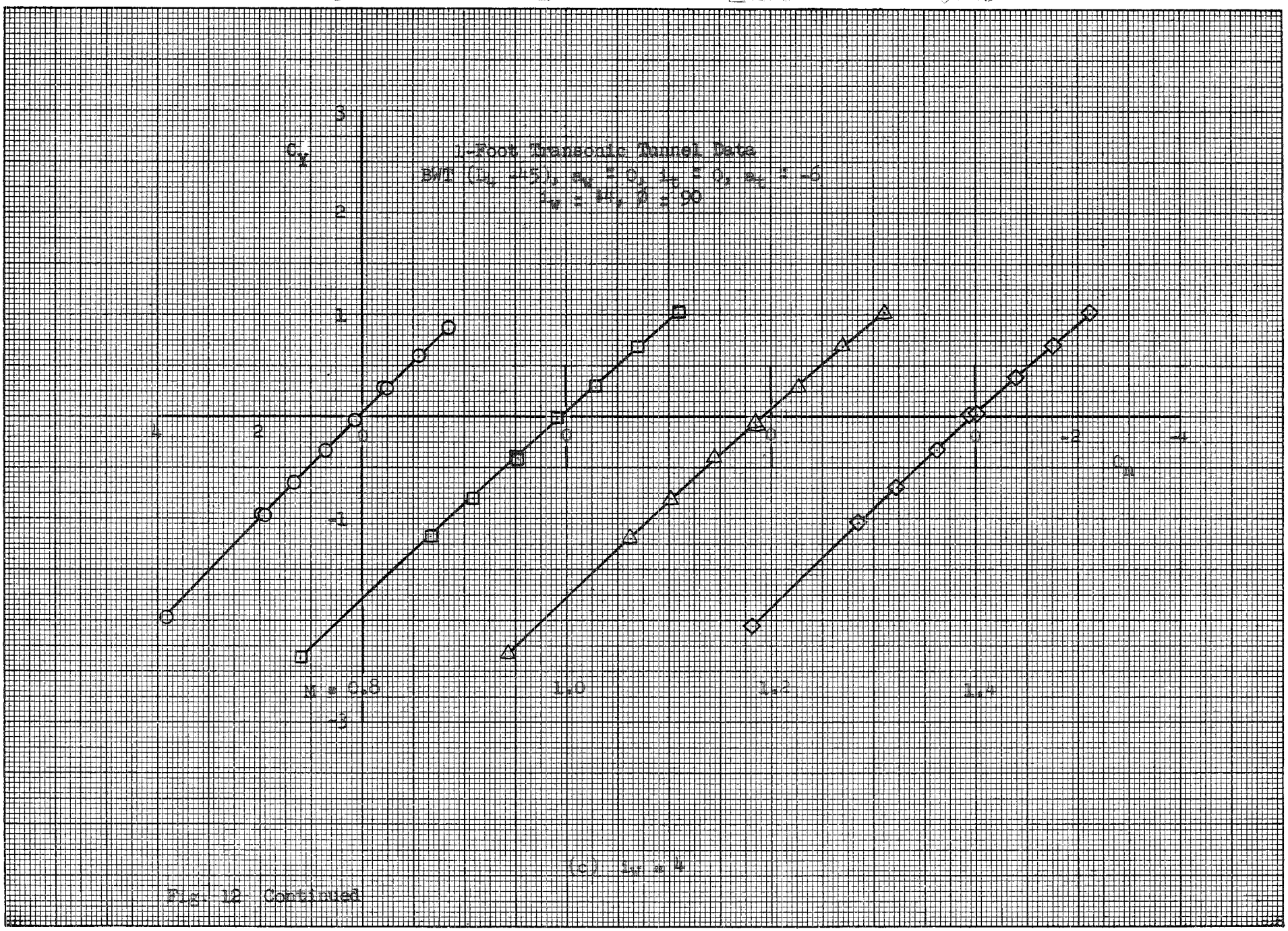

Fig. 12 Continued

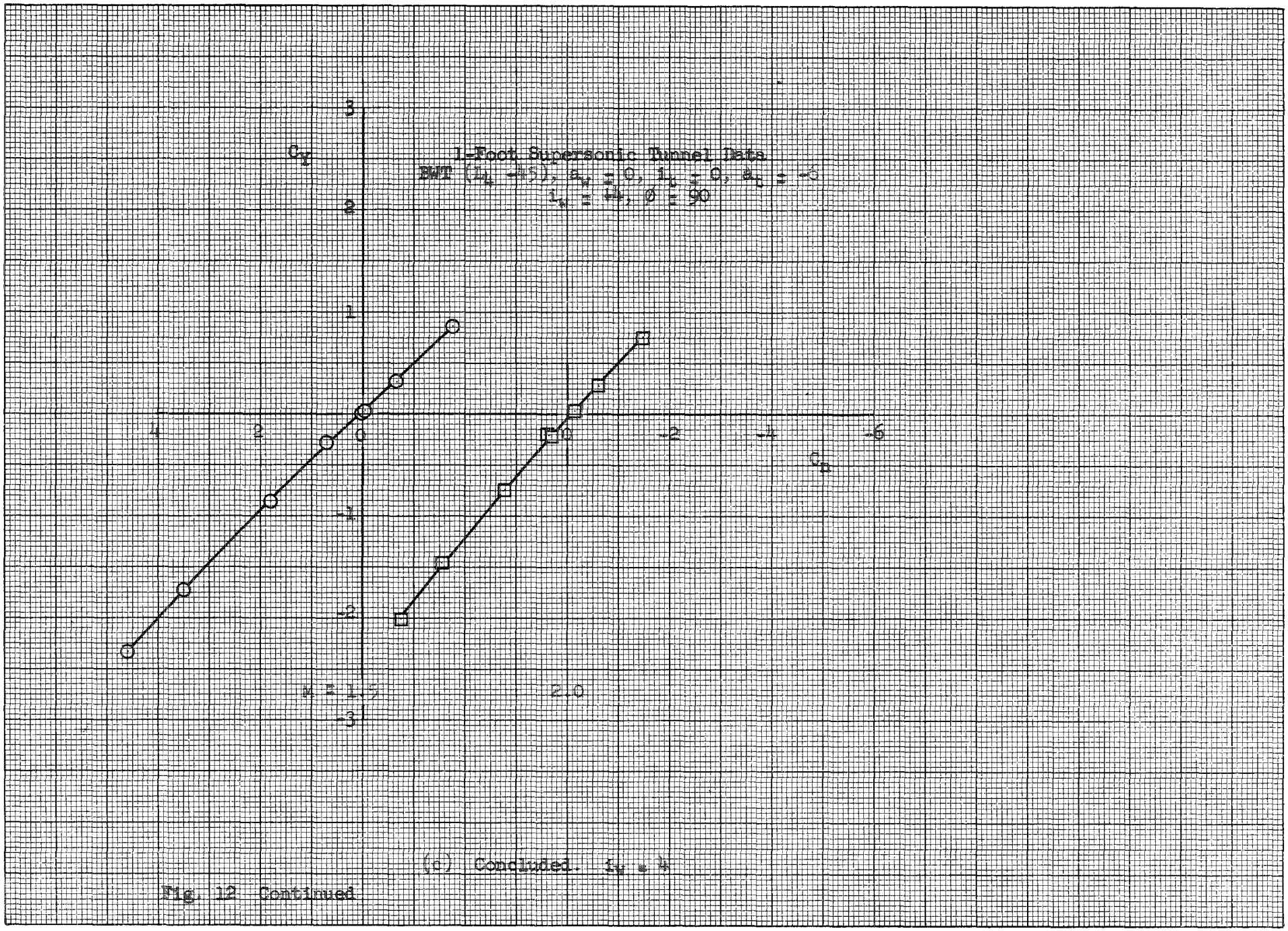

(c) Concluded. i_w = +5

Fig. 12 Continued

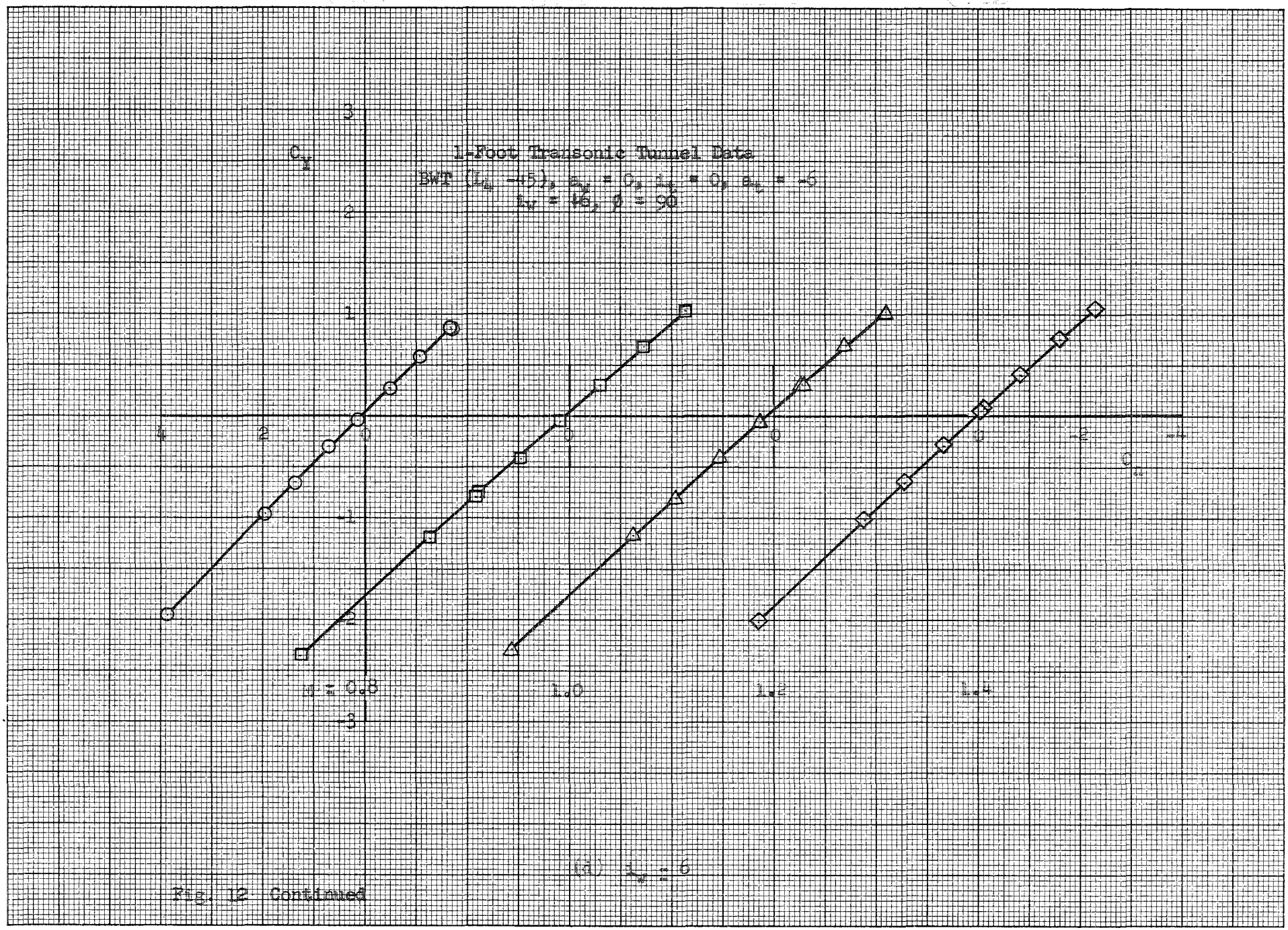

(a) i_w = 6

Fig. 12 Continued

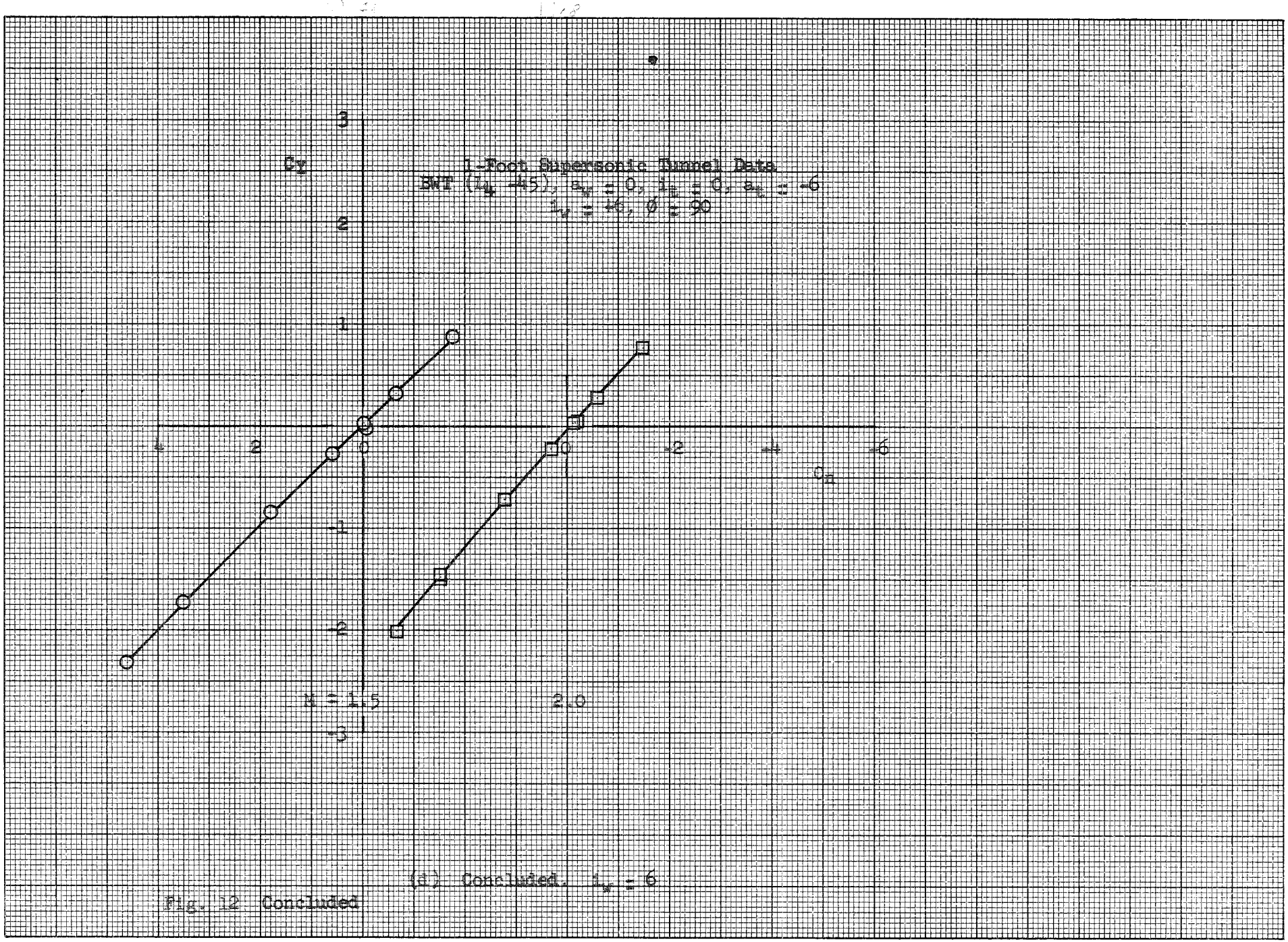

(d) Concluded. l_w = 6

Fig. 12 Concluded

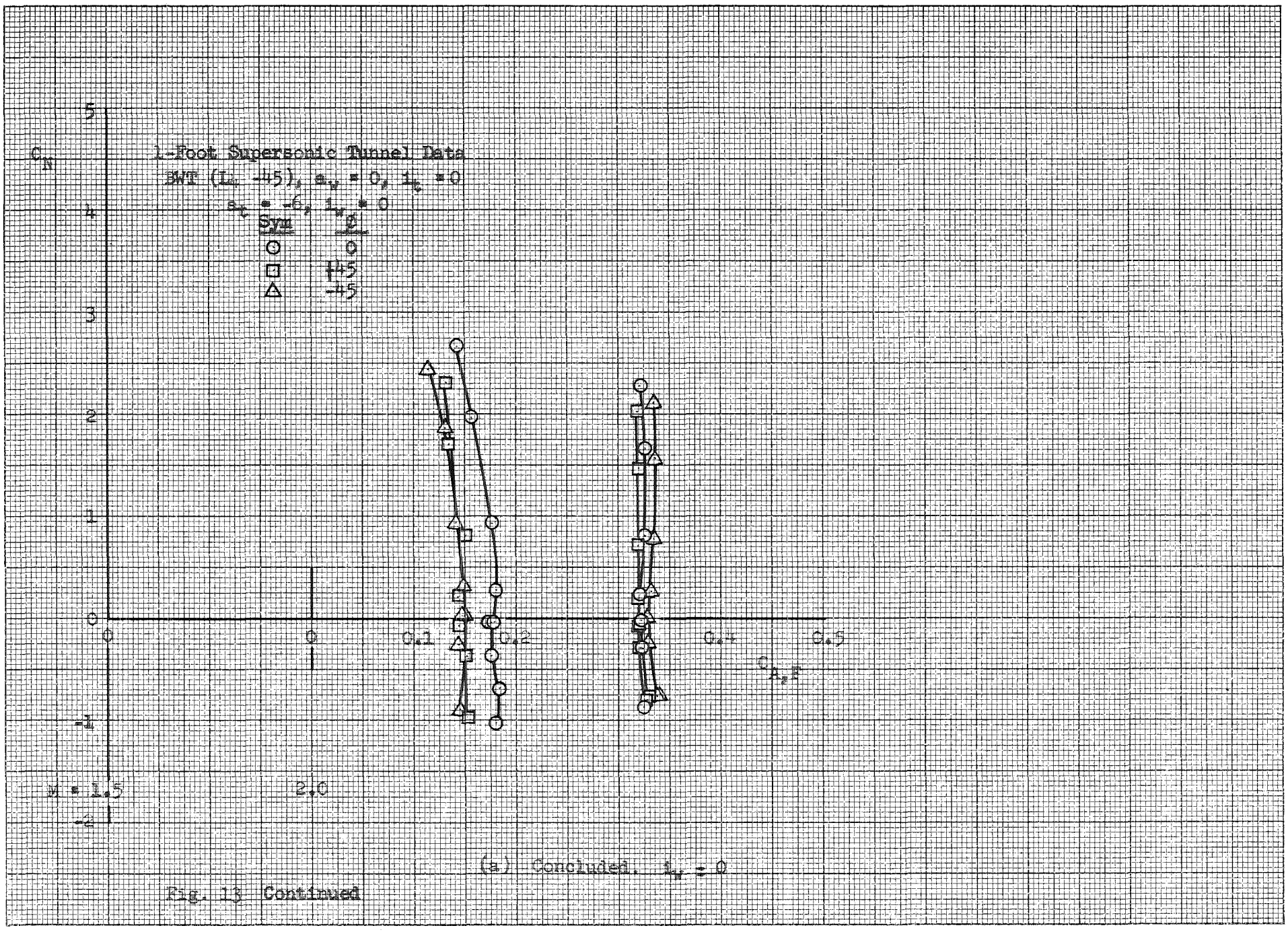

Fig. 13 Continued

(a) Concluded. i_w = 0

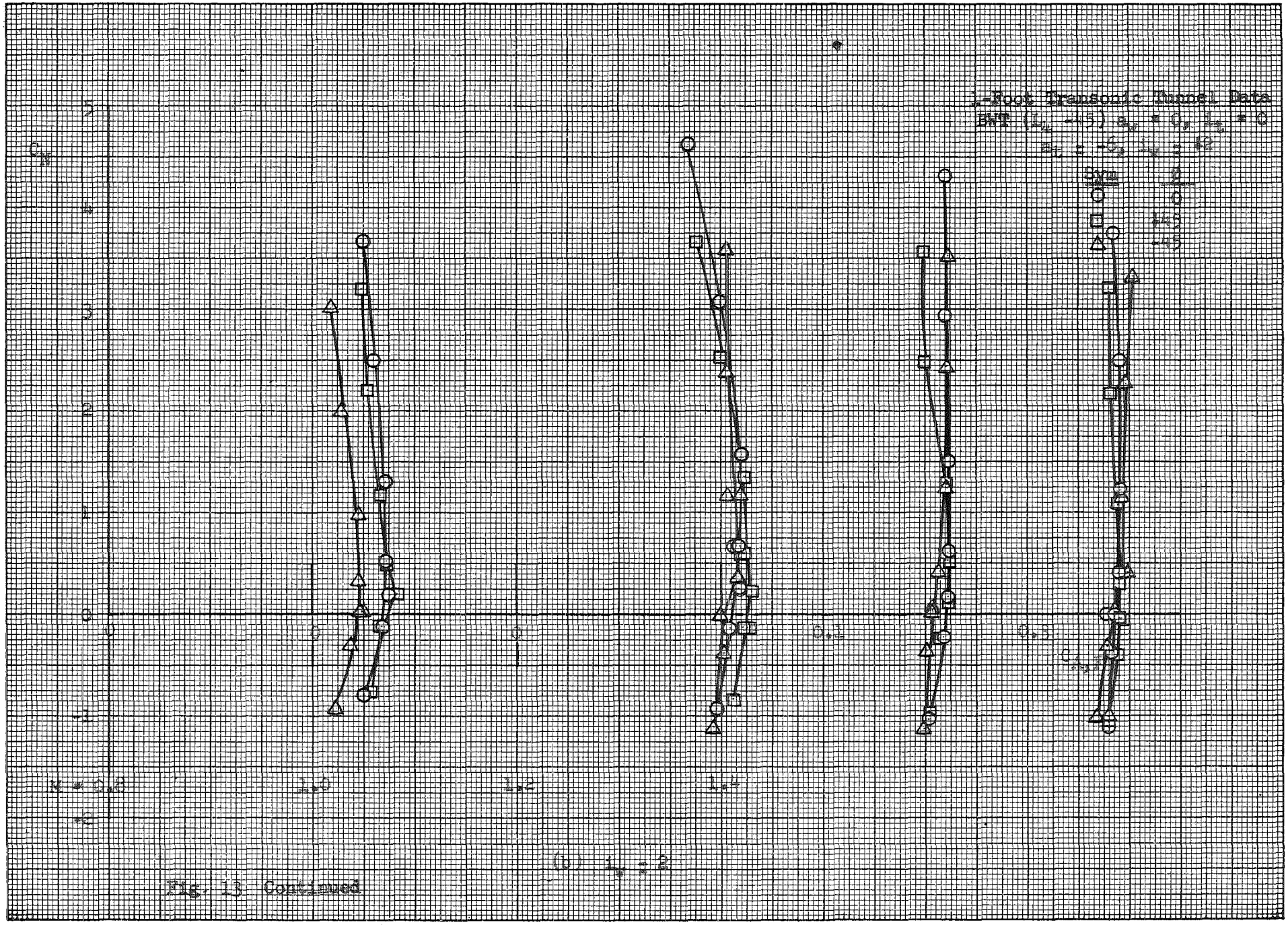

Fig. 13 Continued

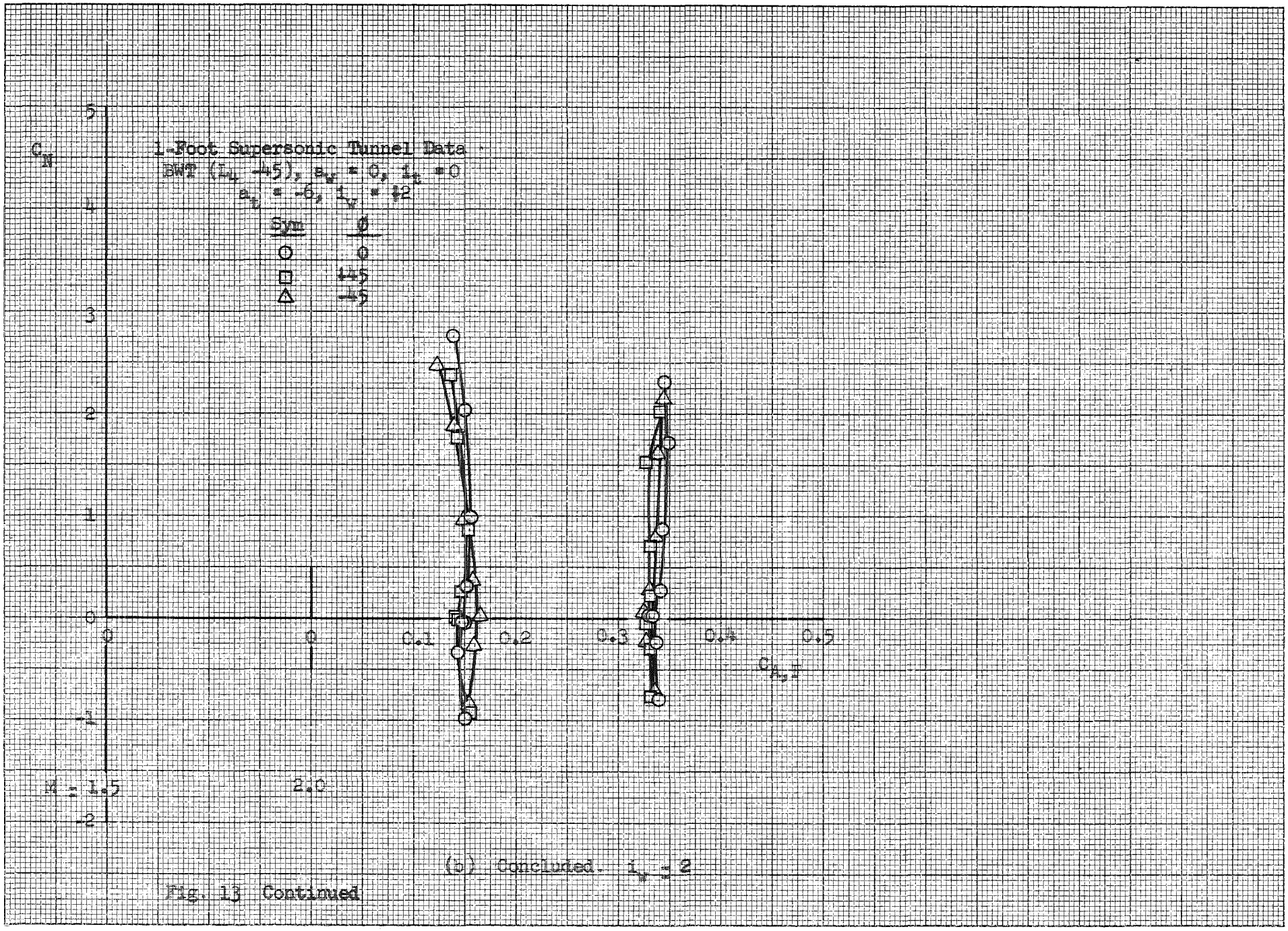

(b) Concluded. $i_w = 2$

Fig. 13 Continued

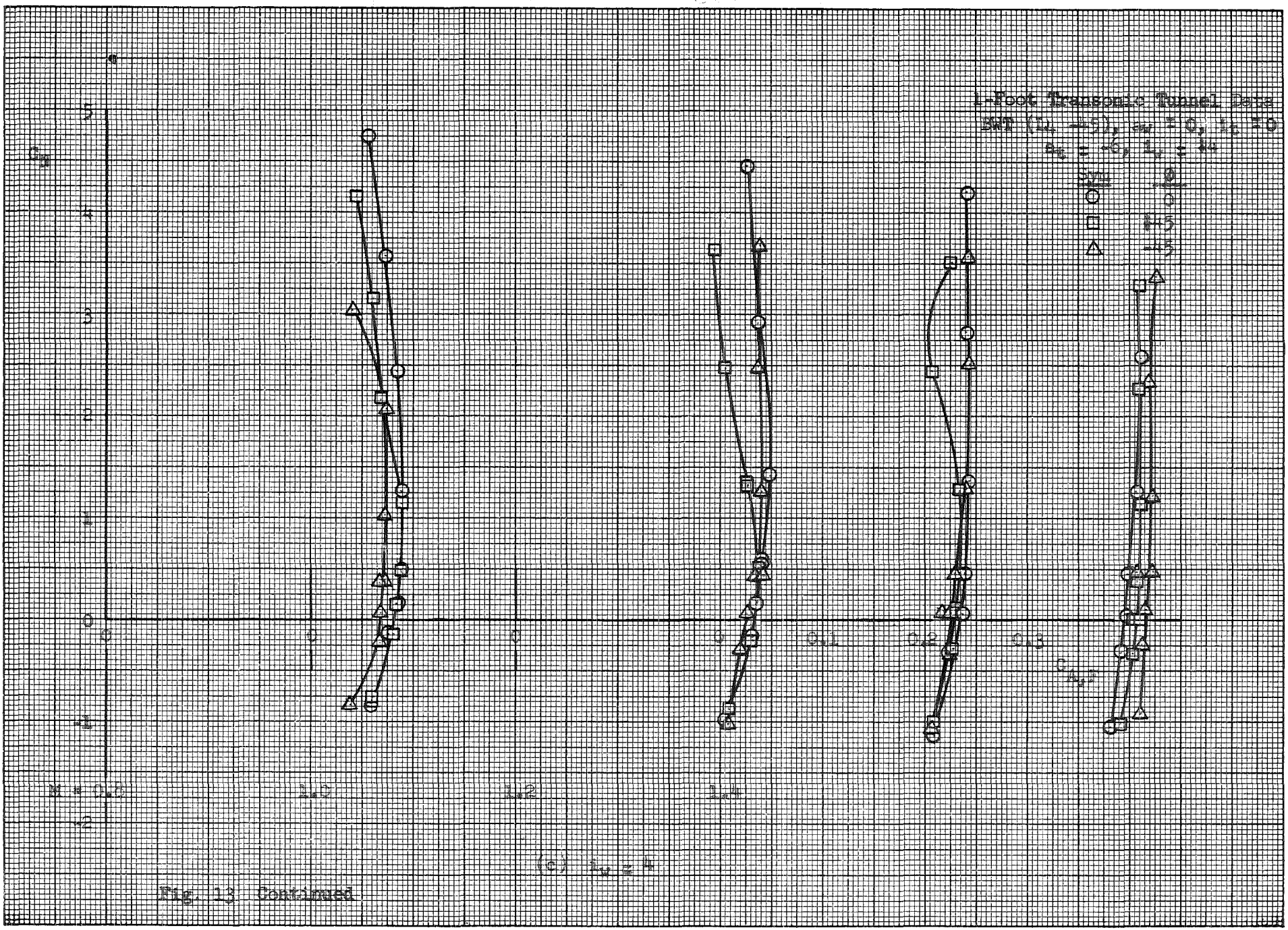

Fig. 13 Continued.

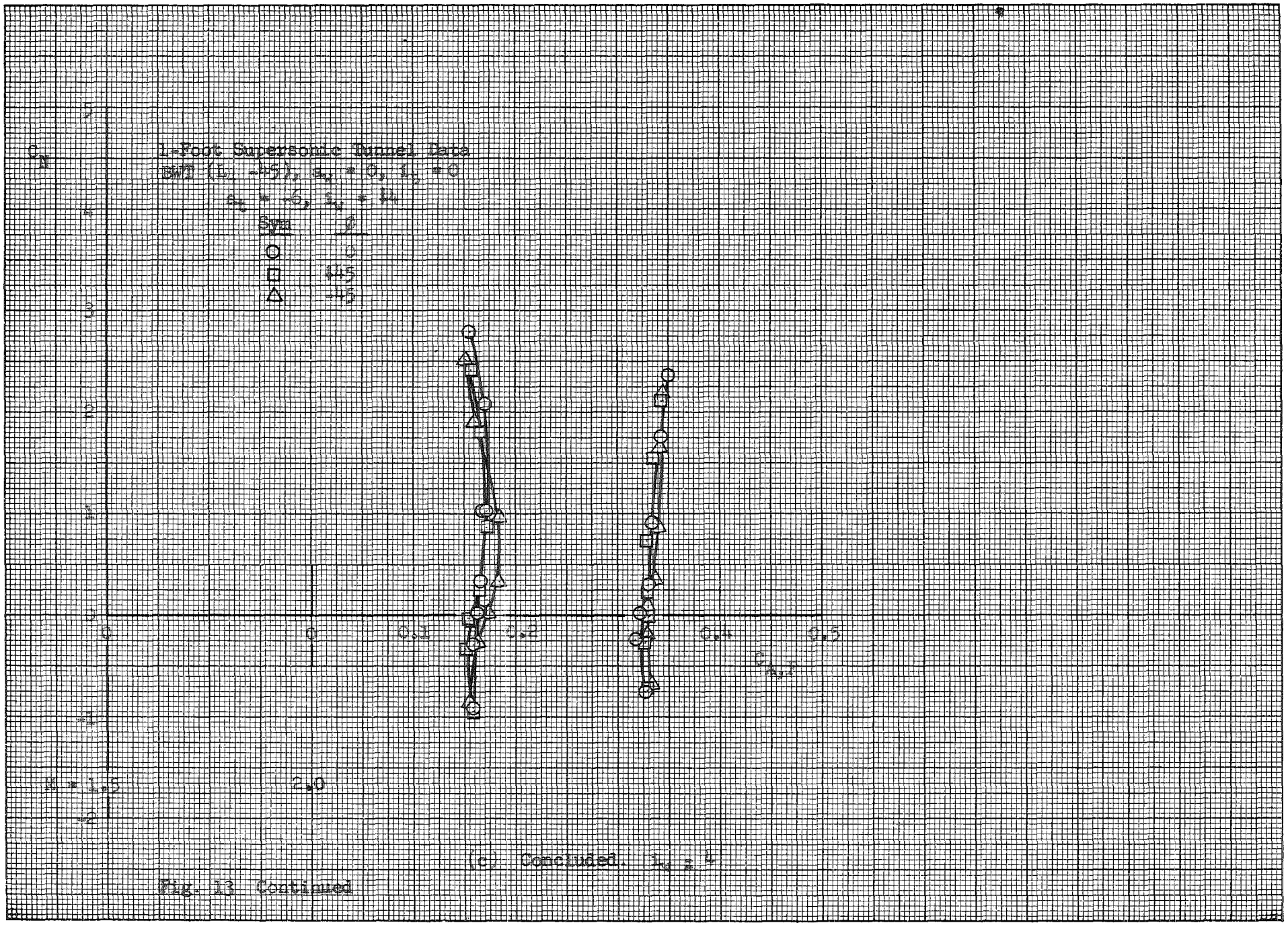

(c) Concluded. $M_\infty = 4$

Fig. 13 Continued

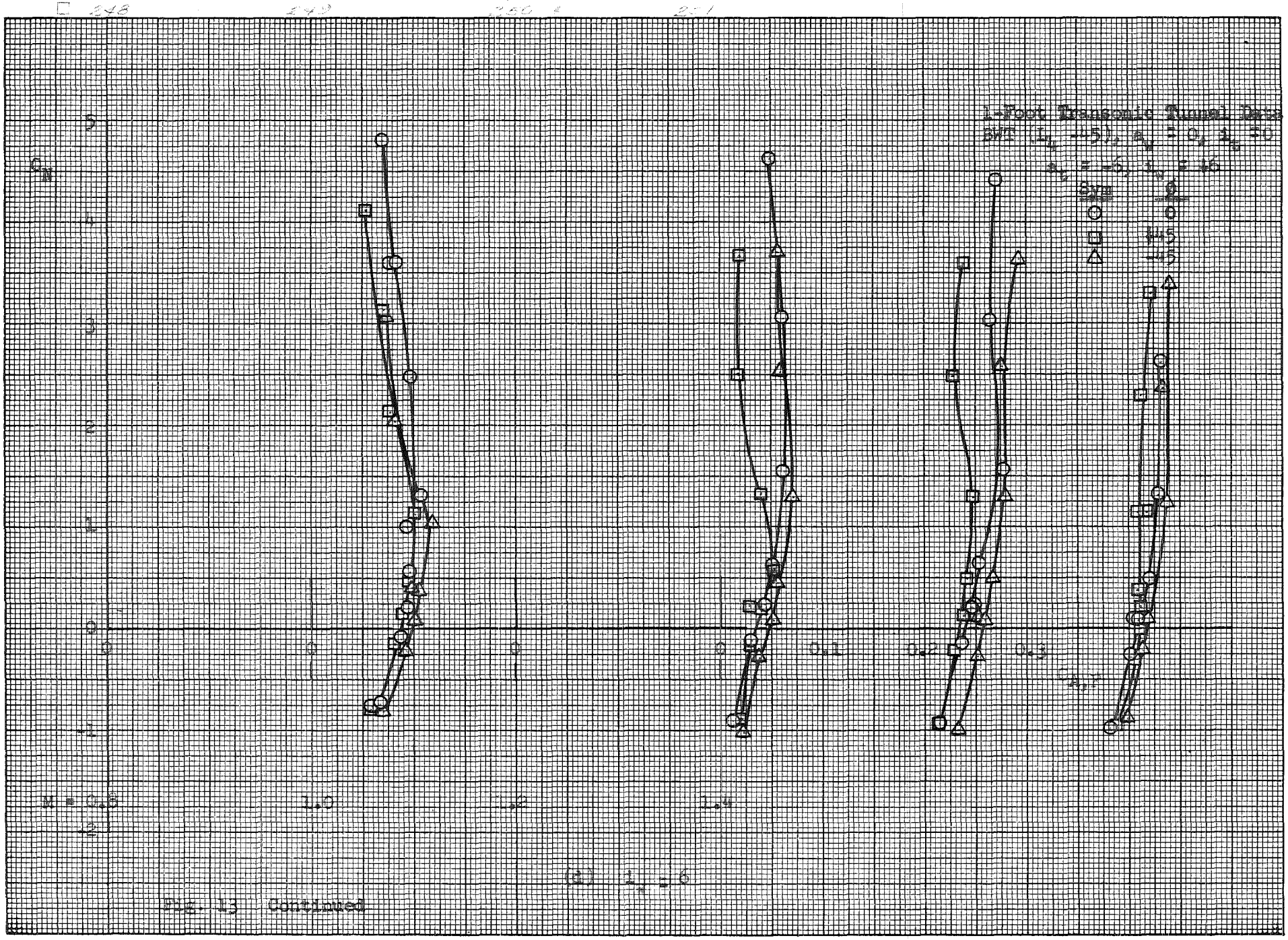

Fig. 13 Continued

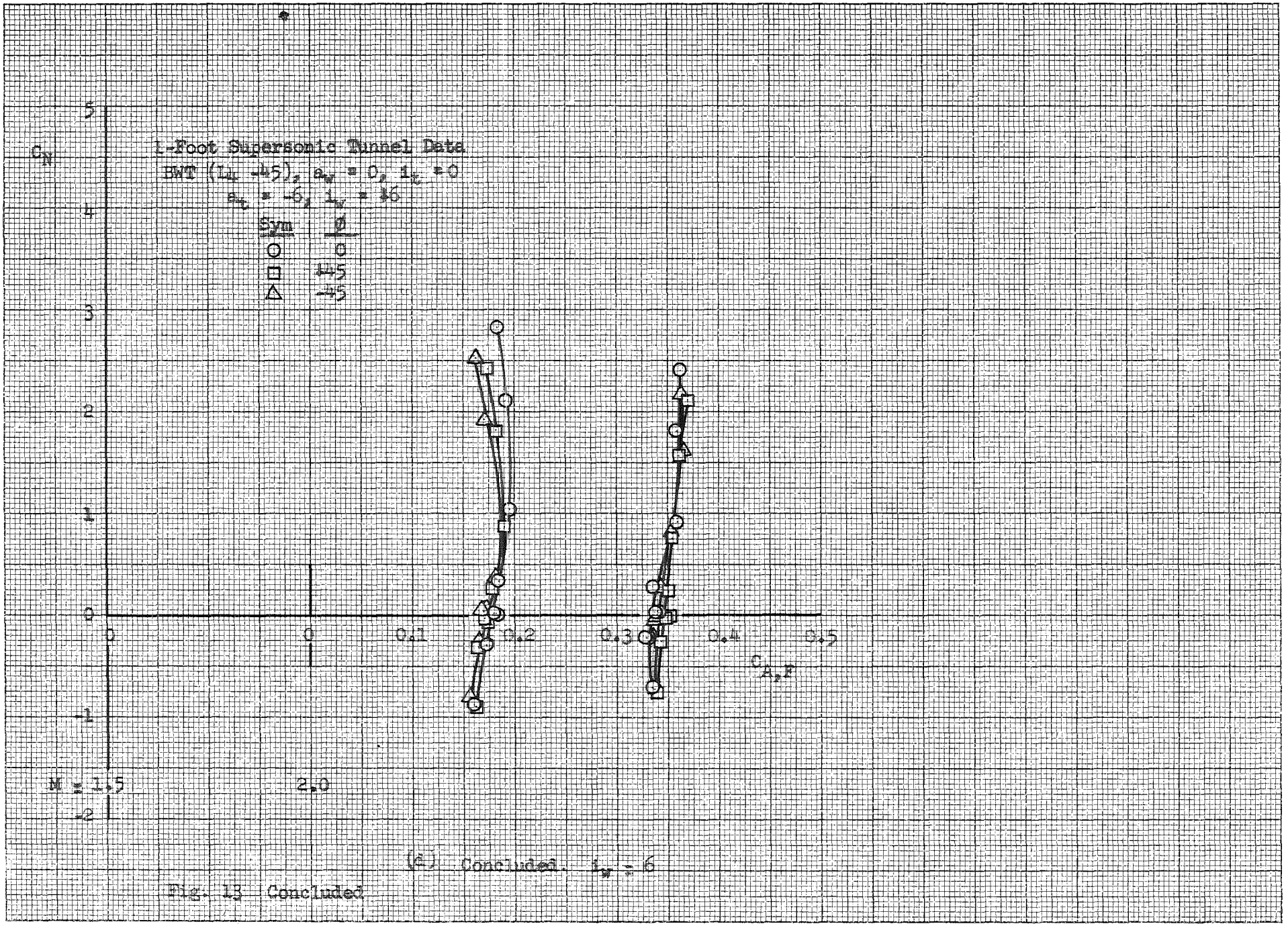

(f) Concluded. i_w = 6

Fig. 13 Concluded

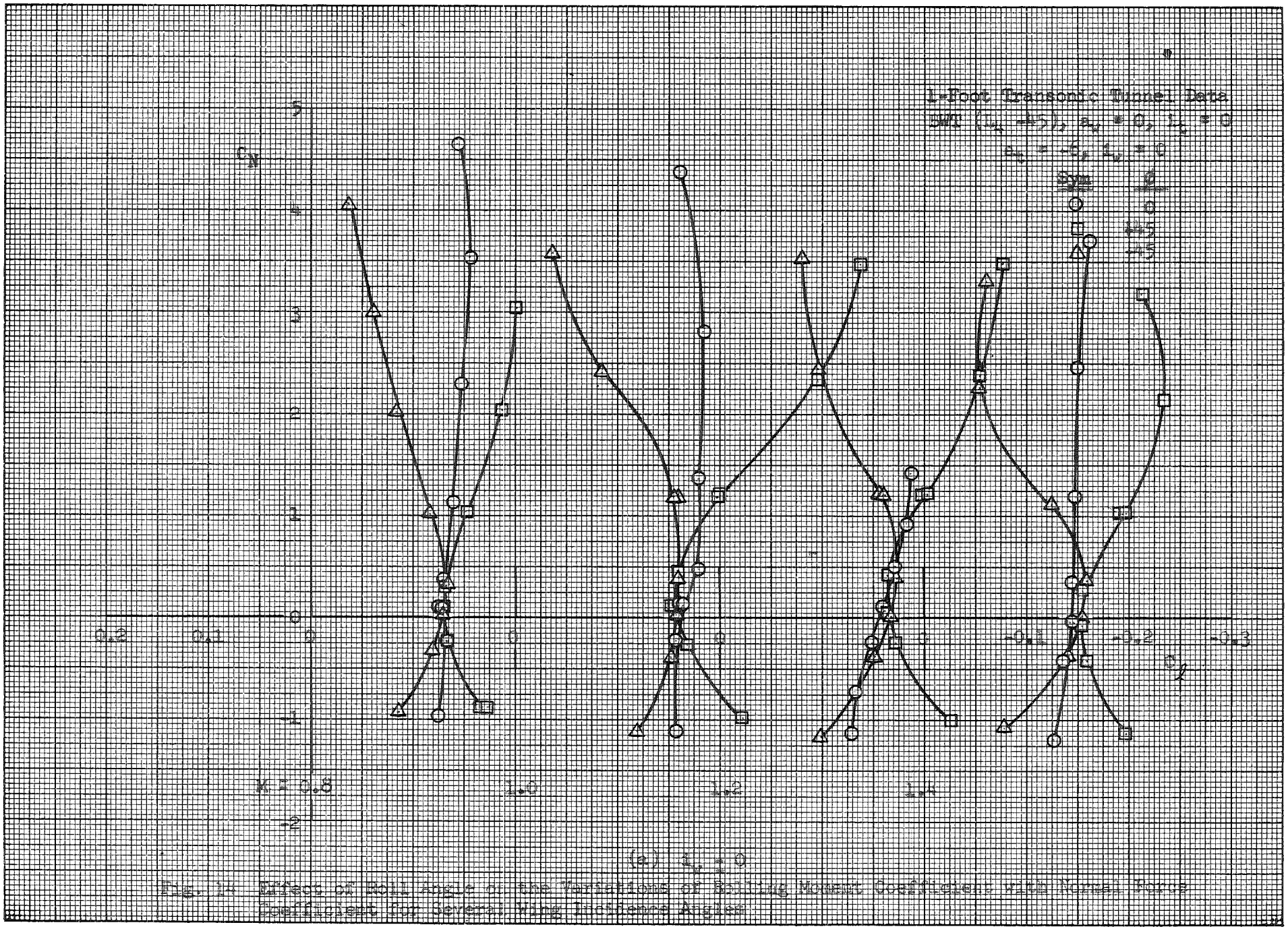

(a) $i_w = 0$

Fig. 14 Effect of Roll Angle on the Variations of Rolling Moment Coefficient with Normal Force Coefficient for Several Wing Incidence Angles

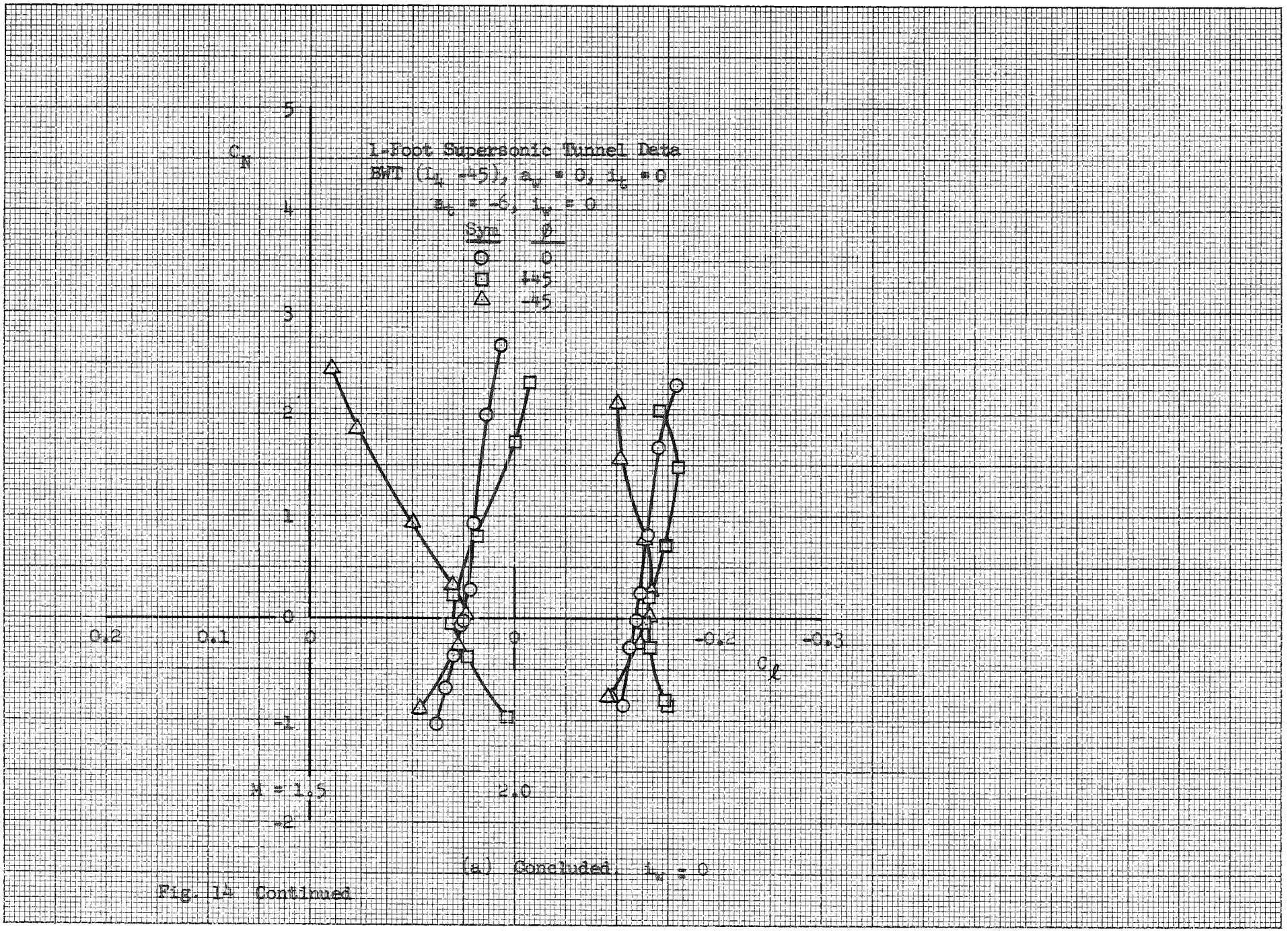

(a) Concluded, $i_w = 0$

Fig. 14 Continued

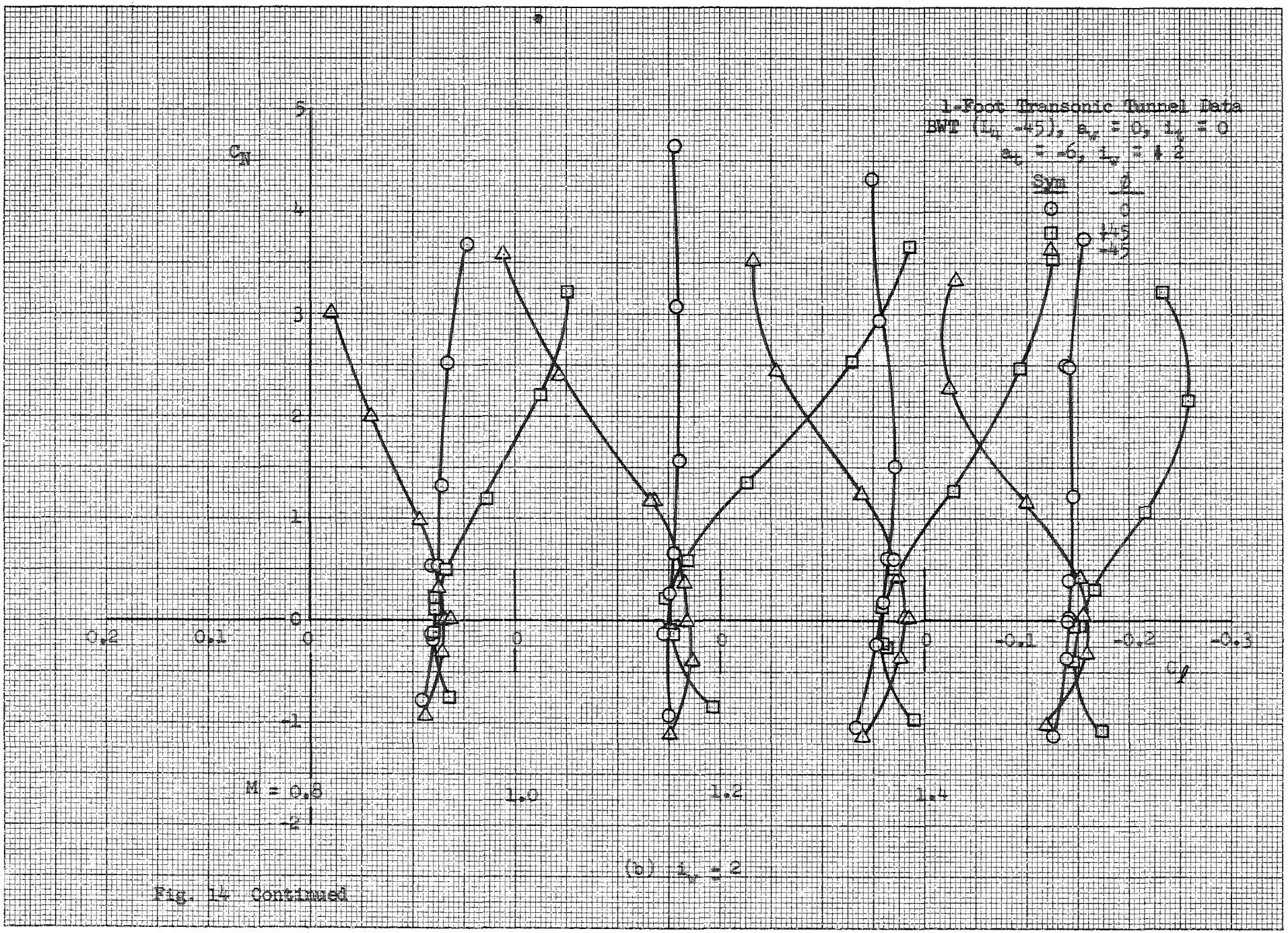

Fig. 14 Continued

(b) Concluded. i_w = 2

Fig. 14 Continued

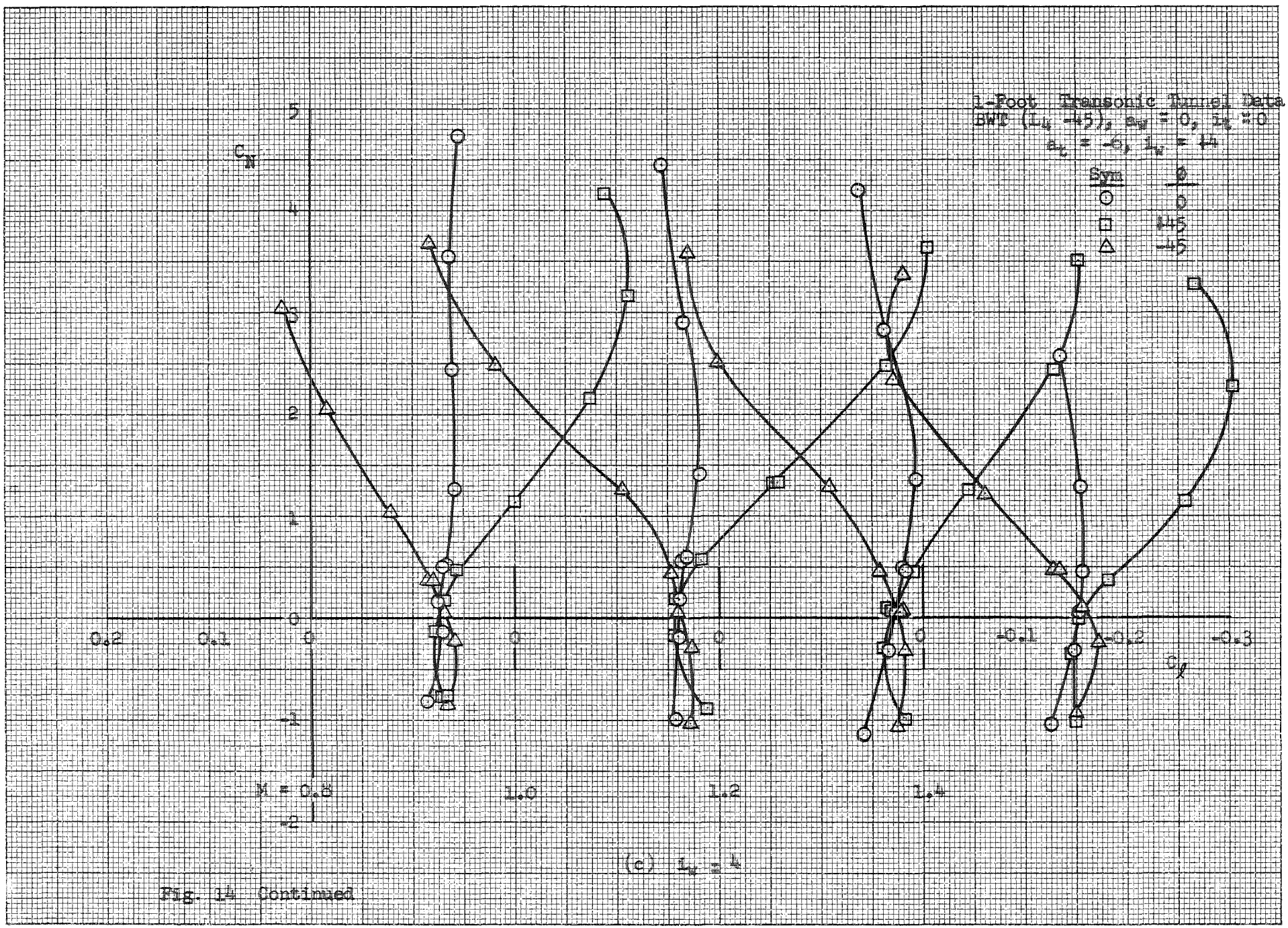

Fig. 14 Continued

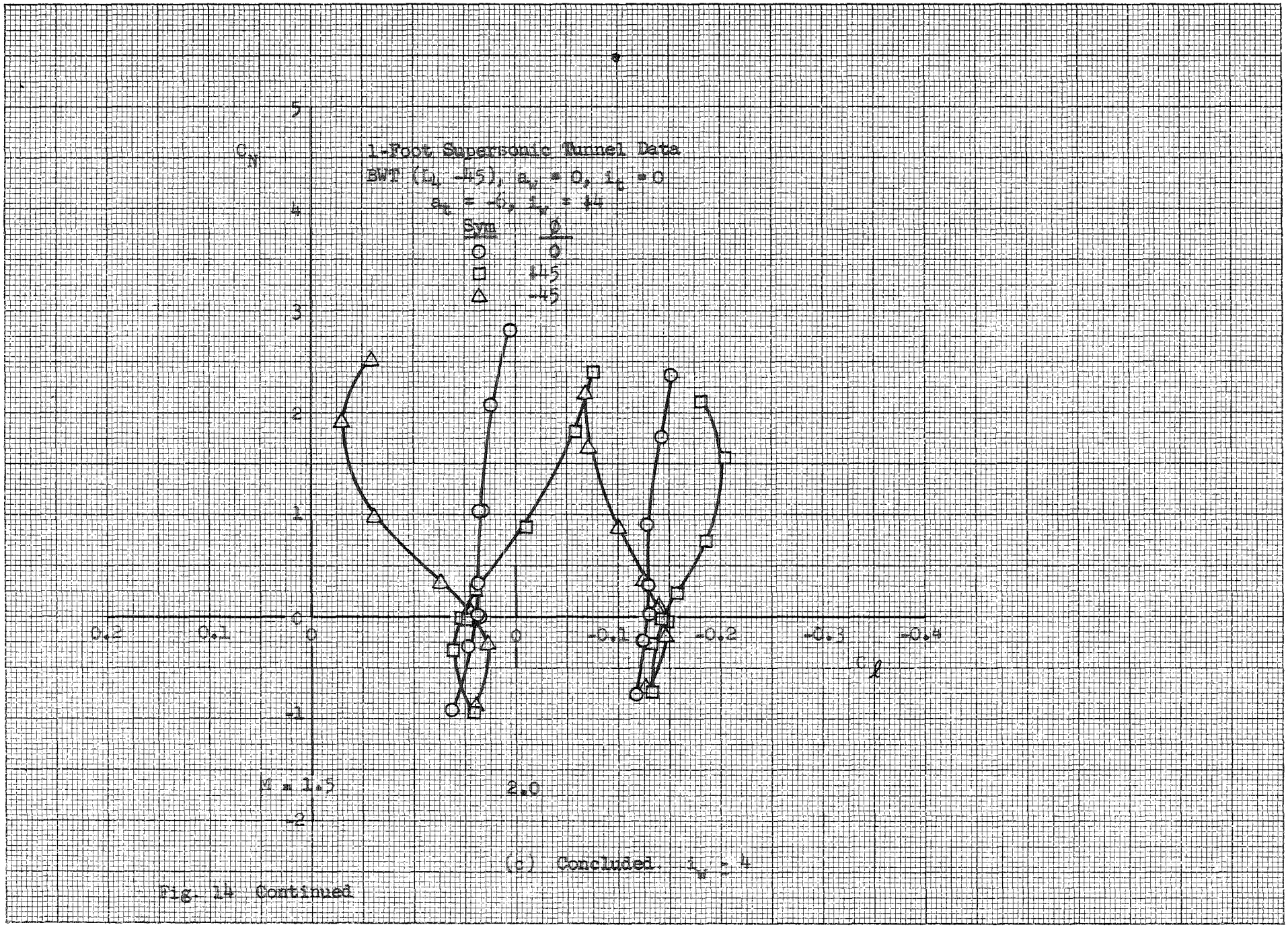

(c) Concluded. i_w = 4

Fig. 14 Continued

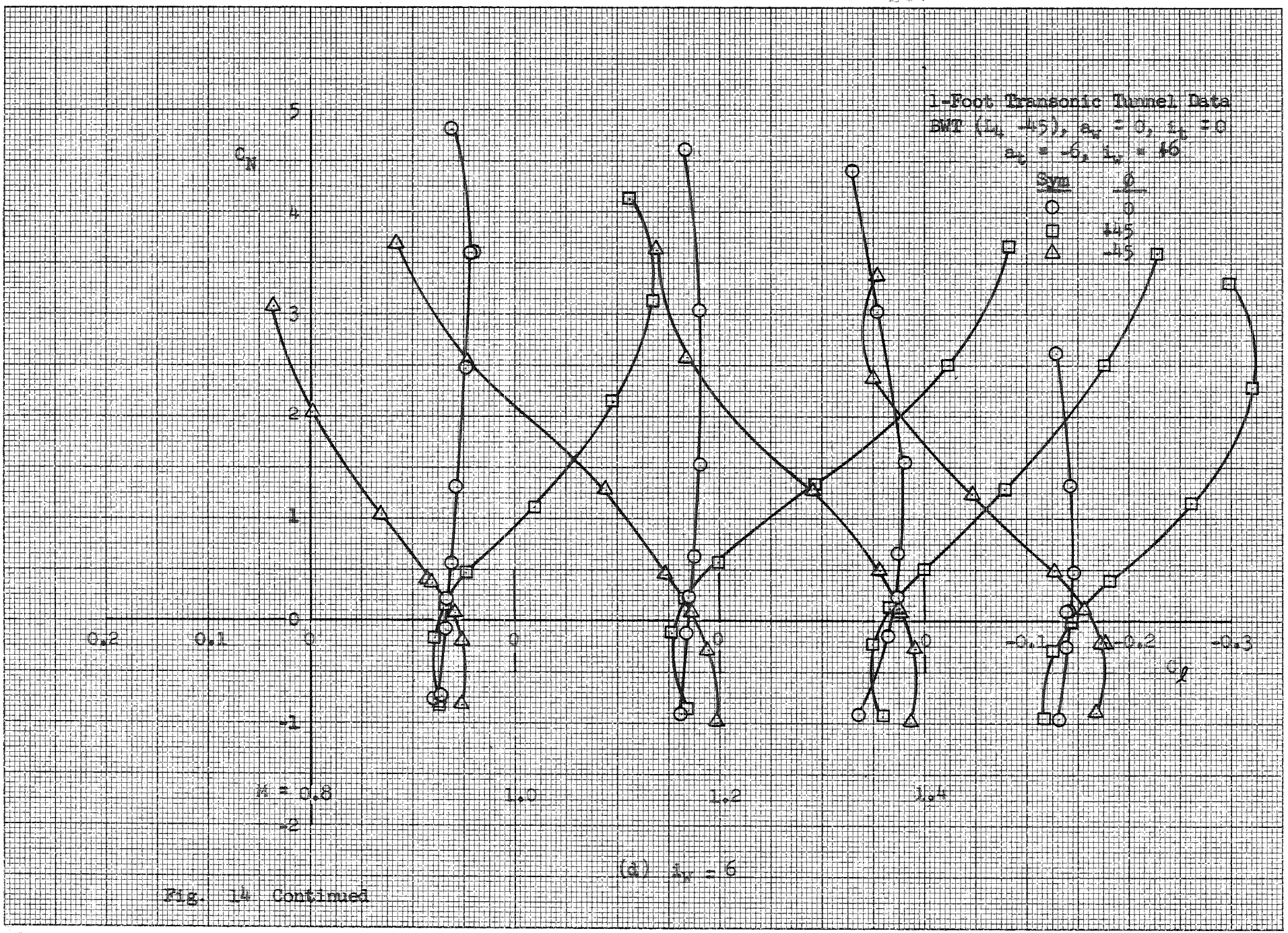

Fig. 14 Continued

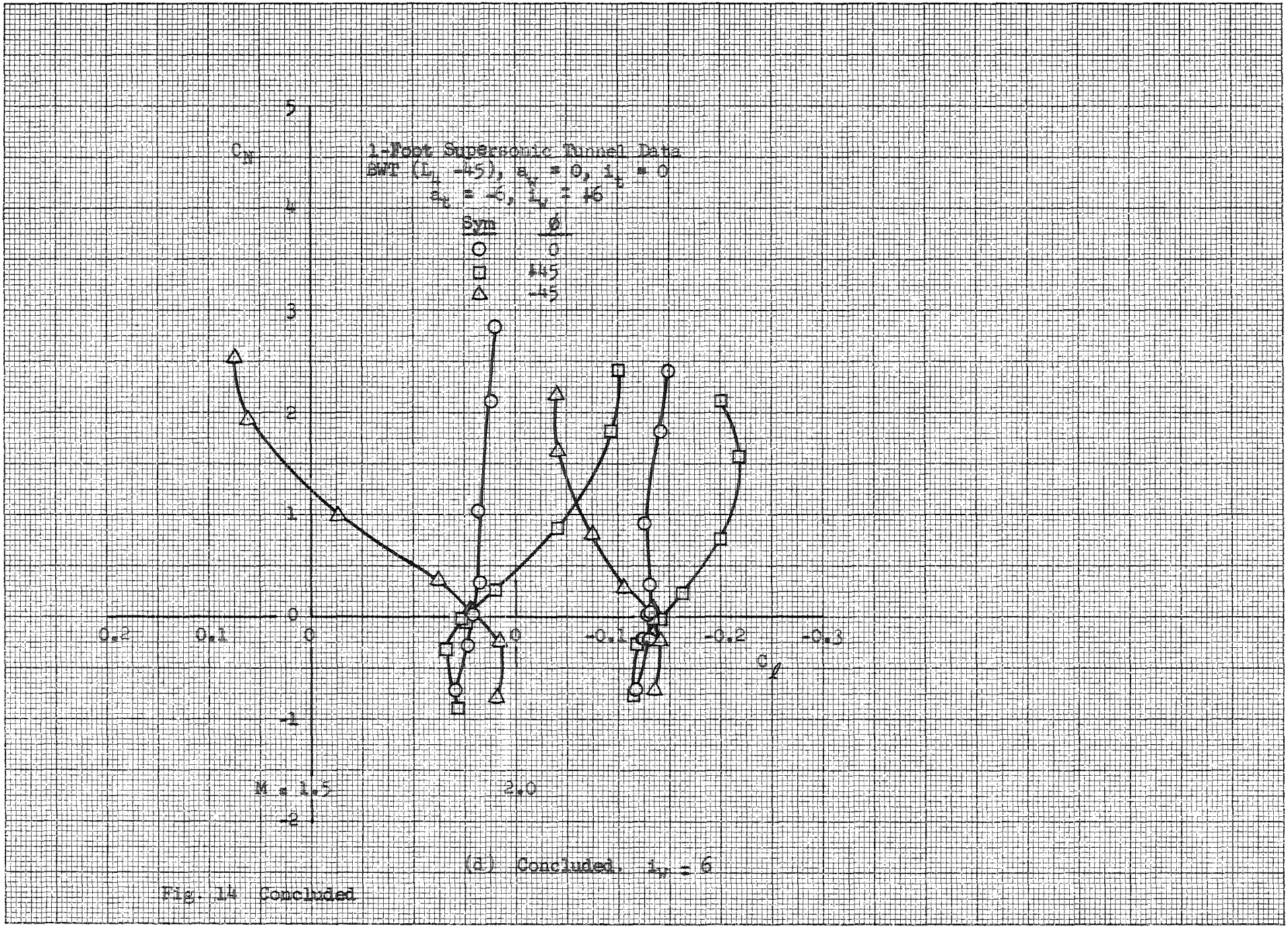

(a) Concluded. $i_w = 6$

Fig. 14 Concluded

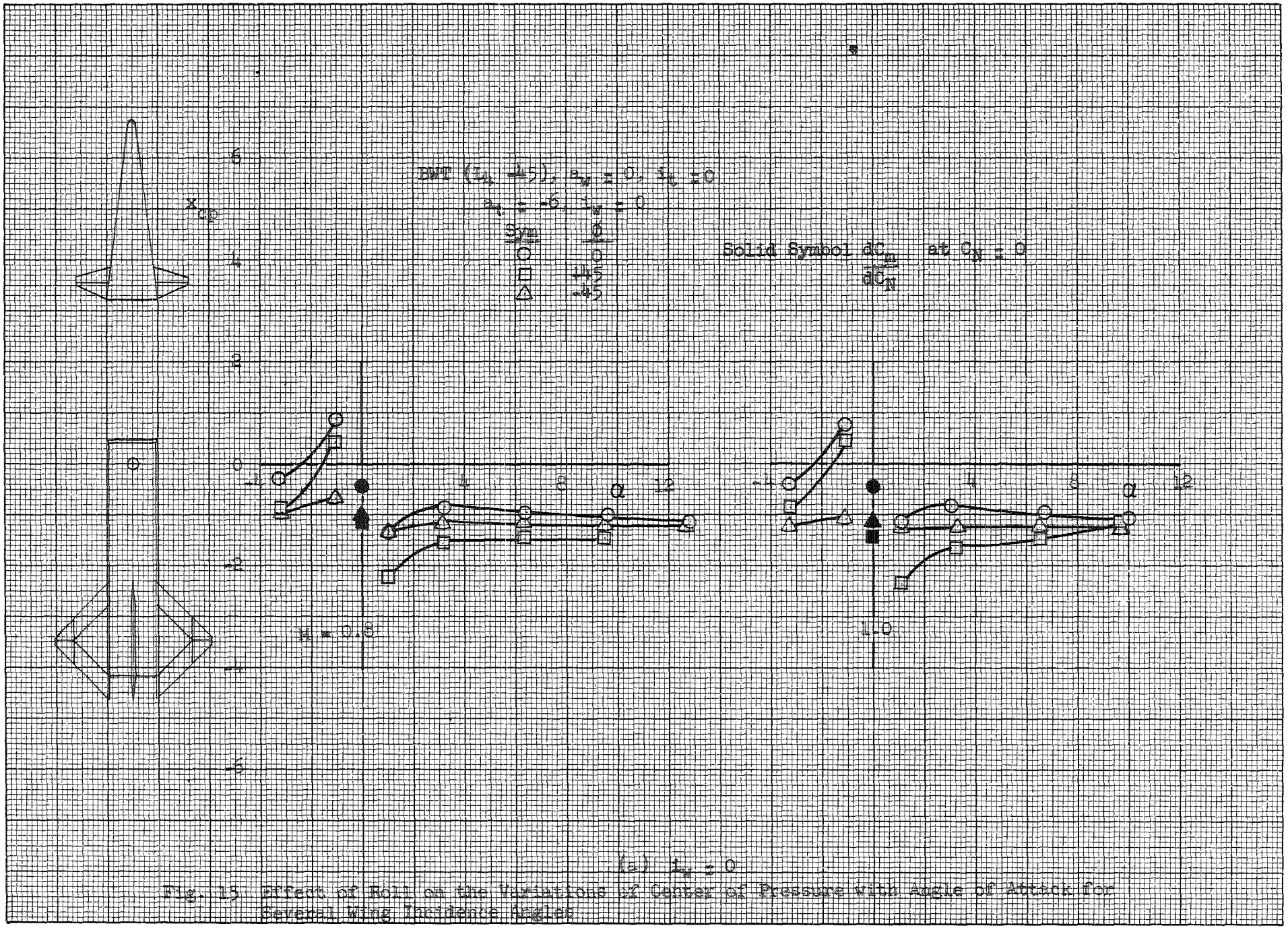

Fig. 15 Effect of Roll on the Variations of Center of Pressure with Angle of Attack for Several Wing Incidence Angles

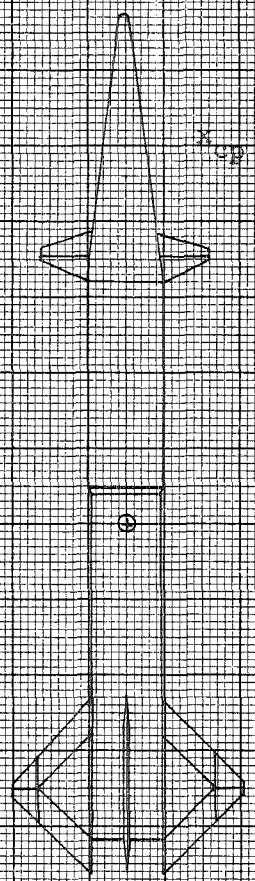

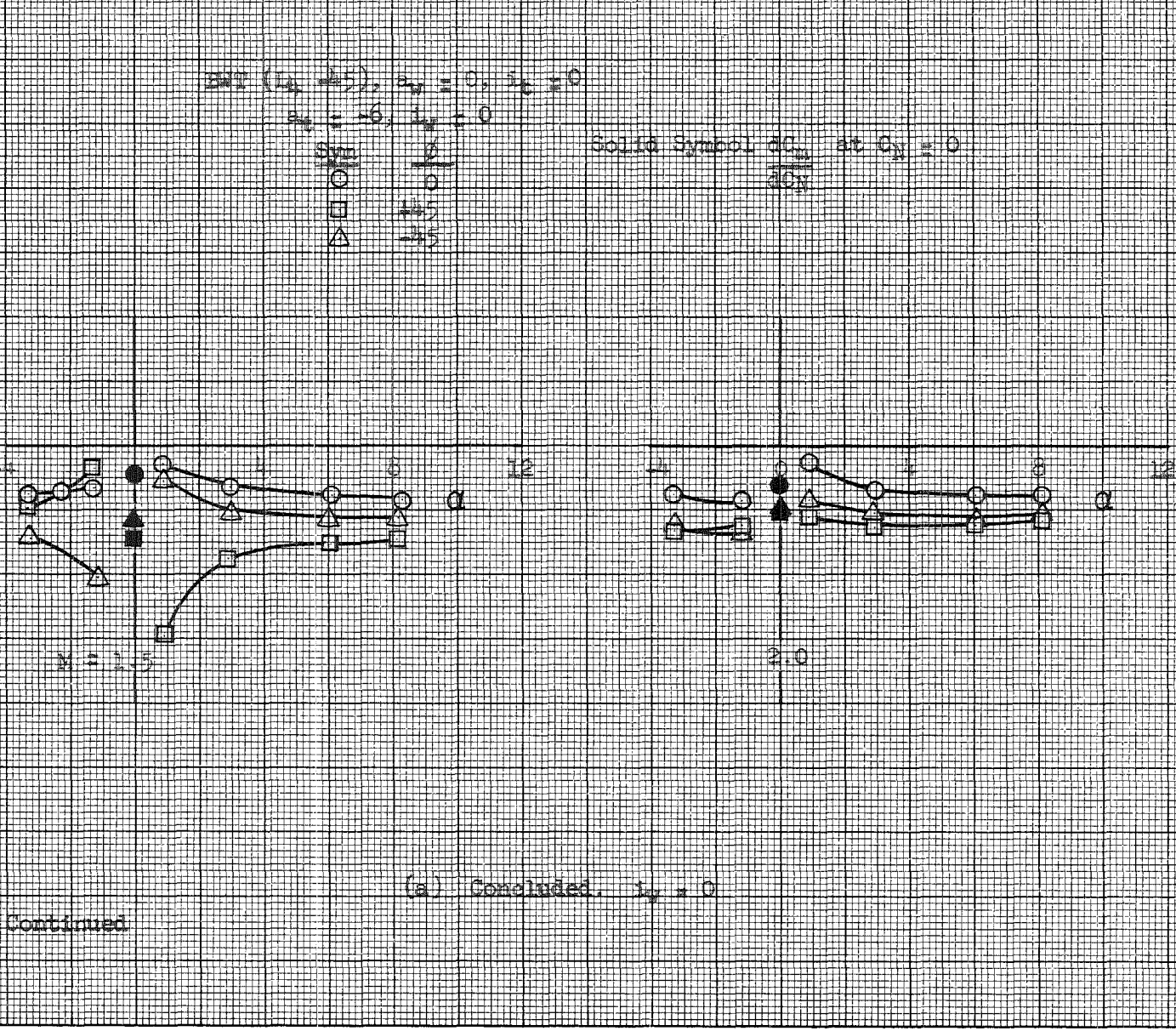

(a) Concluded. i_w = 0

Fig. 15 Continued.

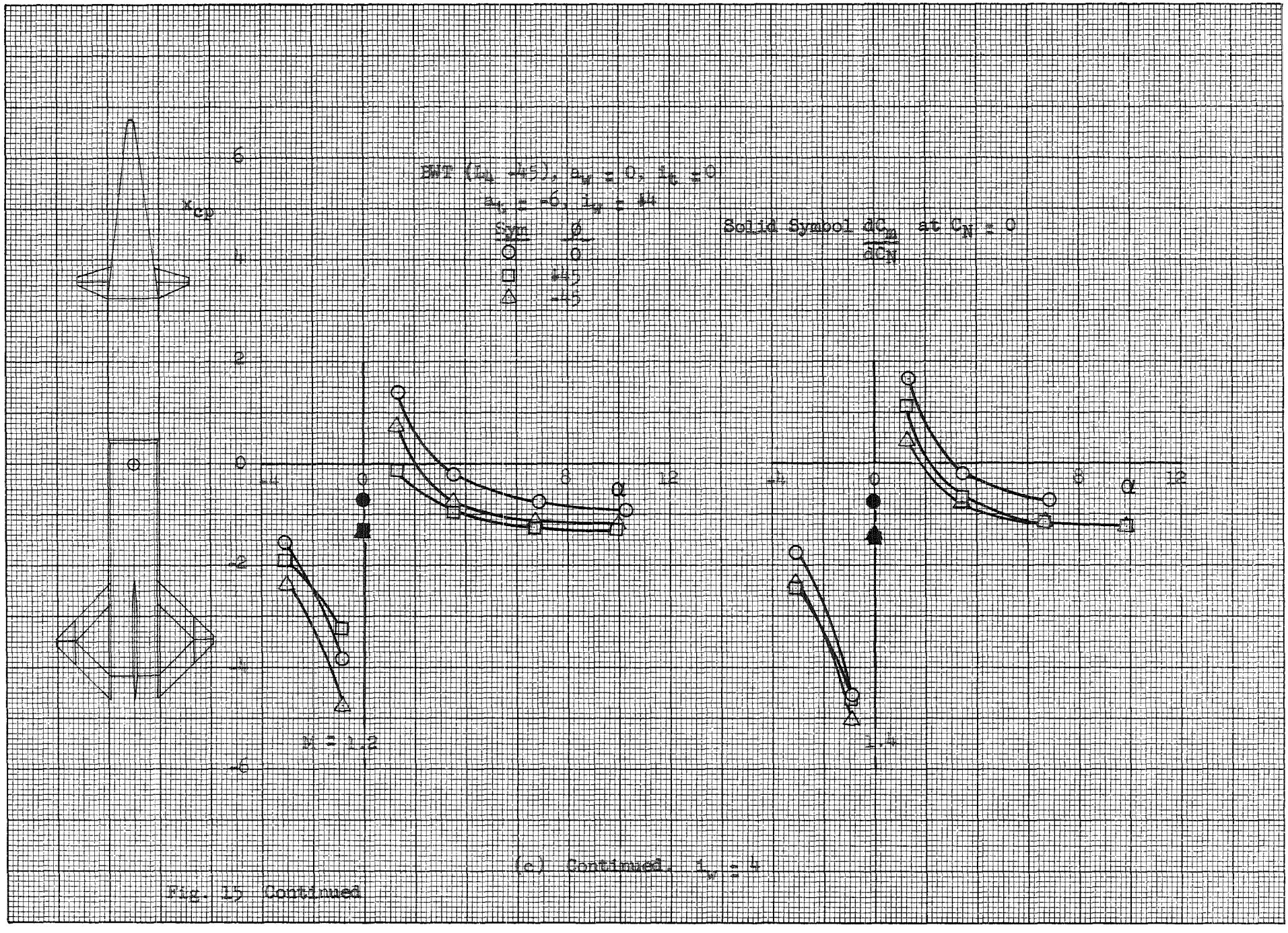

(c) Continued. i_w = 4

Fig. 15 Continued

Fig. 15 Continued

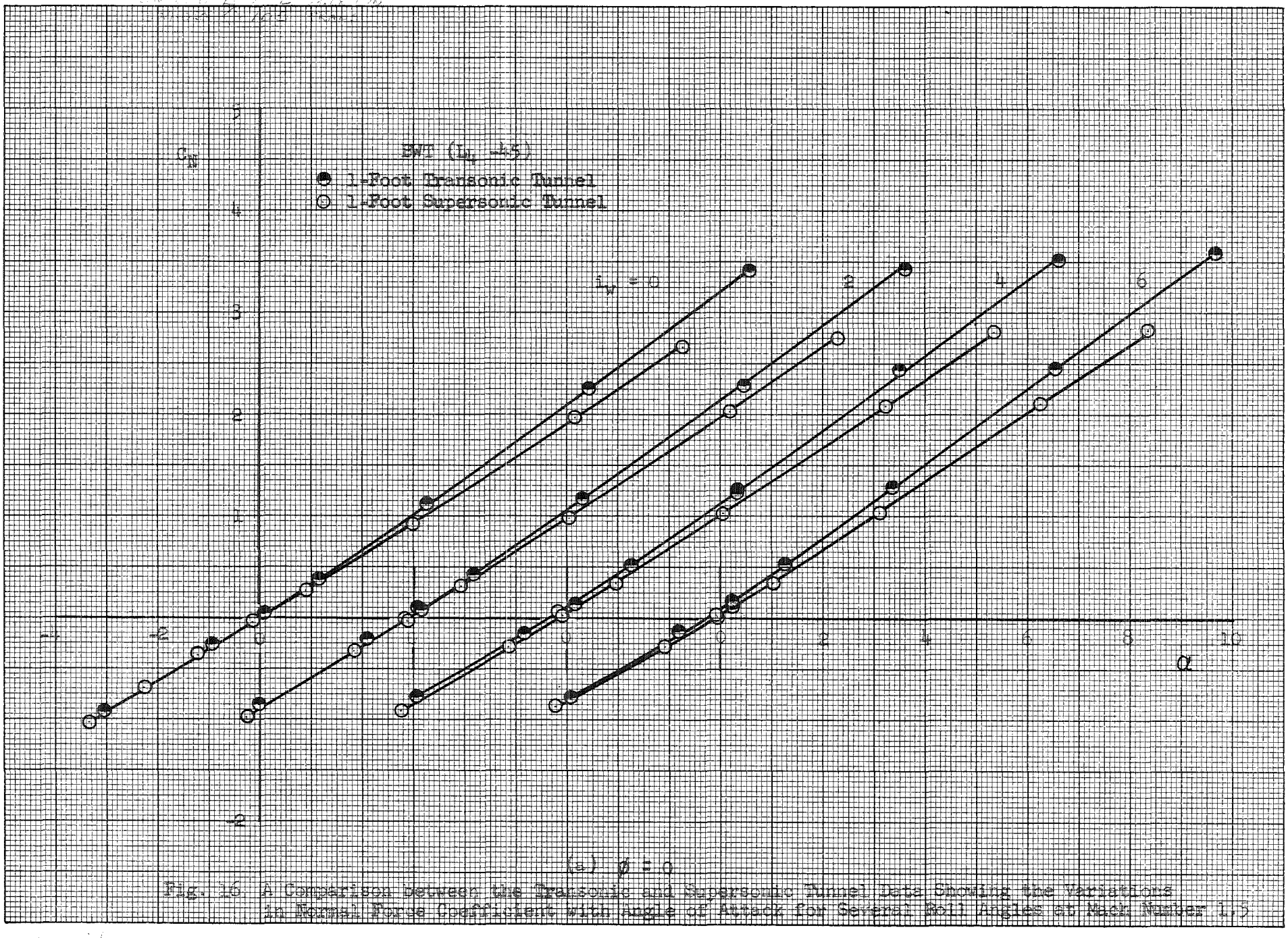

Fig. 16 A Comparison between the Transonic and Supersonic Tunnel Data Showing the Variations in Normal Force Coefficient with Angle of Attack for Several Roll Angles at Mach Number 1.5

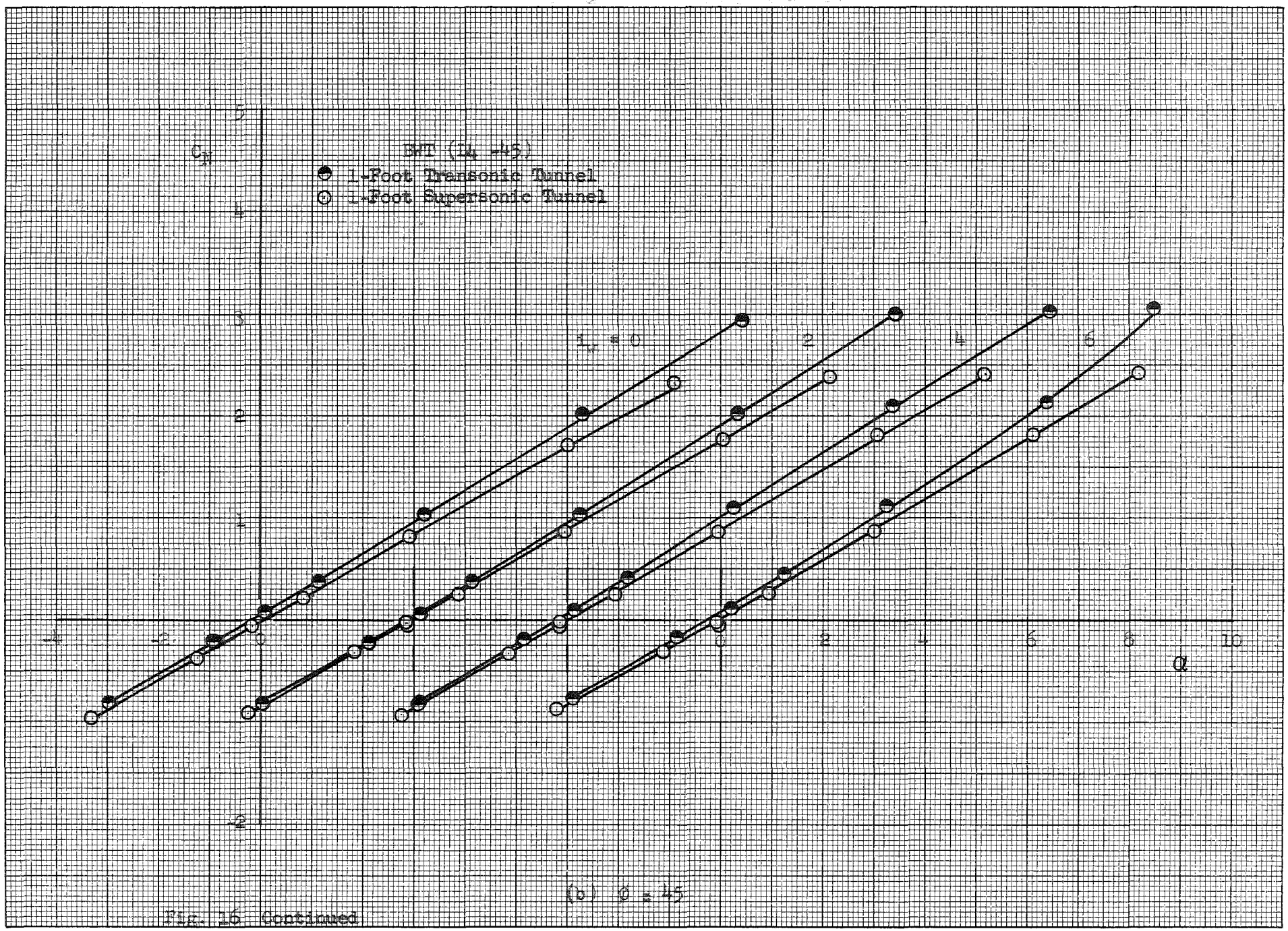

(b) $\phi = 45$

Fig. 16 Continued

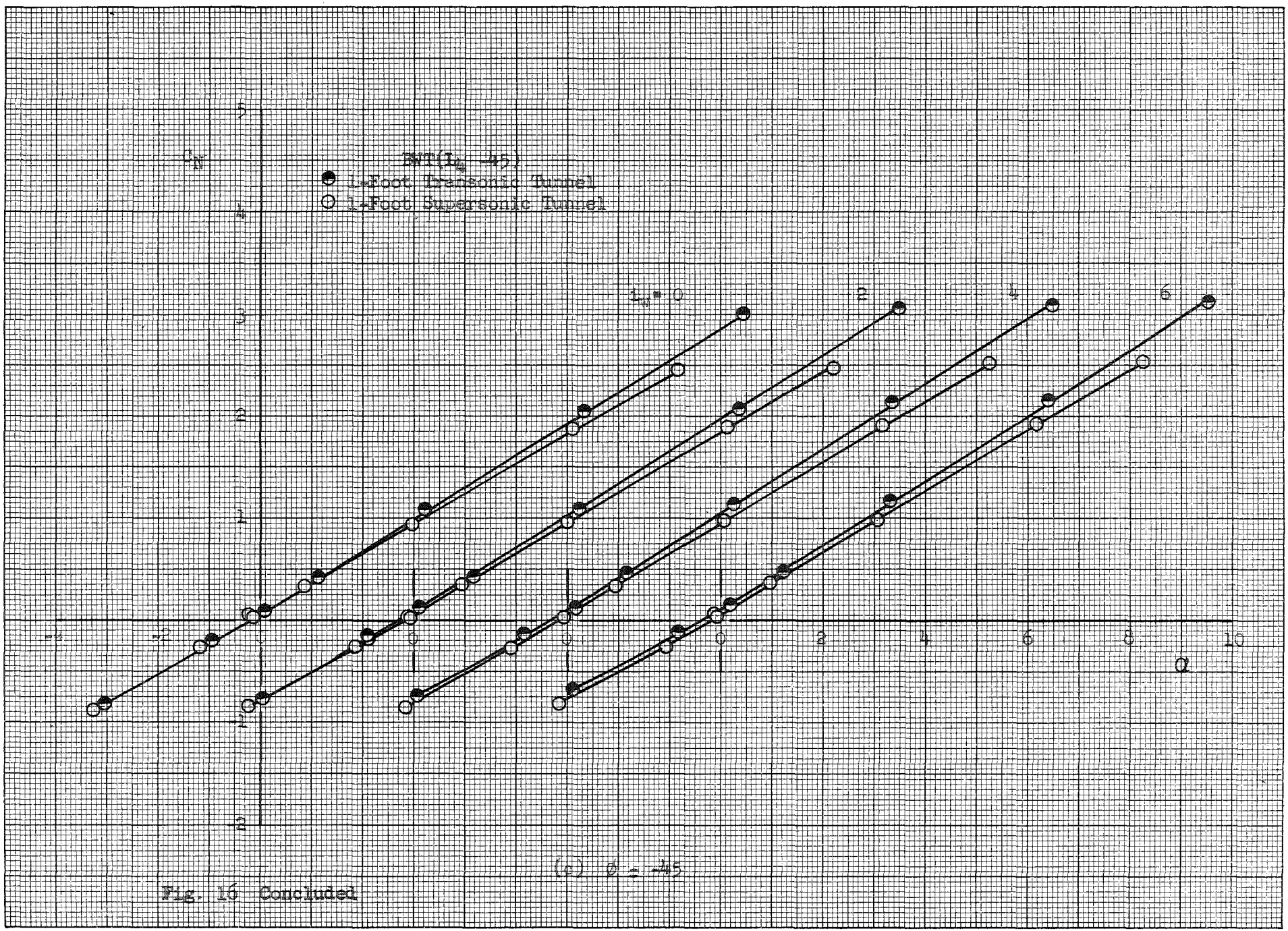

Fig. 16 Concluded

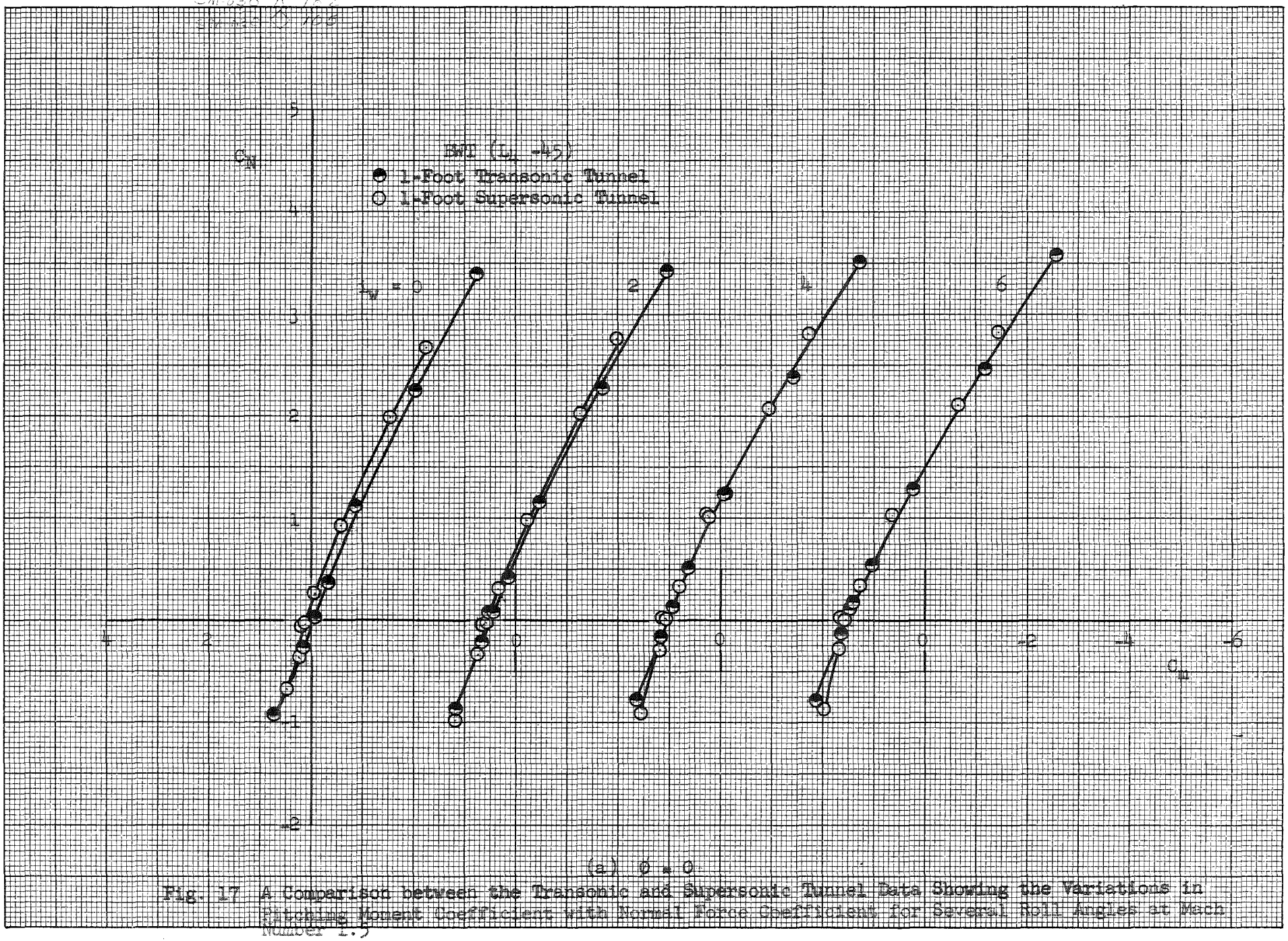

(a) ϕ = 0

Fig. 17 A Comparison between the Transonic and Supersonic Tunnel Data Showing the Variations in Pitching Moment Coefficient with Normal Force Coefficient for Several Roll Angles at Mach Number 1.5

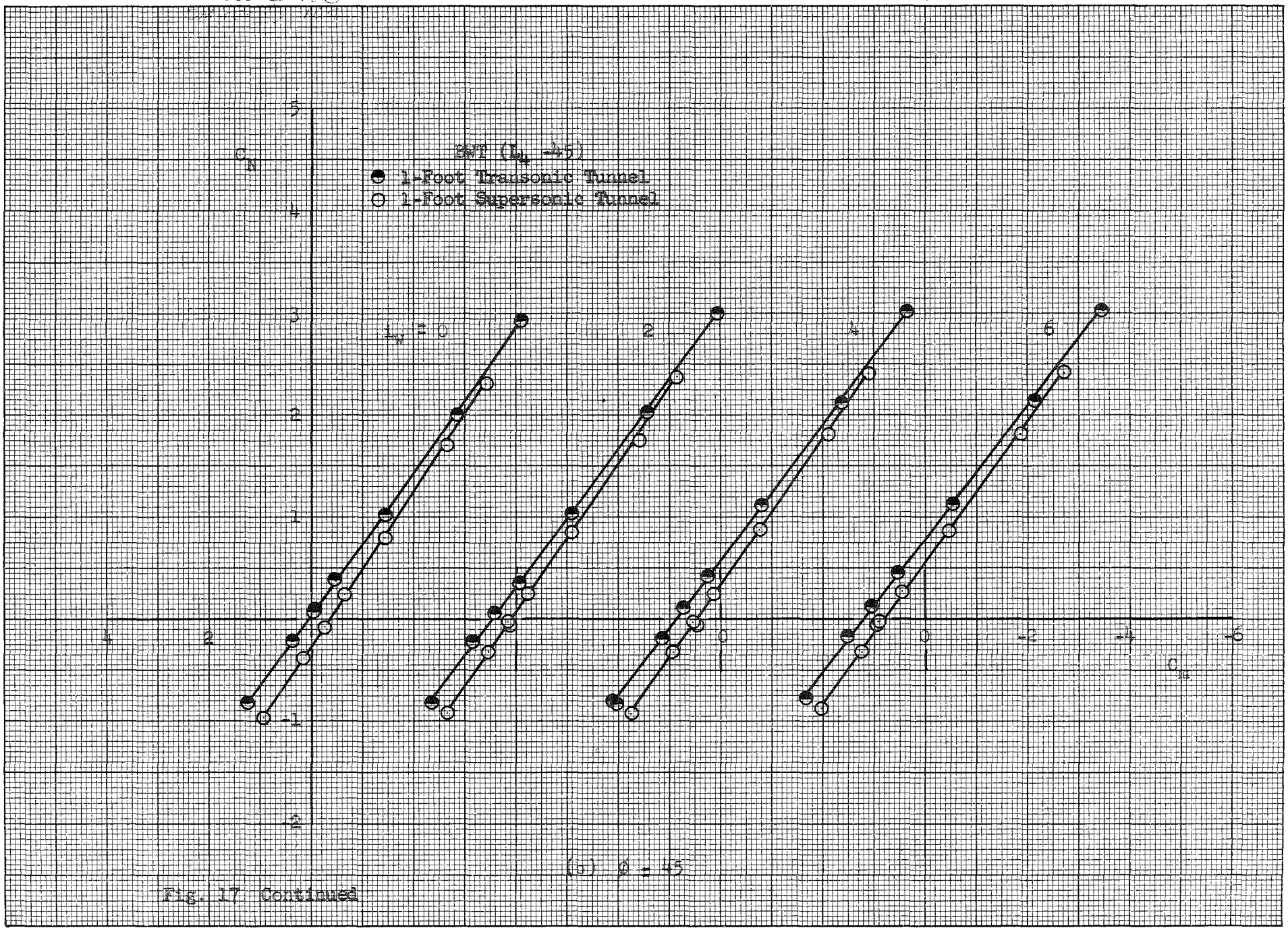

(b) ϕ = 45

Fig. 17 Continued

Fig. 17 Concluded

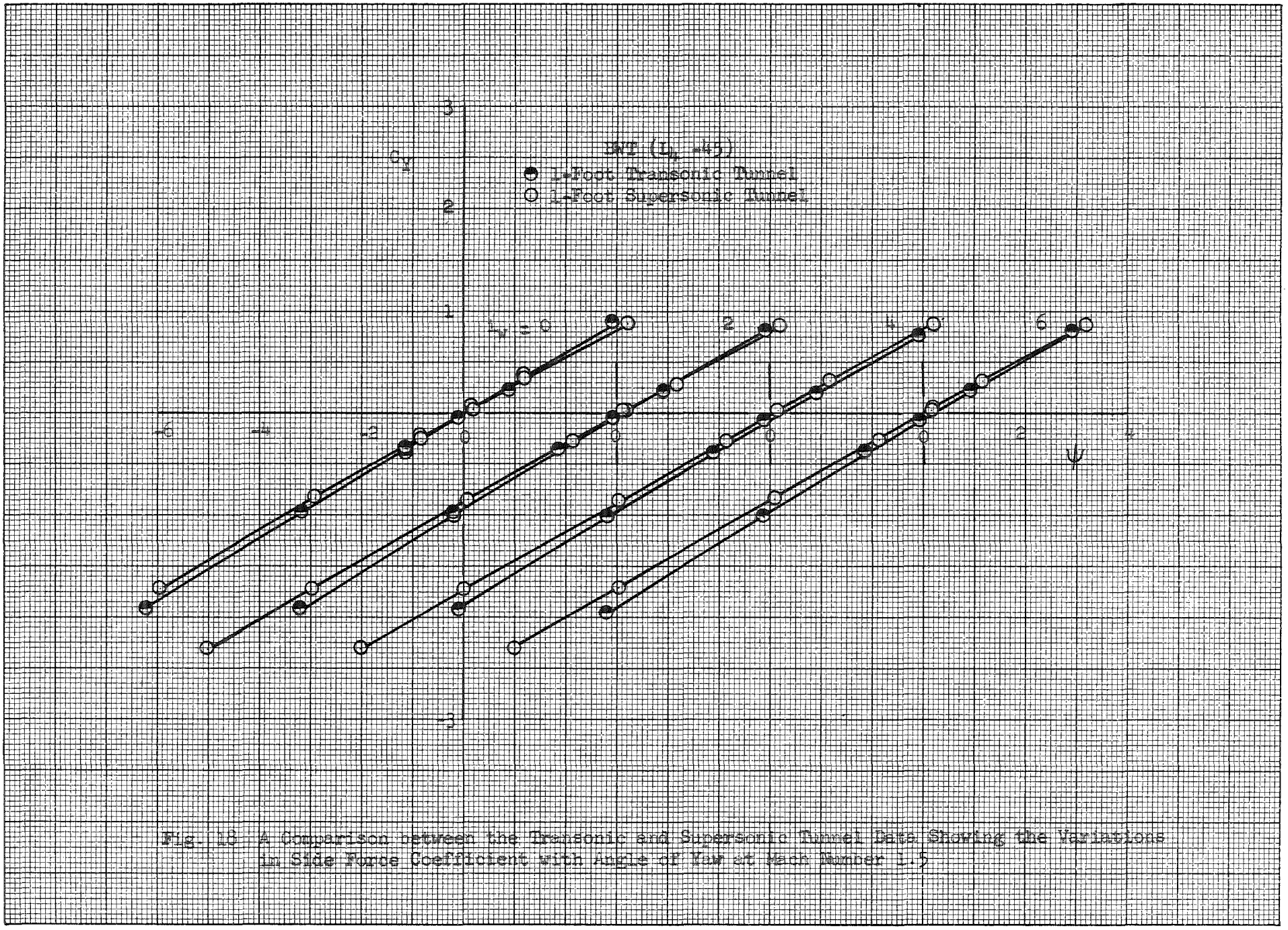

Fig. 18 A Comparison between the Transonic and Supersonic Tunnel Data Showing the Variations in Side Force Coefficient with Angle of Yaw at Mach Number 1.9

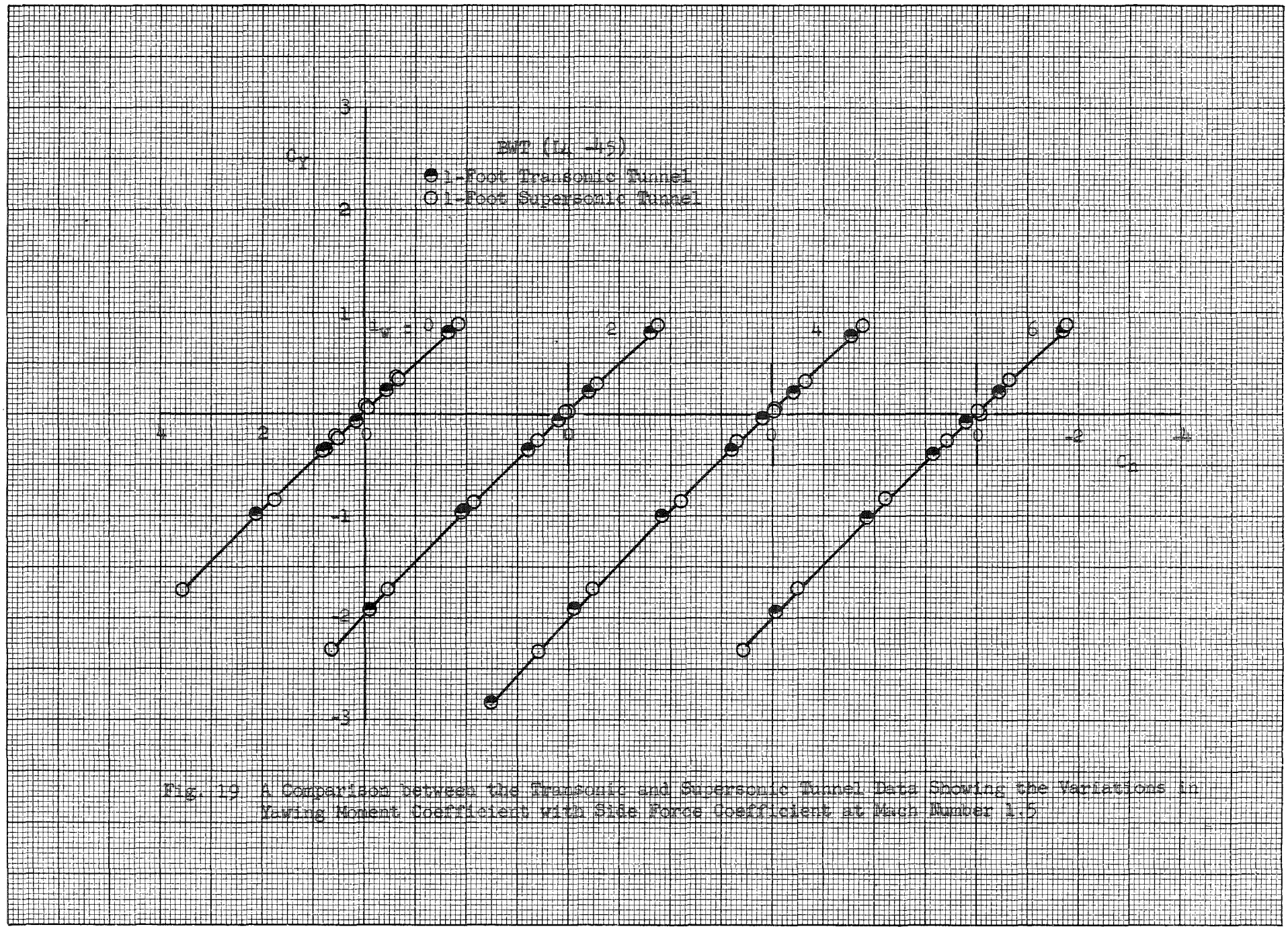

Fig. 19 A Comparison between the Transonic and Supersonic Tunnel Data Showing the Variations in Yawing Moment Coefficient with Side Force Coefficient at Mach Number 1.5

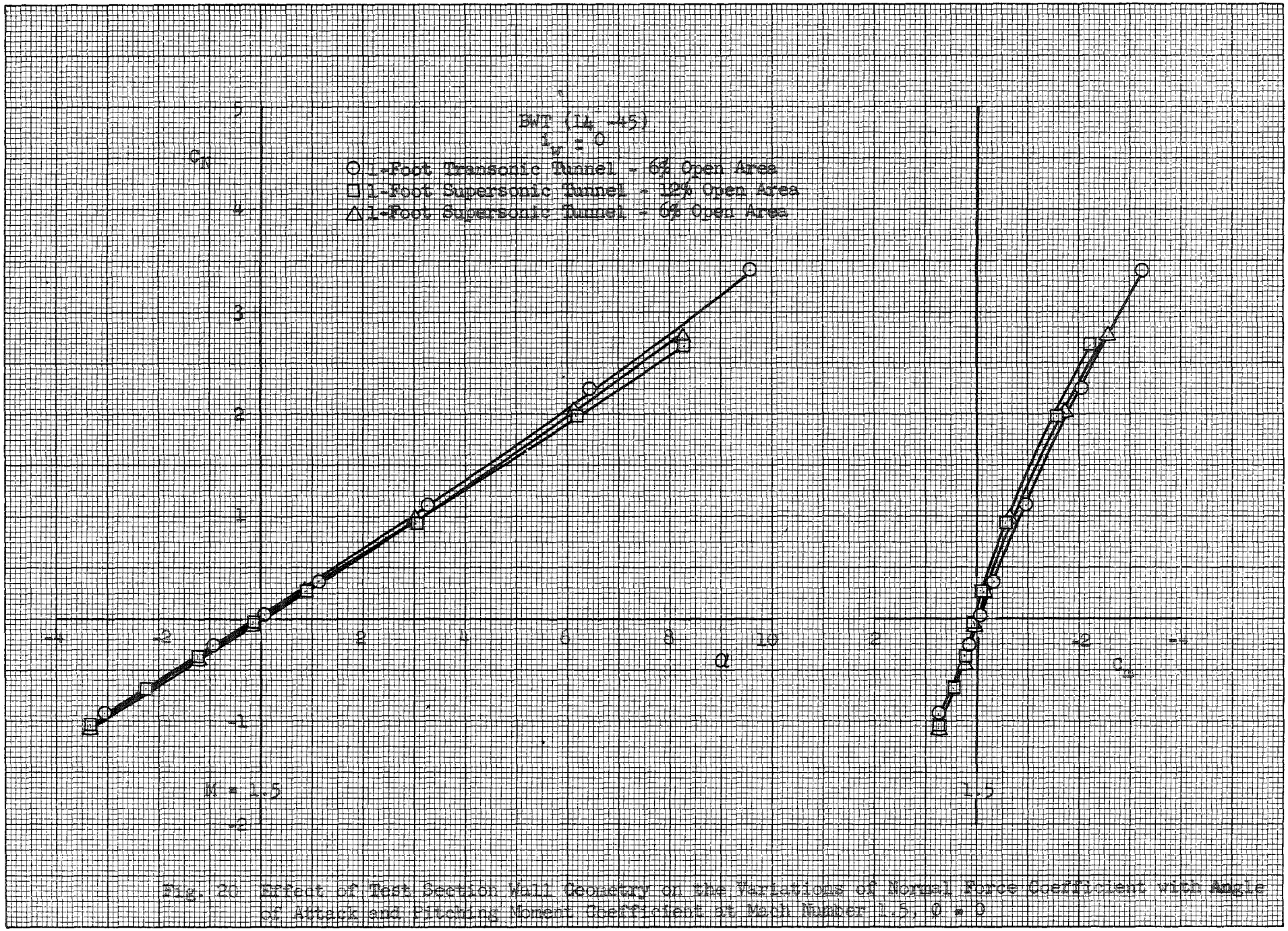

Fig. 20 Effect of Test Section Wall Geometry on the Variations of Normal Force Coefficient with Angle of Attack and Pitching Moment Coefficient at Mach Number 1.5, $\Phi = 0$

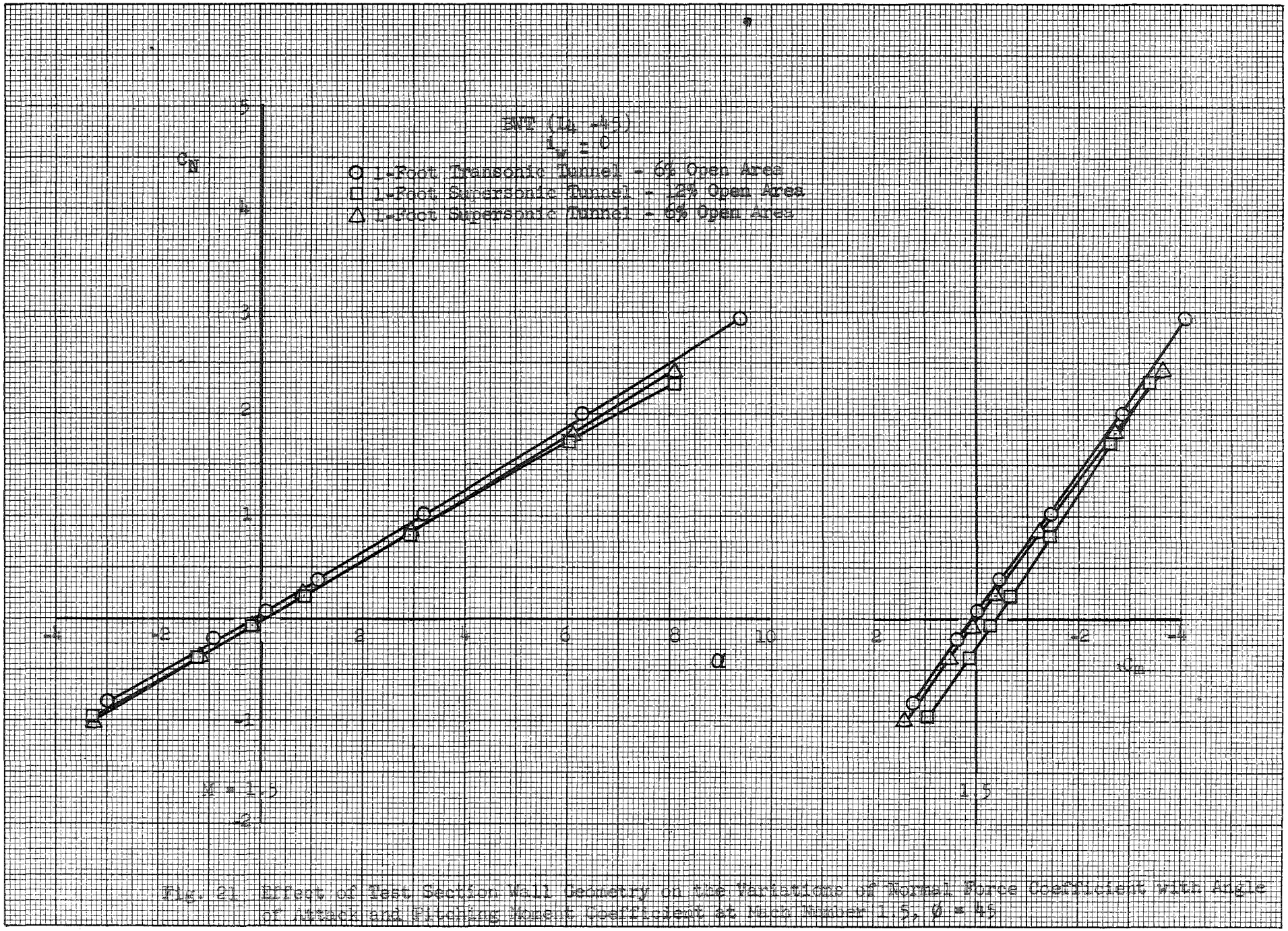

Fig. 21 Effect of Test Section Wall Geometry on Nose Variations of Normal Force Coefficient with Angle of Attack and Pitching Moment Coefficient at Mach Number 1.5, ϕ = 45